Order Number 9315457

The Middle Pleistocene *Homo erectus/Homo sapiens* transition: New evidence from space curve statistics

Dean, David, Ph.D.

City University of New York, 1993

U·M·I
300 N. Zeeb Rd.
Ann Arbor, MI 48106

The Middle Pleistocene *Homo erectus/H. sapiens* Transition: New Evidence from Space Curve Statistics

By

David Dean

A dissertation submitted to the Graduate Faculty in Anthropology in partial fulfillment of the requirements for the degree of Doctor of Philosophy, The City University of New York.

1993

This manuscript has been read and accepted for the Graduate Faculty in Anthropology in satisfaction of the dissertation requirement for the degree of Doctor of Philosophy.

January 11, 1993
Date

Eric Delson
Prof. Eric Delson
Chair of Examining Committee
Department of Anthropology, Graduate Center
The City University of New York

January 29, 1993
Date

Jane C. Schneider
Prof. Jane Schneider
Executive Officer
Department of Anthropology, Graduate Center
The City University of New York

Supervisory Committee:

Prof. Fred L. Bookstein
Center for Human Growth and Development
The University of Michigan

Prof. Timothy Bromage
Department of Anthropology, Graduate Center
The City University of New York

Prof. Court B. Cutting
Institute of Reconstructive Plastic Surgery
New York University Medical Center

Prof. Leslie F. Marcus
Department of Biology, Graduate Center
The City University of New York

Prof. Frederick S. Szalay
Department of Anthropology, Graduate Center
The City University of New York

THE CITY UNIVERSITY OF NEW YORK

Abstract

The Middle Pleistocene *Homo erectus/H. sapiens* Transition: New Evidence from Space Curve Statistics

by

David Dean

Adviser: Professor Eric Delson

Recent models of the evolution of *Homo sapiens*, Out of Africa (OA) and Multiregional (MR) continuity, are polarized over the relative roles of replacement and hybridization. Co-opted by the OA model, Bräuer's (1982) original "Afro-European *sapiens*" hypothesis posited hybridization *with* replacement but gave the upper hand to the role of replacement in the origin of modern humans. Bräuer's original model proposed a polyphyletic origin for *H. sapiens* from developed African and European *H. erectus* populations. The most recent propositions by the principal OA (Stringer, 1991) and MR (Wolpoff, 1992a) advocates have continued to polarize. Stringer posits an intermediate species, *H. neanderthalensis* (i.e., "archaic" *H. sapiens*), between *H. erectus* and *H. sapiens* while Wolpoff would synonymize the last two.

This thesis re-assesses the "Traditional" (TR) model of Howells, Howell, and Delson. The TR model proposed here suggests an African, but possibly European, early Middle Pleistocene cladogenetic origin of *H. sapiens sensu lato*. To test this model three dimensional line tracings of 5 circumvault features were digitized, the glabellar portion

of the brow ridge (GBR), the lateral brow ridge, the temporal line, the coronal suture (CS), and the superior nuchal line (SNL), on samples of *H. erectus sensu lato* (variable numbers for each character), transitional specimens (Bodo, Ndutu, Salé, Broken Hill, Eliye Springs, Saldanha, Petralona, Arago, Swanscombe, Steinheim, and Reilingen), and modern *H. sapiens* (18). Each transitional line tracing was compared directly to an average line tracing for *H. erectus* and *H. sapiens*. A direct morphometric comparison resulted in a chi-square like statistic used to assess affinities of the unknown specimen to the two averages. Space curve averaging and chi square comparisons are discussed in detail. Two of the characters, the GBR and the SNL, indicated that the transitional specimens overwhelmingly sorted with the modern human sample. This result fails to falsify the TR model, but does counter both the MR model and Stringer and Tattersall's current versions of the OA model. The transitional specimens sorted with *H. erectus* for CS, and there was overlap for the other two characters. Perhaps these three characters are plesiomorphic for all populations examined. Results for the possibly "late archaic" Swanscombe and Reilingen crania support an "accretion" model of steady accumulation of Neandertal apomorphies during the Middle and early Late Pleistocene. This model further suggests that since the origin of *H. sapiens* clines of archaic features developed in other regional populations, races, with geographical loci of high

frequency. Most of these late "archaic" populations are assumed to have either dissipated or been largely swamped by modern features. Anatomically modern populations, now thought to have been emerging from Africa throughout the Late Pleistocene, could have played a major role in forming current "racial" populations and clines.

Dedication

To my parents Barbara and Burton who showed me how to love life and learn from it.

Preface

Overview

This section clarifies the use of terminology throughout this thesis. The use of many taxonomic terms, especially those above the species level, varies from author to author. To the casual reader it may appear that I am using taxonomic terms relevant to the *H. erectus/H. sapiens* transition interchangeably; the same will seem so in terms of references to the three dimensional line drawings I made. However, a careful reading will show this is not the case. The usage outlined here is consistent throughout this thesis. A justification for my usage of these taxonomic terms precedes the definitions listed in the Section B, Terminology.

A. Taxonomy

In general I agree with the taxonomic sentiments of Leakey (1963), as exemplified by Szalay and Delson (1979), that family group taxa within the Superfamily Hominoidea are commonly given too high a rank. All of the living ape and human genera, and their close fossil relatives, could be assigned to various subfamilies of the family Hominidae. However, I will defer to the common usage of the supraspecific nomina in this thesis. The Hominidae, after Groves (1989a), is taken to be the family of "large apes" extending back to the early Miocene. At this writing

Hominidae's earliest representative appears to be *Afropithecus* (see Dean and Delson, 1992) if *Proconsul* were not included. Newer craniofacial evidence from Rudábánya and Can Llobateras (Begun 1992, pers. comm.) suggests that the dryopithecines also be included in this family. It is clear that the subfamily Ponginae should include *Sivapithecus*, *Gigantopithecus*, and *Pongo*, but less so *Lufengpithecus*. *Graecopithecus* appears to be the most conservative member of the subfamily Homininae (see: Dean and Delson, 1992); this subfamily also includes the tribes Gorillini and Hominini.

The Hominini includes *Australopithecus* and *Homo*. There is much debate, often acrimonious, over the number of hominin species in the Late Pliocene and Early Pleistocene interval. However, by approximately 1.6-1.8 Ma (million years ago), forms like KNM-ER 3733, 3883, and KNM-WT 15000 mark the start of tenure for a new form, *H. erectus*. Recently it has been argued that several congeners survive alongside the early members of this lineage. For Middle Pleistocene hominin specimens where species attribution to either *H. erectus* or *H. sapiens* is controversial or in question (the primary subject matter of this thesis), I use the term "transitional."

B. Terminology

It may never be possible to adequately diagnose, much less define, the species discussed in this thesis. However the use of these species terms can be defined.

Taxonomic Terms

- australopith: a term for common usage carrying no indication of taxonomic level. Used here to denote members of *Australopithecus (sensu lato)*.
- hominin: a term for common usage to denote members of the Subfamily Homininae, Tribe Hominini.
- *H. erectus* (*sensu stricto*): Those Middle Pleistocene East Asian (from China and Indonesia) fossils almost universally attributed to *H. erectus* (*cf.* Stringer, 1984). It now seems likely that both regions preserve Early Pleistocene *H. erectus* specimens as well.
- *H. erectus* (*sensu lato*): The Old World collection of Early to Middle Pleistocene fossils generally attributed to *H. erectus* (*cf.* Stringer, 1984).
- *H. sapiens*: The sole surviving hominin species. Judging from the results of this thesis, this species has apparent origins in the late Early to middle Middle Pleistocene. Only the single subspecies, *H. sapiens sapiens* survives to the present.
- transitional: Any Middle Pleistocene hominin specimen which has either been questionably identified by one author

or has been variously attributed to both *H. erectus* and *H. sapiens* by several authors.

- "anatomically modern" *H. sapiens*: Living people and their obvious forbears (equivalent to *H. sapiens sapiens*).
- "archaic" *H. sapiens*: All non-modern members of *H. sapiens*, i.e. those not clearly attributable to any living group of people. Related terms include "early," "late," "earliest," and Neandertal (*cf* Stringer, 1988).
- "earliest" *H. sapiens*: Specimens that show the first characters, or apomorphies, unique to *H. sapiens*. While one would expect these to be the oldest specimens it is possible that groups preserving these features alone could survive to coincide with groups displaying additional, perhaps non-modern, apomorphies. This term is general, or lay, rather than jargon and has nothing to do with the formal "early archaic" or "late archaic" *H. sapiens* categories of Bräuer.
- "early archaic" *H. sapiens*: Remains of the entire group of peoples who can be attributed to the earliest radiation of *H. sapiens* (*cf.* Stringer *et al.*, 1979). This term is effectively synonymous with "earliest" *H. sapiens*, but has some status as jargon from its well defined use by Bräuer (e.g., 1984a) and reference to it by others and in this thesis.
- "late archaic" *H. sapiens*: Remains of various groups of people who diverged from the "early archaic" groups (*cf.* Stringer *et al.*, 1979). There is no reason to expect that any or all of the morphoclines that might be detected in

"late archaic" groups would be evidenced in any extinct or extant anatomically modern people. The term "archaic modern" has been applied to the earliest known "anatomically modern" *H. sapiens sapiens* specimens like those from Skhūl, Qafzeh, Omo-Kibish, and Klasies River Mouth. In this context "archaic" also means not clearly assignable to any living racial group, but showing baseline modern morphology.

Neandertal: A group of "late archaic" peoples who appear to have been restricted to Europe and southwest Asia during the late Middle and the first 2/3 of the Late Pleistocene. It is currently unclear if they make any morphometrically measurable contribution to earliest or current European anatomically modern *H. sapiens*.

Morphometric Terms

2D: two dimensional

3D: three dimensional

brow ridge: often used elsewhere in general sense. Used here in a specific sense here for hominins to indicate all morphology, mediolaterally, between the frontal squama, nasion, the orbital rims, and the frontozygomatic suture. In *H. erectus* a continuous torus can be found bilaterally in *norma frontalis* across the region just medial to the orbits beginning at glabella, moving laterally from glabella it is then superior to the orbits and anterior to the frontal squama, and finishes by curving posteriorly onto the side of the vault (*norma lateralis*). It is defined in this thesis to

include a glabellar segment, both superciliary ridges, medially and two lateral segments, the supraorbital tori proper, on either side of the glabellar segment. The term "supraorbital torus" is often generally equated with the brow ridge, however the "proper" usage is adopted here.

☠ curvature maxima landmarks: are the joints along ridge curves or the tops of bubble features on the surface. Only the former are discussed in this thesis.

☠ glabellar segment of the brow: Both superciliary ridges joined at glabella. These two ridges of bone are just superior to the orbits between lines demarcated by the supraorbital notches (see Chapter 2 for fuller discussion).

☠ joint: an inflection point along a line where a change in the curvature gradient occurs.

☠ lateral segment of the brow: The supraorbital torus proper. Beginning above the supraorbital foramen and running laterally to the posterolateral limit of the frontozygomatic suture (see Chapter 2 for fuller discussion). The lateral-most portion can extend laterally away from the skull. When there is little verticality to the frontal (lack of a forehead) this segment can have a triangular flattened dorsal aspect, a "frontal trigone," which would be continuous with the frontal squama.

☠ line tracing: captured data that can be used to represent a 2 or 3 dimensional linear feature.

☠ ridge curve: a three dimensional curving line on the surface of a biological structure. It is defined by a series

of neighboring points that are local curvature maxima on the surface. Often these lines also define the edge of a structure such as a foramen, torus, deep suture intersection, or muscle scar. virtually all of the salient edges found on structures in the body are curvilinear.

- space curve: a three dimensional curving line. There is a family of terms used in this thesis to refer to the three dimensional line tracings which were studied. The term line tracing is probably most general, the term space curve is just as general but refers only to three dimensional line tracings (i.e. the points along the lines have x, y, and z coordinates).

- type I landmark: indicates a discrete juxtaposition of tissues, e.g. a suture intersection. These landmarks often have historical significance and uses. They may have been defined and can only be visualized with special equipment, often in only one plane, e.g., lateral and frontal x-rays. However, many of these landmarks were defined for caliper measurements and are three dimensionally unique (see Bookstein [1991:63-66] for fuller discussion).

- type II landmark: found at local curvature and/or torsion maxima. Examples include tips of pointed or rounded (but not circular) structures, curvature extrema along tori, corners or ovoid extensions around foramina, the bottoms of depressions, or the tops of convexities. Curvature maxima along tori, e.g., inion, are like the Type II landmarks used in this study.

type III landmark: landmarks that act as spanning segments of ridge curves. These ridge curves clearly delimit surface patch gradients of curvature on either side. Often these spans bridge curvature (type II) landmarks (as in this study), diameters, centroids, perpendiculars, and radial intercepts. As spanning segments these landmarks have been defined by a "deficient" criteria, that is changes in their position from specimen to specimen are only meaningful in one or two but not three directions.

Chronological and Institutional Terms

Ka: thousands of years ago, kilo-annum.

Kyr: thousands of years, an interval.

Ma: millions of years ago, mega-annum.

Myr: millions of years, an interval.

AMNH: von Luschan osteological collection, Department of Anthropology, American Museum of Natural History, New York, NY.

CMNH: Hamman-Todd osteological collection, Laboratory of Physical Anthropology, Cleveland Museum of Natural History, Cleveland, OH.

KNM: Kenya National Museum, Nairobi, Kenya.

Acknowledgments

This dissertation project, and my graduate school career in general, were made possible through the concerted efforts of a great many people. The New York subway-hardened students of the anthropology program at the CUNY Graduate School, no matter how hardy, do not succeed without the most exemplary faculty role models. In my case I am sure my degree would not have come to fruition without their assistance and friendship. Time and space do not allow me to adequately thank any of the colleagues I am about to mention.

Eric Delson, my curriculum and thesis advisor, as for so many other students in New York, made available the professional resources essential to success in this field. Moreover, Eric made sure that I and my family were able to survive almost a decade in the harsh economic climate of New York. During this time he has taught me many things, but most importantly to listen. His ability to monitor and master the material relevant to the whole field of physical anthropology has been a constant source of inspiration. His capacity to sense, organize, and articulate a consensus on all topics of paleoanthropology is without match.

My five years' search (beginning with my M.A. thesis work) for a methodology to capture and profitably analyze three dimensional morphometric data ended in a lucky discovery of the work undertaken in Dr. Court B. Cutting's

lab in the Institute of Reconstructive Plastic Surgery at the New York University Medical Center. It was after a technology search that literally took me cross-country, that by chance alone, we finally met. Since that time much, if not most, of what I have been able to achieve has been possible only through the personal advice, shared computer resources, programming assistance, professional backing, and all-too-often direct economic assistance provided me by Dr. Cutting. For the last three years I have been in constant awe of Dr. Cutting's ongoing synthesis of surgery, medical imaging, and morphometrics. As this thesis only scratches the surface of a new approach to craniofacial morphometrics, it is my sincerest hope that our collaboration continue.

Drs. Cutting and Leslie F. Marcus, Department of Biology, Queens College and Graduate School, CUNY, introduced me to Dr. Fred L. Bookstein of The Center for Human Growth and Development, The University of Michigan. All three have been instrumental in educating me in the reasonable uses of the three dimensional data I so eagerly sought. Drs. Cutting and Marcus wrote software that allowed me to undertake these analyses. Dr. Bookstein has given me thoughtful and exacting assistance at several crucial junctures in this dissertation project. My entrance into the field of anthropology was largely due to the excitement at Case Western Reserve University, when I was an undergraduate college student, over the discovery of hominin remains in Ethiopia by Dr. D.C. Johanson and his colleagues William

Kimbel, and Bruce Latimer. Undertaking the morphometric analysis reported here, with the use of today's most powerful graphics workstations, during what can now be called the formation of the "New Morphometrics," has been no less exhilarating. Les Marcus has spent a tremendous amount of time with me painstakingly explaining both new advances in morphometrics and basic concepts of statistics and data analysis. His enthusiastic direction and feedback has spirited my feeble attempts to make this thesis a useful contribution to the morphometric literature.

Dr. Frederick Szalay, Department of Anthropology and Biology, CUNY Graduate School, has served as guardian of my graduate career. He ensured that I gained both income and experience from five straight years of teaching at Hunter College. In my graduate coursework with Dr. Szalay I gained a healthy respect for (and hopefully some knowledge of) the field of systematics and the proper estimation of human ontogenetic and phylogenetic studies among the riches of biological evolution and diversity.

Dr. Timothy Bromage, Department of Anthropology, CUNY Graduate School, came to New York from England as this project was just beginning. He has research interests intermeshing with my own and has freely offered his assistance and advice. I have also enjoyed and benefited from being privy to the synthesis of bone growth histology and morphometrics that Dr. Bromage has pioneered.

Dr. Alan D. Kalvin, IBM Robotics and Augmentation Group, TJ Watson Research Center, and Dr. Marilyn Noz, Department of Radiology, New York University Medical Center, assisted me greatly with many of the computer vision and data handling issues I encountered in this project and other associated research. Along with Betsy Haddad, David Kim, and Deljou Khorramabadi, they form the nucleus of Dr. Cutting's dedicated team. These last three colleagues have provided me daily company and solace throughout the trials and tribulations of this project. I owe special thanks also to Dr. Daniel Karron, Department of Applied Science, New York University, who developed and wrote the 3D digitizing software that I used to collect all the data for this thesis. Dr. Karron also provided me with a full-service account on his workstation in Dr. Cutting's lab the last 3 years. I have also been given access not only to Dr. Cutting's lab but to the entire Institute of Reconstructive Plastic Surgery (IRPS) facility through the good graces of the Chairman, Dr. Joseph McCarthy. Dr. McCarthy and his IRPS colleague, Dr. Barry Grayson, have lent a kind ear and often assistance to the progress and problems of this dissertation project. There are countless other New York area colleagues whose conversations and personal support were pivotal to this project. I only wish I could thank them all with more than the momentary hall chatter that a busy schedule allows.

I owe a great deal of thanks to many other colleagues on an innumerable number of curatorial staffs for making

original material, their offices, libraries, colleagues, and in many cases homes and spare beds, available to me. I especially want to thank: Jens Franzen, Senckenberg Museum (Frankfurt); Jean-Jacques Hublin, Yves Coppens, Monique Tersis, and Dominique Grimaud-Hervé, Musée de l'Homme (Paris); George Koufos, Kalliopi Koliadimou, and George Syrides, Aristotle University (Saloniki); Emmanuel and Harris Kondylis, University of Athens; Reinhard Kraatz, University of Heidelberg; Bruce Latimer, Cleveland Museum of Natural History; Guy Musser, American Museum of Natural History (New York); Thomas Pitsios, University of Athens Medical School; François and Anne-Marie Semah, and Tony Djubiantono, Institut de Paléontologie Humaine (Paris); Christopher Stringer, Peter Andrews, Theya Molleson, Robert Kruzynski, and Tania King, British Museum (Natural History, London); Ian Tattersall, Gary Sawyer, and Jaymie Brauer, American Museum of Natural History (New York); Wu Xinzhi, Dong Xingren, Li Chuan Kuei, Zhou Minchen, Zhang Meeman, and Zhang Yinyun, Institute of Vertebrate Paleontology and Paleoanthropology (Beijing); Xue Xiangxu, Northwestern University (Xian); Reinhard Zeigler, Naturkunde Museum (Stuttgart); Zhou Guoxing and Guan Jian, Beijing Natural History Museum. Also, although we were doing other related work, I especially want to thank Frans Zonneveld, Utrecht University Medical School, and Fred Spoor, University of Liverpool, for the assistance and company they have provided throughout my most recent European travels.

Monetary support for many pilot projects, travel expenses, data collection, and other activities surrounding my thesis project was generously provided in grants directly to me from the Sigma-Xi Society, Senckenberg Museum (Frankfurt, Germany), Wenner-Gren Foundation, LSB Leakey Foundation, and especially a CUNY Dissertation Fellowship. The New York Consortium for Evolutionary Primatology provided me with access to a 3SPACE digitizer and a Silicon Graphics workstation which I used to complete the final data analysis. Ian Tattersall graciously sponsored me for an American Museum of Natural History Graduate Student Research Grant. Indirect support was provided by a National Institute of Health grant to Dr. Cutting. I am eternally grateful to my colleagues Russell Taylor and Alan Kalvin for providing me with an IBM PS/2 Model 70 to interface with Dr. Cutting's Polhemus 3SPACE 3D digitizer during my travels to museums in Europe during the Summer and Fall of 1991. Dr. Bruce Latimer put his complete faith in me, letting me not only study 40 "perfect" Caucasian skulls (complete with morgue data from the Hamman-Todd collection), but also bring them back to New York to digitize, CT-scan, photograph, and study in depth. This database is now archived and housed in the Institute of Reconstructive Plastic Surgery at New York University Medical Center. It would be my pleasure to see this database become a resource to future workers.

Along with Eric Delson, Dr. Lisa Abramson and Sharon Dean assisted with the final copy-edit. However, any typos,

misprints, or other snafus that inevitably snuck through this process are due to my carelessness. Further, I am solely responsible for all of the interpretations made in this thesis, including those I ascribe to others. They deserve all credit for the wisdom I report. All errors and inaccuracies can only be my own.

Lastly, but firstly, I thank my wife Sharon Ellen Dean and son Matthew Evan for surviving a graduate career and attendant family life that graded between commensalism and outright parasitism. My wife has clearly lost the most sleep and life expectancy from this ordeal. I can only hope that the adage of the Central American peoples whom she studies, "whatever doesn't kill you makes you stronger," also applies to marriages. I especially apologize to my son for enduring the downward mobility so common to graduate study. My parents, siblings, in-laws, and Matthew's nanny, Rosa, have also been severely taxed, and along with all of the colleagues mentioned above, have given unwavering support. No matter what the future holds, to all of you I say it was worth it!

Table of Contents

Table Listing

Tables (Continued) Pages

Figure Listing

Figures (Continued) Pages

Equation Listing

I The Problem

"La vraye science et le vray étude de l'homme, c'est l'homme."

Pierre Charron (1601)

"If there were an ancestor whom I should feel shame in recalling, it would rather be a man who, not content with an equivocal success in his own sphere of activity, plunges into scientific questions with which he has no real acquaintance."

Thomas Henry Huxley's response to Bishop Wilberforce (June 1860)

"If we agree that the Australian native, or some other primitive race, may be accepted as a common ancestor for white and black races of mankind, let us ask the following question: How long will it take for the evolution of two such divergent races as the negro and European from such a common stock? In answering that question we have to bear in mind how durable certain modern human types are.

"It is when we approach the antiquity of man from this point of view that we see that we must postulate a very long period of time for the evolution of modern types of man. The whole length of the Pleistocene period does not seem to me sufficiently long for the purpose. Certainly the common ancestor of modern races must have reached a higher stage by the close of the Pliocene period than that represented by *Pithecanthropus*." (The Pliocene ended 400,000 BP for Keith.)

Arthur Keith (1915)

"*Homo sapiens* today is pretty clearly a single species. His races differ, but their skulls are really all much alike in detail. There are far wider differences between the other species of man (such as Neanderthal and Rhodesian), and therefore the natural thing would be to trace *Homo sapiens* back to not more than one of them, if any. If you look for the ancestors of an individual man, you find more and more of them as you go back, but if you look for the ancestors of a race of men you find fewer and fewer -- there are more apples than twigs, more twigs than boughs, and all the boughs go on a single trunk. It may be, as is often suggested, that Neanderthal Man or some other kind mixed with our ancestors (Skhul? Cro-Magnon?), but one cannot explain the very existence of *Homo sapiens* by such an applesauce as this. That would be as if you expected to find a given branch growing on two trees at the same time."

William W. Howells (1944)

"The strict application of unilinear transformationism led Weidenreich (1943, 1946) to find the ancestry of each living racial variety of *H. sapiens* within a distinct subgroup of *H. erectus*."

Anthony P. Santa Luca (1980)

"If, however, *H. s. sapiens* and *H. s. neanderthalensis* had a common post-*erectus* ancestor in such a group as that once known as "pre-neanderthal" or "progressive" (perhaps *H. s. steinheimensis*?) then all three named in this sentence are proper subspecies (Mayr, 1951). But then what about *H. s. rhodesiensis* as a member of this set of subspecies? It can be, and is being, argued that the fossils under this name represent an independent African line of development out of *H. erectus*, in fact one for which at the present time there seem fewer obstacles than for Europe as a direct ancestor for moderns. The same may be said for the new Chinese fossils from Dali and Xujiayao. Thus a European "pre-neanderthal" ancestor for all of *H. s. sapiens*, or for any, may be illusory, an accident of the history of fossil discovery."

William W. Howells (1980)

"... a spectrum of "early archaic *Homo sapiens*" similar to the Rhodesoid morphology can be considered as ancestral to the more modern "late archaic *Homo sapiens*" and to the fully anatomically modern *Homo sapiens* as well. ... Thus, for Africa, the present hominid record makes it appear very probable that the development from archaic to anatomically modern *Homo sapiens* took place in Eastern and/or Southern Africa."

Gunter Bräuer (1984a)

"Whether there was a single African centre of origin for modern humans, followed by a radiation to Asia and Europe later in the Late Pleistocene, or whether other non-European centres of origin existed is unclear."

C. B. Stringer (1985)

"The main elements of the Garden of Eden hypothesis are that modern humans *arose recently* from a small source population, approximately 200,000 years ago in Africa, and that this population was a *new species*. ... A valid explanation of modern populational origins must account for two aspects of the human fossil record, recognized by Weidenreich a half century ago, both of which contradict the Garden of Eden hypothesis. These are the persistence of unique regional distinctions for long periods of time, even across species 'boundaries', and the commonalities of human evolution during the Middle and Later Pleistocene in different regions."

Milford H. Wolpoff (1989)

"... at present, there is no basis for arguing that the evolution of early *Homo sapiens*, as described here, was a particularly important event. Future discoveries may in fact show that it was not an event after all and that what we now call early *H. sapiens* is really an amalgam of several distinct species, evolving along separate trajectories in different regions (Tattersall, 1986)."

Richard G. Klein (1989)

" An opposing view, adopted here, is that *Homo erectus* is a stable taxon, distinct in important ways from all later Pleistocene humans. In this scenario, archaic people [*H. erectus*] were pushed toward extinction and actually replaced by members of an anatomically advanced species" [i.e., *H. heidelbergensis*].

G. Philip Rightmire (1990)

Race

From the time of Darwin to this day a large constituency of paleoanthropologists have devoted efforts to a search for the ancient origin of what are perceived as "racial" traits. At the time of the Piltdown forgery, a Pliocene origin for the modern human races was considered likely (Kieth, 1915). Dubois's original interpretation of Indonesian *H. erectus* was unique in that he was the first to posit a truly "transitional" form between apes and humans, not another race ancestral to humans living in the region today (Theunissen, 1989). Schwalbe (1901) was the first of many to suggest the limits of the racial approach to hominin systematics had been reached. He held that Neandertals represented a separate species from *H. sapiens*, "*H. primigenus*." For those who persisted with a strict racial approach it became more and more difficult to incorporate new specimens, especially with the discovery of additional

Indonesian and Chinese *H. erectus*.

By the end of the 1930's the New Synthesis had also aligned systematics and its half sister, paleoanthropology, with the principles of genetics and population biology. Some paleoanthropologists, however, remained immune to the new priorities. Simpson (1944) chided Weidenreich for basing the weight of characters on how well they sorted taxonomic groups rather than weighting a character strongly on the basis of some "causal reason for its greater importance."

Hooton (1930), Hrdlička (1930), Weidenreich (1946), and later Coon (1962) continued to be fascinated by theories of race formation. All four of these authors assumed a universal "Neandertal" phase through which a worldwide diaspora of *H. erectus* passed on the way to becoming *H. sapiens*. It would seem that their views have found fresh, more or less, American-trained advocates in the supporters of the "Multiregional" (MR hereafter) model of human evolution (discussed below and in Chapter IV, "Conclusions").

In the 1940's European debate on the origin of *H. sapiens* coalesced around the denial of any role for Neandertals in the evolution of modern humans. It was assumed that Neandertals had had a common origin with *H. sapiens* but were thought to have later diverged from more sapient forms such as Steinheim, Swanscombe, and Fontéchevade (Kieth, 1939). Instead, these authors looked to the east for late *H. erectus* or so-called "pre-sapiens"

populations, e.g. the Zuttiyeh craniofacial fragment, which might have given rise to the Cro Magnon people who would later (re)colonize Europe (Vallois, 1949). This position is still prevalent in much of Europe (e.g. Saban, 1991). For these theorists it can almost be assumed that any specimen that is not anatomically modern or a Neandertal is reasonably ascribed to *H. erectus*.

Mayr's (1951) call to unite Early and early Middle Pleistocene, post-australopith, hominin taxa as *H. erectus*, and all later hominin groups including Neandertals into *H. sapiens*, was a largely successful attempt to apply systematic methods to the hominid fossil record. In the late 1950s and early 1960s a succession of fossil discoveries, especially in East Africa, and advances in techniques that allowed them to be accurately dated, made it clear that the European and Asian hominin record was probably no greater than 1 million years. Weidenreich's successors (e.g. Arambourg, Bishop, Dart, Howell, Howells, von Koenigswald, Leakey, Napier, and Tobias) accepted most of Mayr's views and were by this time convinced Africa was the site of origin of *H. erectus*. For most of the last 30 years the evolution of the species *H. sapiens* (including various "archaics", Neandertals, and the highly polytypic modern forms), from the panmictic Middle Pleistocene species *Homo erectus* was an accepted fact in the mainstream anthropological literature (e.g., Campbell, 1985; Brace, 1988). Questions surrounding the nature of this speciation

event, if one occurred at all, were left intentionally vague. However, during the past 10 years, since Bräuer's "Afro-European *sapiens*" hypothesis (1982), a heated controversy has grown over the timing and location of the appearance of the earliest anatomically modern *H. sapiens sapiens*. At the bottom of the current debate are changing views on what constitutes a biological species, how the fossil evidence for the evolution of *H. sapiens* squares with these theoretical definitions, and how the documented Pleistocene climatic and cultural changes might indicate such major shifts.

The "Out of Africa" and "Multiregional" Models

Largely because of the backlash to Coon's (1962) opus, especially his work on the origin and demographics of the "racial" osteological features of living peoples, study of Pleistocene human evolution has been an unwelcome stepchild for Anglophone physical anthropologists during the last 30 years. The breach was filled by discussions of punctuation and stasis in *H. erectus* alongside furtive debate over the fate of the Neandertals (Brace, 1964; Howells, 1974; Bräuer, 1981; Stringer and Burleigh, 1981; Trinkaus, 1982; Stringer, 1982; Trinkaus and Smith, 1985). Even so, theories as to whether Neandertals had been replaced or assimilated had to be couched in terms that were bullet-proof against charges of racism (Graves, 1991).

Questions over differing views of *H. erectus*,

irrespective of the Neandertal problem, began to resurface with a seminal critique of the use of this taxon by Howells (1980). Immediately after this searching paper most discussion of *H. erectus* was then diverted back to debate over the pace and degree of change within the assumed 1.5 Myr tenure of *H. erectus* (Eldredge and Tattersall, 1982; Wolpoff, 1983; Rightmire, 1981a, 1985, 1986). However the taxon began to become unglued at the 1983 Senckenberg conference (Andrews and Franzen, 1984) where several papers were presented that questioned the utility of retaining the Early Pleistocene African *H. erectus* specimens (primarily KNM-ER 3733, 3883, and OH 9) in a taxon originally defined for the Asian representatives (Stringer, 1984; Andrews, 1984; Wood, 1984).

European workers were also beginning to ask questions about the taxonomic treatment of "archaic" or early *H. sapiens* (Stringer *et al.*, 1979) and the origin of anatomically modern people (Bräuer, 1981; Protsch, 1975; Howells 1976, 1980). The latter topic quickly outstripped the attention given the former even though the mid 1970's to early 1990's saw the discovery of several Middle Pleistocene specimens (e.g., Apidima [Coutselinis, *et al.*, 1991], Bodo, Dali, Eliye Springs, Jinniushan, Ndutu, and Yunxian) that would obviously prove useful to discussions of the *H. erectus/H. sapiens* transition. New dates in the vicinity of 100 Ka doubled the age of anatomically modern human remains from Skhûl, Qafzeh, and Klasies River Mouth, and the

emergence of the mitochondrial (mtDNA) "Eve" hypothesis rekindled debate over the origin of anatomically modern humans. While the redated early "modern" sites and mtDNA Eve model have received wide attention, the new Middle Pleistocene finds were largely neglected and casually attributed to nebulous "archaic" *H. sapiens* or late *H. erectus* categories. At this writing actively used textbooks still advocate hominin species attribution on the basis of time lines drawn around "chronospecies" (Wolpoff, 1980a; Campbell, 1985) or clubs of "grade" members (Brace, 1988) despite complaints by many that such practices are less than useful (Howell, 1984; Rightmire, 1988).

Bräuer (1982, 1984a, b, c, 1989) confronted this theoretical gap with his "Afro-European *sapiens*-hypothesis", later renamed the "Out of Africa Hypothesis" (OA hereafter). Although Bräuer's (1984a, 1992) attempts to identify "early-" and "late archaic" grades within a broadly defined *H. sapiens* was superficially similar to Stringer *et al.* (1979) it was the first proposal for an African origin of anatomically modern humans to review the worldwide Pleistocene hominin fossil sample (see also: Thoma, 1973; Protsch, 1975; Bräuer 1978; Bräuer and Protsch, 1980). Stringer *et al.*'s (1979) two "late archaic" *H. sapiens* "grades" refer mainly to the position of specimens relative to the Neandertal lineage. Bräuer noted that such Eurocentric ideas about the origin of modern humans were still held tenable by many, including those supporting the

"pre-sapiens" model of parallel lines of modern and Neandertal stock in Europe. Instead, Bräuer concurred with others that the European and southwest Asian evidence suggested one line leading to Neandertals (Howells, 1976, 1980; Hublin, 1982; Santa Luca, 1978). He went further, however, in saying that the Neandertals and another less well known line in eastern Asia were both "genetically replaced" (i.e., "hybridization with replacement") by anatomically modern humans who arose in Africa by 30 Ka. Extending and largely concurring with Stringer *et al.'s* (1979) model, Bräuer (1984a, 1992) also proposed the existence of two additional populations of "early" and "late archaic" *H. sapiens* existing in Africa during the period from 500 to 30 Ka in Africa. The "early archaics" in Africa include Bodo, Kabwe (Broken Hill), Ndutu, and Saldanha (Elandsfontein) (See Chapter IV for discussion of "late archaics"). One of the first tests of the "early" and "late archaic" *H. sapiens* categories, the Eliye Springs cranium, was described by Bräuer and Leakey (1986) as intermediate. Bräuer (1984a, 1989) refers to the use of the "early" and "late archaic" *H. sapiens* categories as "grades."

While he posited a monocentric origin for *H. sapiens* in subsaharran Africa, he gave an unspecified role to hybridization and his illustrations (Bräuer, 1984a:159, 1989:125) suggested polyphyly. Specifically, he indicates an independent origin of African "archaic *H. sapiens*" and European ante-Neandertal/"archaic" *H. sapiens* from separate

"developed *H. erectus*" stocks in Africa and Europe. He calls attention to similarities between Petralona and Bodo and between Broken Hill and Dali, but stops short of claiming phylogenetic ties between them that would obviate this apparent polyphyly. Stringer (1991, pers. comm.) has modified his earlier views of the entire "archaic" period, now making the claim that all "archaics" belong to a single species, *H. neanderthalensis*. He would attribute only anatomically modern forms, which he sees as having a separate, later origin in Africa, to *H. sapiens sapiens*.

Thus, Bräuer's hypothesis (1992) is inconsistent with Stringer's current view because, although replacement is the dominant mode of transition, it claims more of a role for hybridization in the origin of early through anatomically modern *H. sapiens*. Bräuer's model is consistent with Hublin's views (1986; 1992). However, Hublin offers the possibility that most of the differences seen in the Far Eastern *H. erectus* sample may be due to unimportant hormonal differences and that direct continuity of surviving *H. erectus* with immigrating Afro-European *H. sapiens* (i.e. hybridization) is a possibility. To date Bräuer has proposed regional, independent evolution of a Neandertal line in Europe (Bräuer and Rimbach, 1990; *contra* Brace, 1991) and a less well defined, but independent lineage in Eastern Asia with hybridization-replacement by modern humans occurring in the latest Pleistocene, perhaps even the Holocene in these regions. The "early" and "late archaic" *H. sapiens* problem

is discussed in Chapter 4.

Largely in response to claims that the origin of anatomically modern humans could be found in the late Middle Pleistocene, Wolpoff (1989a and b; Wolpoff *et al.*, 1984) and others (Frayer, 1992a; Groves, 1989a and b; Habgood, 1989a; Li and Etler, 1992; Pope, 1992; Smith, 1984 and 1992a; Smith *et al.*, 1989a and b; Smith and Paquette, 1989; Simmons and Smith, 1991; Thorne and Wolpoff, 1981; Wu and Wu, 1985; Wu, 1990, 1991) have entertained Weidenreich's (1943, 1945) ideas of "Multiregional" (MR model) continuity of features that region's earliest indigenous inhabitants, i.e. *H. erectus sensu lato,* through its modern human inhabitants. They propose that after the initial radiation of *H. erectus* from Africa that regional features began to differentiate at the periphery. However all populations remained in genetic contact through gene flow. According to this model in each major region of the Old World, Africa, Europe, Northeast, and Southeast Asia, populations would accumulate regionally unique features. Recently, Wolpoff (1992a, b; Thorne and Wolpoff, 1991) has removed the apparently arbitrary *H. sapiens* threshold by arguing that *H. erectus* should be sunk into *H. sapiens*. Dhobzhansky (1963) chided Weidenreich for going overboard in his theories of *H. erectus* to *H. sapiens* anagenesis, while noting that it was quite possible the two forms were synchronic and sympatric in the Middle Pleistocene. The premise of this thesis, that *H. sapiens* autapomorphies are first present in the Middle Pleistocene,

is therefore in contradistinction to the MR hypothesis. It proposes to test theories of Middle Pleistocene cladogenetic origins of *H. sapiens*, including variants of the OA model (*cf.* Foley and Lahr, 1992).

The specific model tested by this thesis, the Traditional Model (TR) of Howells (1980), Howell (1978), and Delson (1981), posits a late Early to early Middle Pleistocene cladogenetic event resulting in the origin of *H. sapiens*. While it is likely many regionally significant racial populations would have developed after this time, reticulate evolution within the species would predominate. The Traditional model is supported by Bräuer's recognition of "early archaics" in Africa (e.g., Bodo, Broken Hill, Eliye Springs, Ndutu, Saldanha, and Salé), ante-Neandertals in Europe (Arago, Apidima*, Atapuerca*, Bilzingsleben*, Ehringsdorf*, Mauer, Petralona, Reilingen, Swanscombe, Steinheim, and Vértesszöllös*; *too damaged, incomplete, or permission not granted to digitize for this project), and similar forms in Asia (Dali*, Jinniushan*, and Yunxian*); a geochronological correlation of the specimens digitized for this project is presented in Figure 1.1 and documented in Tables 2.1 and 2.2 (*permission could not be secured to digitize for this project). If supported, a Middle Pleistocene origin of this single species, *H. sapiens*, would fall in the middle of the MR and OA theoretical spectrum (see Chapter 4 for other intermediate hypotheses). Additional taxonomically useful characters obtained from

this analysis might also obviate the need for continued use of chronospecies or grades.

Figure 1.1: Geochronology of *H. erectus* and "early archaic" *H. sapiens*.

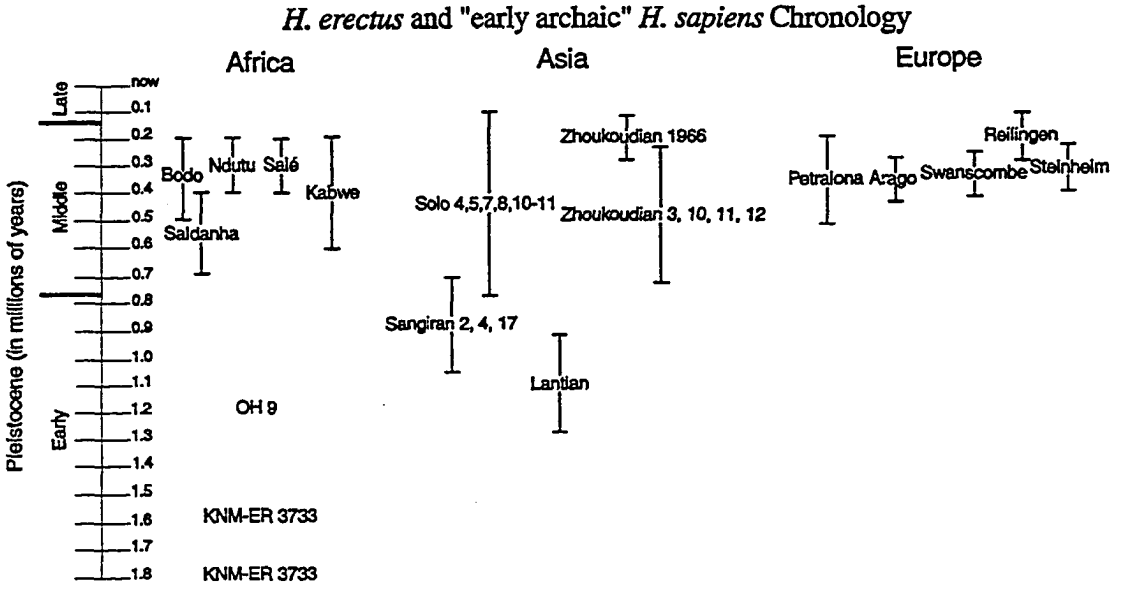

If one accepts this position, the uncertain dating of the earliest specimens attributable to *H. sapiens* -- especially in Europe and Africa -- it cannot be said with certainty where this speciation event occured. Europe,

southwest Asia, East and North Africa cannot be ruled out.

Morphological support of the single origin hypothesis would further highlight the need for a broader diagnosis of the species *H. sapiens* (Howells, 1973; Day and Stringer, 1982; Stringer and Andrews, 1988; Wolpoff, 1992a and b). A broader diagnosis would include characters that were the result of discrete transformation, robust autapomorphies. It is likely that quantification of these characters need be adjunct, not secondary, to the character definition. While not a reason for adopting a phylogenetic position, it should be noted that such a diagnosis of *H. sapiens* would support the discarding of the "waste-basket" taxon "archaic" *H. sapiens* (e.g., in favor of demonstrable "racial" populations), assist biogeographic study (e.g. Tillier and Vandermeersch, 1982), and would be consistent with widespread traditional and current informational use of the term *H. sapiens*.

No specimens definitively attributable to *H. erectus* are known from Europe (Howell, 1976; Howells, 1976; Stringer, 1981; Hublin, 1982; Bonis, 1986; Rightmire, 1988; Jelínek, 1980a and b; but see Gibbons, 1992). However, if Africa is considered the location of the transition, the best test of such a model have been the findings supporting a lack of morphological continuity between the latest *H. erectus* (e.g., Zhoukoudian and Hexian) and the earliest *H. sapiens* (e.g., Dali, Jinniushan, and Yunxian) in China (*cf.* Groves 1989a, b; *contra:* Li and Etler, 1992; Pope, 1991). However,

the possibility that there was a Middle Pleistocene origin of *H. sapiens* in Africa, with subsequent intra-species evolution and eventual replacement of *H. erectus,* has not previously been part of the OA-MR debate.

If *H. sapiens* had a Middle Pleistocene origin, arguments over hybridization between moderns and Neandertal or other "archaic" *H. sapiens* become a question of movement of subspecific populations and changing geoclinal variation. Attempts to localize the *H. erectus-H. sapiens* transition will benefit from additional fossils, but attempts at understanding this process might best begin with the youngest known *H. erectus,* in sub-Saharran Africa there are a few specimens: OH 11, 12, 22, and 28. There are several late Early to early Middle Pleistocene sites outside of sub-Saharran Africa that produced candidates in Europe (e.g. the Dmanisi mandible) or northwest Africa (e.g., the Ternifine mandibles and parietal). The Dmanisi mandible has yet to be subject to critical comparative study.

As it stands today, the conventional perspective on the *H. erectus-H. sapiens* transition has given way to two nearly bipolar views: the OA (Out of Africa) model and the MR (Multi-Regional) model. The nature of the dichotomy has been brought out in several recent conference volumes (Mellars and Stringer, 1989; Trinkaus, 1989; Bräuer and Smith, 1992). Advocates of both the MR and OA models generally agree that during the Early and Middle Pleistocene, *H. erectus* populations spread from Africa through eastern and

southeastern Asia and possibly into Europe (Stringer, 1984; Bräuer, 1984a; Wolpoff, 1971, 1980a). There is disagreement, however, over the contribution any of these extra-African *H. erectus* groups made to later or in some cases nearly synchronic groups of "archaic" *H. sapiens*. Thus, while most participants would agree that the earliest Pleistocene, approximately 1.6 Ma BP, saw the appearance of a group of clearly non-australopith forms, *H. erectus*, there is no agreement on when or where the earliest *H. sapiens* appeared.

The earliest specimens presenting the *H. erectus* morphology include KNM-ER 3733 and 3883, and KNM-WT 15000. The existence of anywhere from one to three species or hominin morphs in the immediately antecedent Plio-Pleistocene is now a topic of serious debate (Bilsborough and Wood, 1986; Clarke, 1990; Rightmire, 1990; Wood, 1991; Delson, 1992). Craniofacially, however, the earliest *H. erectus* skulls present an overall morphology and several distinct characters that mark what appears to mark a speciation event. Howell (1978), Groves (1989a), and Rightmire (1990) have made strong arguments for the integrity of the taxon *H. erectus sensu lato*. Rightmire and others (Stringer, 1984; Andrews, 1984; Hublin, 1986; Turner and Chamberlain, 1989; Kennedy, 1991) have recently reviewed the characters listed in Table 1.1 as diagnostic of this species apart from other proposed species of earlier *Homo*, *Australopithecus*, and *H. sapiens*. These characters have been more recently reviewed by Bräuer (1992; Bräuer and Mbua,

1992), especially the subset which Andrews (1984), Stringer (1984), and Wood (1984, 1992) have proposed as limited to Asian forms. Bräuer's findings are discussed in Chapter 4.

Table 1.1 Craniofacial characters typical of *H. erectus (sensu lato)* after Rightmire (1990:189) except 11.

1) The brow is thickened and continuous, and there is a depressed or at least flattened supratoral shelf behind.
2) The frontal and anterior interparietal exhibit midline keeling.
3) There is an angular torus at the posteroinferior corner of the parietal bone.
4) The occipital squama is wide and sharply angled.
5) The morphology of the transverse torus of the occiput is distinctive, as noted by Wood (1984) and others, although there is a good deal of variation.
6) The glenoid cavity is narrowed medially to produce a deep fissure between the (large) entoglenoid pyramid and the tympanic plate.
7) The tympanic bone, which presents a strong petrosal crest, terminates in a blunt process supratubarius
8) The petrosal crest is separated from the mastoid bone by a fissure.
8) The vault bones are relatively thickened.
9) Endinion and inion are widely separated
10) Endocranial volume is increased to approximately 1000ml.
11) Anterior nasal spine, acute nasoalveolar clivus angle, anterolateral eversion of piriform margin (Franciscus and Trinkaus, 1988)

There is very little disagreement that the Asian *H. erectus* forms from Indonesia and China, what Stringer (1984) refers to as *H. erectus sensu stricto,* belong to a single species (but see Dong, 1989). One reason for the proposed separation is that these forms show autapomorphies (e.g., angular torus, thick cranial bones) that preclude them from being on the direct line to living humans (Stringer, 1984). Stringer (1984) also notes that the current use of this taxon, *H. erectus sensu lato,* was defined for the Asian forms.

Hublin (1983), Stringer (1984), and Wood (1984, 1991;

Bilsborough and Wood, 1986) have all suggested the smallish, conservative, KNM-ER 1813 as possibly similar to the ancestral morphotype of *H. erectus sensu lato*. Sounding the same note, Leakey (1966) and Andrews (1984) have called attention to the fact that at any given time during the Pleistocene, forms living in sub-Saharan Africa seem more similar to living humans than do any of their extra-African contemporaries. Leakey (1972) claimed that late-surviving early Middle Pleistocene *H. habilis* was ancestral to *H. sapiens*, not *H. erectus sensu lato* which for him included OH 9. Leakey was convinced that Steinheim, Swanscombe, Fontéchevade, Vértesszöllös, Kanjera, and Omo 1 represented Middle Pleistocene *H. sapiens*. However, he interpreted Kabwe, Solo, and Neandertals as hybrids between *H. erectus* and *H. sapiens*. Clarke (1990) proposed that the Asian *H. erectus* (*sensu stricto*) apomorphies occurred in a lineage that diverged (left Africa?) before the appearance of forms such as Early Pleistocene African KNM-ER 3733, 3883, and KNM-WT 15000. Thus he would recognize a separate species *H. leakeyi* (includes Early and Middle Pleistocene African *H. erectus*), with OH9 as the type specimen (Heberer, 1963a and b); *H. leakeyi* would later give rise to *H. sapiens*. Wood (1992) argues for the addition of KNM-ER 730 and 992 to Clarke's *H. leakeyi*, without OH 9 and other Olduvai *H. erectus*, and renames this hypodigm *H. ergaster*. Wood aligns *H. ergaster* as the sister group of *H. sapiens*. Along with the Asian specimens, Wood allocates specimens from Olduvai,

Baringo, and Swartkrans to *H. erectus sensu stricto.*

It is currently difficult to dispute this position in regards to the time frame when "archaic" *H. sapiens* is thought to have appeared, sometime between 1.0 and 0.4 Ma, because there is very little diagnostic cranial material dated with certainty to this period. It is possible there is a gap in the middle Middle Pleistocene Indonesian record; these specimens are notoriously poorly dated. It could be that some of the Sangiran specimens are older than 1.0 Ma (Pope, 1988) while there are claims that the Solo specimens date to as late as 200 Ka (Bartstra *et al.*, 1988; but see Aziz *et al.*, 1991). In China the Lantian (Gongwangling) site could be as old as 1.2 Ma (An and Ho, 1989; Pope, 1988). Without the Chenjiawo mandible and Yuanmou incisors another potential gap would exist between the Early and Middle Pleistocene fossils in China. The oldest specimens at Zhoukoudian could date to no more than 500-250 Ka (Li and Wang, 1991; Pope, 1992). The less widely known cranium from Hexian appears to be typical of those at Zhoukoudian and is reported to be little older than 250 Ka (Wang, 1989; Chen and Zhang, 1991). Irrespective of a potential gap, there does seem to be morphological continuity for both the Indonesian and Chinese *H. erectus* samples over the time span they represent (Rightmire, 1990).

The latest dates for Hexian and Zhoukoudian appear to be the best evidence of late surviving Asian *H. erectus*, increasing the likelihood of sympatry with rather than

transformation (local continuity) into "early archaic" *H. sapiens* such as those known from Dali, Jinniushan, and Yunxian (Pope, 1988, 1992; Chen and Zhang, 1990; Li and Etler, 1992) during the period from 300-150 Ka. So far, perhaps because of the attention being given the origin of anatomically modern humans, little attention has been paid to the possibility of a replacement, or replacement with hybridization, event in the late Middle Pleistocene of China. It is clear that populations similar to the Chinese "early archaic" *H. sapiens* existed earlier in Europe and Africa.

Advocates of the MR model argue that Eurasia remained populated throughout the Middle and Late Pleistocene and that processes of mate and culture exchange facilitated worldwide gene flow among the disparate groups throughout this land mass. Many regional differences seen in modern human populations (especially those with skeletal indications) are presented as regional synapomorphies, having arisen and become most prevalent in the furthest reaches of the human range during the Pleistocene (Thoma, 1973; Habgood, 1989a; Thorne and Wolpoff, 1981, 1991; Wolpoff, 1985, 1989a, 1992a). The search for continuity has stretched the limits of the patchy fossil record of Eastern Asia. But it has found some support from workers who were skeptical at the outset (Pope, 1991, 1992; Habgood, 1989a; Hublin, 1986; Hublin and Braun, 1992).

Character Analysis

In positing either regional continuity of characters, or the emergence of synapomorphies suggesting the evolution of a new species, documentation and testing of characters is the single most important activity. Much of the data cited in the literature as relevant to the *H. erectus/H. sapiens* transition has been of a binary nature, e.g., presence/absence features. In these cases, however, there is often much more agreement over the status of a character state, whether it is present or absent, than when the character morphology as presented varies, perhaps clinally, and must be quantified. Without advanced morphometric techniques it is often a very difficult problem to quantify morphological variation. Traits that relate directly to linear measurements, indices of such measurements, angles or volumes of cavities are notable exceptions.

Smith and colleagues (Smith and Ranyard, 1980; Smith *et al.*, 1989b; Simmons and Smith, 1991; Simmons *et al.*, 1991) attempted to differentiate morphological states of brow development on the basis of three linear measurements taken along the supraorbital torus. Pope (1991) attempted to illustrate Far Eastern continuity in the outlines of the lateral edge of the zygomatic process of the maxilla (buttress of the zygomatic arch). Howells (1973, 1989) has had very good results with discriminant analysis of linear measurements and angles. The major assumption behind this attempt at discrimination is that the blanket of

measurements reflects the underlying populations' genetic integrity and phylogenetic history. The ties of such analyses of linear measurements and angles to descriptive diagnostic morphological variation are much more tenuous. Are good characters actually being measured or are the "characters" just the measurements that are easiest to collect? Indices have the benefit of size independence, but at best they have a discernible allometric relationship with changes in the three dimensional morphological state we usually hold in our mind's eye. Howells' (1973, 1989) approach collects a great many measurements in the hopes of adequately representing craniofacial form without over-representing (i.e. overweighting) any aspect of it.

Very few workers have applied more direct morphogenetic techniques, using 2 or 3 dimensional landmark data, to problems of hominin evolution. Hershkovits *et al.* (1991) used moire photography to collect contour data and make visual comparisons of recent human fossils. Landmark-based morphometric tools, especially tensor methods such as finite element scaling analysis, have also been used to compare phylogenetic counterparts (Richtsmeier, 1989; Richtsmeier *et al.*, 1991), sexual dimorphism (Cheverud and Richtsmeier, 1986), and biomechanical models (Endo and Adachi, 1988) among other primates. Matrices of linear measurements between all the landmarks taken from an object, Euclidean Distance Matrix Analysis (EDMA), provide an alternative descriptor for similar analyses (Richtsmeier *et al.*, 1992).

A variety of landmark data techniques have been applied to two-dimensional projections of objects in order to study ontogenetic changes in cranial profiles (Olshan *et al.*, 1982; Hazout *et al.*, 1990; Rohlf and Bookstein, 1990; Delfino *et al.*, 1991; Bookstein, 1991), phylogenetic changes amongst primate scapulae (Albrecht, 1991) and mandibular (Straney, 1990; Daegling, 1992) form. The use of landmark data in a way that ties together anatomical shape (i.e., morphology) and the statistical representation of that shape has been described as the "New Morphometrics" (Rohlf and Marcus, in press).

The New Morphometrics offers new possibilities to quantify morphological states and express these comparisons visually with a likeness of the object. This allows debate to center on important aspects of character analysis, especially the assumptions behind the choice of the character. The assumptions that underlie a character supply its robusticity, its weight, in the overall analysis. The nature of the character, especially polarity (i.e. the possibility of homoplasy), should not be reducible to a measurement. Knowledge of a character's ontogeny, potential roles, and actual biorole allows the disentangling of features that are correlated to a single process. Discerning such related features prevents redundant characters and overweighting of character complexes. Intimate knowledge of a character also allows better judgment as to the observed state's heritability, an assumption necessary for the

character to have phylogenetic importance. The same criteria hold for presence/absence characters, which are very often the most robust (i.e., well understood) traits in an analysis.

For many the cladistic revolution is little more than a justification for collecting characters to run through a parsimony analysis. From this purely empirical perspective all observations are characters deserving of equal weight because each is a hypothesis that the next observer may come along and fell. It is assumed that with enough characters the "law of large numbers" will take over and the correct result will be hit upon. This is actually a return to the phenetic approach to which cladistics was a reaction. Morphometrics has the same potential for abuse. However, many in-depth character analyses, i.e. the robustification of characters, have made clear the value of quantized characters.

A similar situation comes into focus when one compares the two competing models of *H. sapiens* evolution. OA advocates have largely disagreed with MR hypotheses that point to particular specimens which evince intermediate characteristics, i.e. transitional fossils, as disproof of the OA model. OA advocates concede that hybridization likely did occur at the boundaries between groups of terminal "late archaic" and modern *H. sapiens* (e.g. in the Levant and Western Europe; few have considered hybridization between *H. erectus* and "early archaic" *H. sapiens*, e.g., in China), but

in most cases it is expected that the aboriginal group did not contribute significantly to future gene pools (Stringer, 1989a and b). If it can be demonstrated that hybridization did not lead to significant regional (i.e. genetic) continuity (i.e., known evidence supports full replacement) then the extreme taxonomic arguments of some OA advocates, that each region's *H. erectus* and "archaic" *H. sapiens* population should be treated as separate species (Tattersall, 1986), are made possible. Most MR advocates argue that the *H. erectus-H. sapiens* transition occurred worldwide, over time, with panmictic gene and culture flow keeping all populations on a relatively equal footing.

Neither camp has carefully addressed the fundamental criterion for positing a transition: an analysis of the proposed character transformations from one to the other side of the interspecies boundary. The data available from the fossil record allow for the testing of character transformation hypotheses based on strong data from comparative and functional anatomy. Table 1.2 lists some of the character transformations noted to have occurred cranially at the *H. erectus/H. sapiens* transition. All of the characters listed in Table 1.2 are amenable to digitization on the original or cast specimens, scoring, and statistical differentiation.

Table 1.2 Character transformations associated with the emergence of *H. sapiens* from *H. erectus* (for many of the original sources see Wood, 1984).

A. SKULL VAULT

1) thinning of cranial bones (Rightmire, 1990; GE Kennedy; 1991)
2) expansion of occipital lobe (with overall increase in cranial capacity, appearance of "hemi-bun" (sensu Smith, 1984), and coincidence of inion and endinion (Stringer, 1984: Kennedy, 1991))
3) diminution of occipital (angular) torus laterally and movement inferiorly (Wood, 1984)
4) increased angle of occipital bone (100^{o} -> 160^{o} (Rightmire, 1984))
5) decreased length of upper scale versus lower scale of occipital bone (Stringer, 1984)
6) development of a true external occipital protuberance (Rightmire, 1990)
7) loss of sagittal keeling on frontal and parietals (Rightmire, 1990)
8) increased biparietal breadth (Rightmire, 1990; Stringer, 1984)
9) reduction of postorbital constriction (Rightmire, 1990)
10) great expansion of the frontal lobe, especially antero-laterally (Grimaud-Hervé, 1991)
11) lengthening of superior sagittal suture chord to be longer than squamosal suture chord on parietal (Bräuer, 1981; reverses in Neandertals)
12) increase of brain size to greater than 1000cc (Wood, 1984)

B. SKULL BASE

1) universal presence of sphenoid spine (Rightmire, 1990; Hublin, 1986)
2) medial tilt of sphenoid spine (Rightmire, 1990)
3) increasing coronal orientation of petrous bones (Weidenreich, 1941; Dean and Wood, 1982)
4) tympanic fusion with mastoid (Stringer, 1984)
5) elevation of widest skull point above (bimastoidal) cranial base (Santa Luca, 1980)
6) sphenoidal clivus plane changes from horizontal slope to inferior slope (Laitman *et al.*, 1978)
7) increased flexion of cranial base, especially evident on basisphenoid and basioccipital (Laitman *et al.*, 1978; Rightmire, 1990)

C. FACE

1) post supraorbital-torus (sot) sulcus diminution (Rightmire, 1990)
2) sot loses uniformity (e.g. bar-like in *H. erectus*); remains massive in most males, usually over mid-orbit, less so laterally and at inferiorly depressed glabella (Rightmire, 1990)
3) glabellar brow ridge segment (i.e. supraorbital tori between supraorbital notches, ie. both superciliary ridges joined at glabella) becomes prominent (see description in Chapter 2)
4) decrease in interorbital width (Hublin, 1986)
5) decreased overall prognathism, increased midface (Stringer, 1984)
6) face discontinues ontogenetic elongation, i.e. reaches maximum height (Maier and Nkini 1984),
7) changed distribution and possible increase in pneumatization of facial bones (personal observation)
8) development of articular tubercle on inferior zygoma (Picq, 1990, nd)

D. MANDIBLE (and related surfaces)

1) decreased robusticity (Stringer, 1984)
2) opening up of glenoid fossa (Stringer, 1984)
3) chin protrudes (Rightmire, 1990;)
4) development of mental trigone with mandibular tubercles (Rosas *et al.*, 1991)
4) reduction of planum alveolare as symphysis becomes vertical (Rosas, 1987)
5) less rounded precanine dentition, more in frontal plane, less in sagittal, not scoop shaped (personal observation)
6) no more crowding and medial tilting of M3 (personal observation)
7) mandibular fossae internal to cranium in norma posterioralis (Wood, 1984)

The research for this dissertation was designed to test the morphometric reality of five characters that I hypothesized to be distinctive of earliest *H. sapiens*. These characters involve specific conformations of: the glabellar (superciliary) brow ridge segment, the lateral brow ridge segment, the temporal line, the coronal suture, and the superior nuchal line (see Chapter 2 for more detail).

The Garden of Eden

The primary hypothesis presented here, that *H. sapiens* first evolved in the Middle Pleistocene (although we cannot rule out the late Early Pleistocene), will more likely find favor with OA proponents than workers supporting the MR hypothesis even though it does not coincide with the extreme version of either model. The OA model would be largely supported if much of the anatomically modern morphotype originated in sub-Saharan Africa and was disseminated outward by perhaps several population movements. OA advocates consistently refrain from positing total replacement of indigenous "archaic" populations within Europe and Asia by early moderns.

A recent trend by MR model proponents has been to minimize the phylogenetic importance of morphological change in hominin populations since the Early Pleistocene that arose due to migration, isolation (drift), mutation, extinction, and adaptation. In fact it is argued that *H. erectus* should be synonymized with *H. sapiens* (Thorne and Wolpoff, 1991; Wolpoff, 1992a and b). MR arguments have primarily countered models of a late Middle or early Late Pleistocene origin of anatomically modern features in African and/or Near Eastern populations by claiming that none of the specimens is actually over 40,000 BP (*contra* Shreeve, 1992). This is the MR *H. sapiens sapiens* chronological rubicon for synchronous appearance of these characters. Processes of gene flow are assumed to have

allowed all populations to nearly simultaneously cross the species threshold with all modern features eventually appearing in outlying populations via continuous gene flow. Recently, in a similar vein, MR advocates have claimed that those specimens over 40,000 are too robust to be considered anatomically modern (Wolpoff and Caspari, 1990; Smith, 1992b). Wolpoff (1989a, 1992a; Smith *et al.*, 1989a) suggests that new findings of older dates for the African and Middle Eastern "early modern" sites has spurred a regional competition for status as the "Garden of Eden."

Supposedly, further doubt is cast on the early origin of modern traits in sub-Saharan Africa by comparing the relevant specimens with modern Africans. MR advocates claim that if African populations were the source of anatomically modern features, then the people carrying these features out of Africa, and their earliest descendants, should have exhibited certain modern "regional" African features (Wolpoff, 1989a). A circular argument at best. These ideas have been countered in turn by OA-advocate arguments that the exodus of proto-Eurasians occurred before any individuals (in or outside of Africa) would be expected to exhibit features associated with the modern African morphotype (Stringer, 1989a and b; Habgood, 1989b). It is also possible that proto-Eurasians had been allopatric to, and somewhat segregated from, proto-Africans, at least the population that contained the eventual founders for living Africans, for some time before the exodus (Cann *et al.*,

1987; Stringer, 1989b).

To counter the identification of characters demarcating *H. erectus* from *H. sapiens,* or "archaic" from modern morphology, MR advocates propose gene flow models that would prevent hominin speciation throughout the Middle and Late Pleistocene. Mayr's "center and edge" model of trait distribution (Wolpoff, 1985; Thorne and Wolpoff, 1981) has been invoked as a mechanism for telegraphing all such features. Populations at the edge of the human range could, according to this model, develop regional features, and many of these should survive to the present in the peoples of those regions. The search for "regionally continuous" characters has delved back to Early and Middle Pleistocene *H. erectus* populations.

Efforts to study "race formation" (i.e., the traditional search for an ancient character to the features which separate the living races) continue despite lessons from population biology on the geographical distribution of "racial" traits and the evidence from morphometry (Howells, 1973, 1989; Wright and Kamminga, 1990) that osteological features seen in living geographical populations cannot be positively identified on specimens from the same region before 30-40 Ka (Bräuer, 1978; Habgood, 1989b). Thus, not unexpectedly, the earliest known specimens of "anatomically modern" humans putatively older than this date (e.g. at 90+ Ka in the Levant [the center?], East Africa, and South Africa) give no evidence of regional continuity in any of

the features they present.

Alternatively, some OA advocates point to these morphological discontinuities as marking what they envision as subsequent waves of peoples out of Africa throughout the Pleistocene, the vast majority of which are thought to have become extinct. An extreme view has been taken by Tattersall (1986, 1992a and b) and adopted by Klein (1989) that most of these populations constitute distinct species. For them the genetic support for the recent origin of anatomically modern humans in sub-Saharan Africa translates into evidence of a speciation event. Mitochondrial DNA data, showing strong clustering of most African populations versus a few African populations and all non-Africans, has been used to point to a common ancestry of all living peoples approximately 200,000 BP in Africa (Cann *et al.*, 1987; Stoneking *et al.*, 1992a; but see Maddison *et al.*, 1992), i.e., the "Eve" hypothesis. Other genetic markers studied show a similar clustering (Rouhani, 1989) but see Maddison *et al.* (1992) have rejected the overall African versus extra-African patterning seen by these and other earlier workers. The influence of the date given the human-chimp split on the timing of the origin of modern humans has received a lot of attention (Stoneking *et al.*, 1992b), with at least one model (Pesole *et al.*, 1992; Saccone *et al.*, 1992) supporting a 0.3-0.8 Myr date consistent with the Traditional Model presented in this thesis.

Of course proposals for a Late Middle or Late

Pleistocene speciation event assume total replacement of all "archaic" populations by the first waves of modern humans from Africa. Nowhere does this seem more possible than in Western Europe. It does appear however, that there is evidence for hybridization between Neandertals and moderns in central and eastern Europe (e.g. Hahnöfersand, Vindija, and Mladeč: Bräuer, 1981; Frayer, *et al.*, nd), suggesting that the eventual supplantation of Neandertals by moderns in Europe was an uneven process. Bräuer (1984), Hublin (1992), and Thoma (1973) also discuss the mixing of "archaic" and modern features in Africa and the Far East.

It is hoped that the "early archaic" *H. sapiens* characters proposed in the next chapter are sufficiently robust to provide tests of hybridization between earliest *H. sapiens* and *H. erectus*, especially in the Far East. The current fossil record suggests that of all regions, this appears to be the most likely place where late *H. erectus* and early *H. sapiens* might have been synchronic if not sympatric (Chen and Zhang, 1991).

II Materials and Space Curve Statistics

"Geometry is the only science that it hath pleased God hitherto to bestow on mankind."

Thomas Hobbes (1651)

"Let us inscribe in a system of Cartesian co-ordinates the outline of an organism, however complicated, or a part thereof: such as a fish, a crab, or a mammalian skull. ... Ear, eye and nostril, and all the other great landmarks of cranial anatomy, not only continue to exist but retain their relative order and position throughout our transformations. ... In these transformations of ours every point may change its place, every line its curvature, every area its magnitude; but on the other hand every point and every line continue to exist, and keeps its relative order and position throughout all distortions and transformations."

D'Arcy Thompson (1917)

"Biologists interested in the processes regulating shape over ontogeny or phylogeny need tools for coherent quantitative reports that do not waste data."

Fred L. Bookstein (1991)

Overview

This chapter discusses three components of this thesis. The first part, Section A, is a listing of the extant and fossil hominin material that was digitized. The second, Section B, explains how and why the five characters, all skeletal features, were chosen. The last, Section C, discusses the methodology used for data capture and analysis. It includes a summary of the data analysis method and a section on possible improvements. Many of the terms used below have been defined or discussed in the Preface, Introduction, and chapter 1.

In brief, the five characters surveyed were: 1) the glabellar or mid-segment of the brow, 2) the lateral brow,

3) the temporal line, 4) the coronal suture, and 5) the superior nuchal line. Three-dimensional (3D) line tracings representing these characters were collected from casts and specimens chosen to represent *Homo erectus*, the "transitional" group, and modern humans.

Every one of the five lines (seven if the two lines present bilaterally are treated separately) that could be completely traced from the transitional specimens (most of the specimens are fragmentary and don't preserve all 5 characters) was compared to two "average" homologous space curves, one representing the *H. erectus* sample and the other, a modern human (*H. sapiens sapiens*) sample. These comparisons require some initial processing of the curve data. First, homologous curvature maxima landmarks (Type II landmarks *sensu* Bookstein, 1991, see "Geometric Landmarks" below) are found along all the curves. Second, both average curves must be computed. Third, the "transitional" curve must be resampled to have the same number of points as both average curves. Then, the transitional curve can be compared directly, point-by-point, to both average curves.

To do this, the chord between the endpoints of the transitional curve is matched to the homologous chord of an average curve through the Procrustes (least squares) matrix approximation technique (Rohlf, 1990). The transitional specimen is then rotated around the shared endpoint-to-endpoint chord to a position with minimum residuals between

the homologous curvature maxima landmarks (as seen in Figure 2.1).

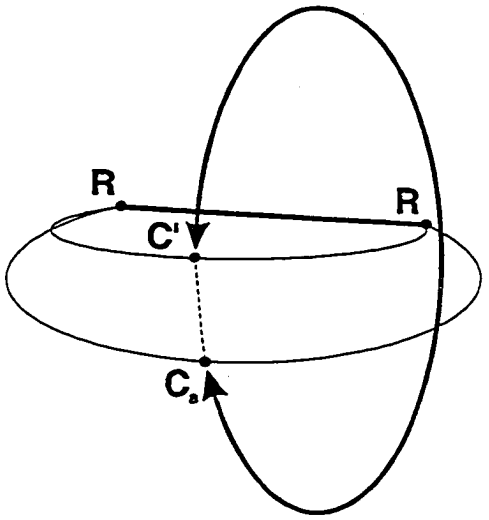

Figure 2.1 Curve Comparison: The two curves are registered at their endpoints (R). The transitional curve is then rotated about their shared chord (thick line) to minimize the (dashed-line) distance(s) between one or more of its curvature maxima (C') and the homologous point(s) on the average curve (C_a).

Next, the straight line distances between all points on both curves (point 1_a to 1', point 2_a to 2', etc.) are calculated. Then these point by point "residuals" are squared and summed, producing a sum of squares. This quantity is used to produce a chi square-like statistic. This "chi square" shows the likelihood that the transitional space curve could be attributed to the species arche-morphotype represented by each average space curve.

A. Study Specimens

The *H. erectus* Sample

Ashton (1950), Mayr (1951), Santa Luca (1980), Turner and Chamberlain (1989), and Rightmire (1990), amongst others, have all strongly advocated the specific unity of African and Asian *H. erectus* samples. Stringer (1984) has referred to this inclusive taxon as *H. erectus sensu lato* and a restricted taxon with just the far eastern members as *H. erectus sensu stricto*. I used the position of Rightmire and Santa Luca, *H. erectus sensu lato*, in the selection of specimens for the *H. erectus* sample in this study. Of the specimens allocated to *H. erectus*, there is, perhaps, most disagreement over the position of those from Solo. The level of intra-sample variability within the *H. erectus* samples surveyed should provide information on this question (Marcus *et al.*, in prep.).

Table 2.1 The *H. erectus* sample: Key: o = original, c = cast, (1) the glabellar or mid segment of the brow, (2) the lateral brow, (3) the temporal line, (4) the coronal suture, and (5) the superior nuchal line. (See geochronological chart: page 13, Chapter 1.)

Specimen	Char.s	Date	Dating Source(s)
KNM-ER 3733 (c)	1-5	1.78 Ma	Feibel *et al.*, 1989
KNM-ER 3883 (c)	1-5	1.57 Ma	Feibel *et al.*, 1989
OH 9 (c)	1-5	ca. 1.2 Ma	Hay, 1990
Sangiran 2 (o)	1-5	900 ± 200 Ka	Shizumu *et al.*, 1985
Sangiran 4 (o)	4, 5	900 ± 200 Ka	Shizumu *et al.*, 1985
Sangiran 17 (c)	1-5	900 ± 200 Ka	Shizumu *et al.*, 1985
Solo 4 (c)	1, 2	450 ± 350 Ka	Aziz *et al.*, 1991
Solo 5 (c)	1-5	450 ± 350 Ka	Aziz *et al.*, 1991
Solo 7 (c)	1-5	450 ± 350 Ka	Aziz *et al.*, 1991
Solo 8 (c)	4	450 ± 350 Ka	Aziz *et al.*, 1991
Solo 10 (c)	1,2,3,5	450 ± 350 Ka	Aziz *et al.*, 1991

Table 2.1 The *H. erectus* sample (continued).

Specimen	Char.s	Date	Dating Source(s)
Solo 11 (c)	1-5	450 ± 350 Ka	Aziz *et al.*, 1991
Solo 12 (c)	1-5	450 ± 350 Ka	Aziz *et al.*, 1991
Lantian (c)	1, 2	1.1 ± 125 Ka	An and Ho, 1989
Zhoukoudian 3 (c)	1-5	500 ± 250 Ka	Chen and Zhang, 1991
Zhoukoudian 10 (c)	1,2,3	500 ± 250 Ka	Chen and Zhang, 1991
Zhoukoudian 11 (c)	1,3,4,5	500 ± 250 Ka	Chen and Zhang, 1991
Zhoukoudian 12 (c)	1-5	500 ± 250 Ka	Chen and Zhang, 1991
Zhoukoudian 1966 (c)	1,2	200 ± 50 Ka	Chen and Zhang, 1991

Many of the original specimens were digitized on a research trip conducted between August 26 and December 6, 1991. Casts were studied in the Departments of Vertebrate Paleontology and Anthropology at the American Museum of Natural History.

The Transitional Sample

Fossils from the Middle Pleistocene (780-128 Ka) are the earliest to present the diagnostic characters (synapomorphies) of *H. sapiens*, and thus these are the earliest potentially "transitional" human forms. While no mandibular characters were surveyed for this project, perhaps the Mauer mandible and Ternifine mandibles and parietal are the earliest *H. sapiens* fossils now known, currently dated to about 0.6 Ma (Kraatz, 1991; Hublin, 1985, 1992), that may belong to these transitional populations. Only specimens from this earliest transitional group, what Bräuer (1984a, 1992) calls "early archaics", were chosen for this grouping. Thus, for example, in Europe no specimens with full-blown Neandertal "en bombe" vault shape (the earliest being perhaps Biache ca. 190 Ka or Fontéchevade ca.

120 Ka) were included. Larger brains overlain by more vertical, less constricted brows, and expanded parietals, among other advanced characters, argued against inclusion of "archaic" specimens from Africa (e.g., Djebel Irhoud I and II, Omo-Kibish I and II, Singa, Ngaloba, Florisbad, etc.) and Asia (e.g., Zuttiyeh, Narmada, and Maba), because like Neandertals they would come under Bräuer's (1984a, 1992) "late archaic" rubric.

The relevant morphological characters present on "early archaic" *H. sapiens* (*sensu* Bräuer) from the Middle Pleistocene were digitized. The entire "transitional" sample, the characters digitized, and most recent dating of these specimens is listed in Table 2.2 below.

Table 2.2 Transitional Specimens: Key: o = original, c = cast, (1) the glabellar or mid segment of the brow, (2) the lateral brow, (3) the temporal line, (4) the coronal suture, and (5) the superior nuchal line. (See geochronological chart: page 13, Chapter 1.)

Specimen	Char.s	Date	Dating Source(s)
Bodo (c)	1,2	350 ± 150 Ka	White, 1986
Ndutu (c)	5	300 ± 100 Ka	Clarke, 1990; Hay, 1990
Salé (o)	3,4,5	300 ± 100 Ka	Hublin, 1985
Broken Hill (o)	1-5	400 ± 200 Ka	Delson, pers. comm. (estimate)
Eliye Springs (c)	4,5	200 ± 100 Ka	Bräuer and Leakey, 1986
Saldanha (c)	1, 2	550 ± 150 Ka	Klein and Cruz-Uribe, 1991
Petralona (o)	1-5	350 ± 150 Ka	Latham and Schwarcz, 1992
Arago (c)	1-3	350 ± 50 Ka	Yokoyama *et al.*, 1991
Swanscombe (o)	5	325 ± 50 Ka	Bowen, *et al.*, 1989
Steinheim (o)	1-5	300 ± 50 Ka	Adam, 1985; cf. Bowen *et al.*, 1989
Reilingen (o)	4,5	200 ± 50 Ka	Dean and Zeigler, in prep.

Many of the original specimens were digitized on the research trip cited above, and casts were obtained from the same sources, as mentioned above.

The Modern Human Sample

A sample of 20 Caucasian specimens aged 18-55 from the CMNH, evenly split between males and females, were studied. An effort was made to use specimens that preserved nearly all of their teeth and that were in generally good health at the time of death. The cause of death is known not to have been a wasting disease. All of the skulls were listed as "white." It is probably safe to assume, based on known demographics, that most of this population is Central-Eastern European (Hungarian/Polish ancestry). The sample is largely brachycephalic.

Table 2.3 The Modern Human Sample: Key: AMNH = American Museum of Natural History, Department of Anthropology; CMNH = Cleveland Museum of Natural History, Laboratory of Physical Anthropology.

Museum	Cat. No.	Age	Sex	Race
CMNH	514	30	F	Caucasian
CMNH	560	23	M	Caucasian
CMNH	630	22	M	Caucasian
CMNH	667	24	M	Caucasian
CMNH	681	28	F	Caucasian
CMNH	856	23	M	Caucasian
CMNH	881	38	F	Caucasian
CMNH	883	39	F	Caucasian
CMNH	919	42	M	Caucasian
CMNH	920	42	M	Caucasian
CMNH	939	50	M	Caucasian
CMNH	962	44	M	Caucasian
CMNH	1157	25	F	Caucasian
CMNH	1253	31	F	Caucasian
CMNH	1273	34	F	Caucasian
CMNH	1759	40	F	Caucasian
CMNH	2048	52	F	Caucasian
CMNH	2401	22	M	Caucasian
CMNH	2584	23	M	Caucasian
CMNH	2860	46	F	Caucasian

Table 2.3 The Modern Human Sample (continued).

Museum	Cat. No.	Age	Sex	Race
AMNH	1439	e 40	M	S. Chinese
AMNH	1440	e 40	F	S. Chinese
AMNH	2382	e 25	M	W. African
AMNH	2386	e 25	F	W. African
AMNH	8173	e 25	M	Australian
AMNH	8175	e 25	F	Australian

Additionally, one male and one female skull of each of 3 groups (Australian Aborigine, southern Chinese, and West African Black) were studied/digitized from the von Luschan collection of the AMNH. The health status and age of these specimens were surmised by traditional osteological criteria. Data from the non-Caucasian AMNH specimens was essential to characterizing the range of variation seen in modern humans for the five characters under study (see Chapter III). These data also demonstrated the utility of using any of the Caucasian average ridge curves as a measurement of affinity with *H. sapiens*. A character was considered suspicious if some of the AMNH specimens showed stronger affinities with the *H. erectus* and others with the *H. sapiens* mean (i.e., overlapping affinities).

B. The Characters

Five space curves were digitized with a hand-held electromagnetic digitizer. Landmarks, often traditional cephalometric landmarks (as opposed to the curvature maxima landmarks discussed later in this chapter), were identified

at the beginning and the end of each curve, later to be used as registration points. Each curve was traced 3 times (only the first was used in this study). The digitizer-PC interface software displayed a good overlap of these three tracings from multiple views. The use of multiple tracings and multiple views proved to be very useful for error correction and confirmed that the same curve could be found on repeated attempts, as did multiple tracings of several of the modern human specimens performed at greater than one month intervals. The multiple tracings (in one session) also confirmed that a slip of the hand had not occurred during the procedure. Curvature maxima landmarks are numbered (see below) for each curve in the order in which they were traced (e.g., the registration point closest to landmark 1 was the starting point).

The five curves digitized were: 1) the glabellar or mid-segment of the brow, 2) the lateral brow, 3) the temporal line, 4) the coronal suture, and 5) the superior nuchal line. All five were found on every modern human specimen and where available on "transitional" and *H. erectus* specimens. The endpoints of these curves were used as registration points (R in Figures). Curvature maxima (C in Figures), or geometric landmarks, were located along each line tracing.

The character and specimen naming scheme is used hereafter in the text. The five characters traced were chosen because they are clearly identifiable and presumably homologous on all the specimens surveyed. All are prominent

bony tori, muscle scar edges, the borders of foramina, or suture boundaries and are referred to here as "ridge curves" (see Preface and Section C). Since both Character 1 and Character 2 depend on an understanding of the supraorbital torus, a discussion of the significance of the hominin brow follows.

The Brow Ridge

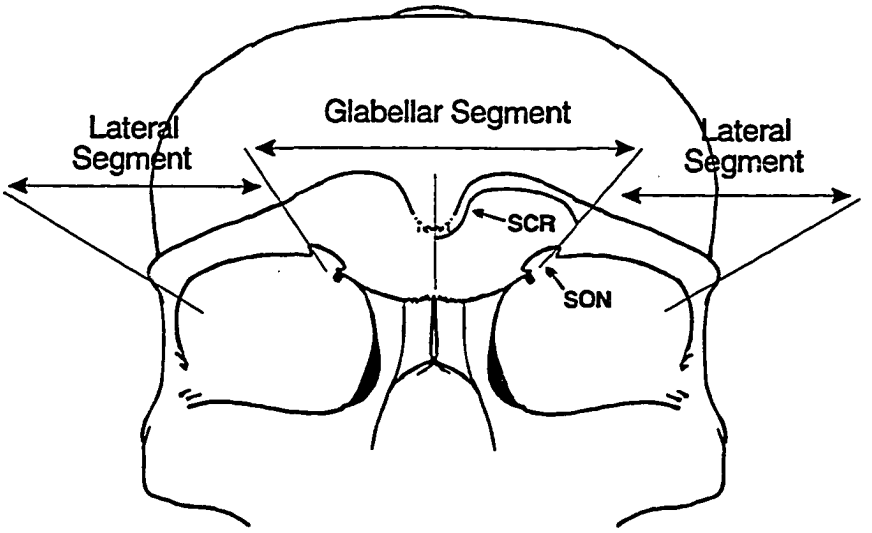

Figure 2.2 Modern Supraorbital Torus: The glabellar segment (both superciliary ridges [SCR] joined at glabella) is separated from the lateral segment (the supraorbital torus proper) of the brow by the supraorbital notch (SON [modified from Russell, 1983]).

Numerous qualitative descriptions and morphometric breakdowns of the primate supraorbital region have been developed to bolster biomechanical and phylogenetic models (e.g., Endo, 1966; Smith and Ranyard, 1980; Russell 1983) regarding the brow. The biomechanical significance attached to the brow has frequently been used to imply the attainment of a new adaptive level, perhaps the result or cause of a speciation event. However, recent *in vivo* and morphological

studies of the catarrhine brow suggest that the morphological basis for bony build-up at the brow is more subtle than the bony struts and beams that crowd the literature. It would now seem that most theories of supraorbital ontogenesis and phylogenesis offered over the last century are no longer tenable.

Strain gauge tests done *in vivo* by Picq and Hylander (1989; Hylander *et al.*, 1991a and b) on the macaque and anubis baboon brow suggest that there is no pronounced biomechanical role for the middle segment (between, i.e. medial to, both supraorbital notches) of the brow in primates. Their studies measured strain at glabella, at the midpoint on the dorsal surface of the supraorbital torus just superior to glabella, and approximately at the midpoint on the dorsal supraorbital torus, just lateral to the supraorbital notch. Their findings include: 1) no increase in brow strain due to incision, 2) no support for the classical model that the balancing side brow will be compressed while the working side is under tensile stress, and 3) a tendency in the catarrhine supraorbital region for there to be a greater build-up of bone than is necessary for resistance to normal masticatory-related strain.

There is still a question as to whether the lateral brow segment (supratoral buildup rarely extends inferior to the frontozygomatic suture in catarrhines) is put under strain during postcanine mastication by the anterior temporalis muscle. This region sits atop the superolateral corner of

the orbit and if there is great post-orbital constriction it would appear that this area would come under strain during constriction of the anterior temporalis muscle. This would be expected in macaques and other primates with high degrees of post-orbital constriction, but to date no strain gauge test results have been published for this area. Postorbital constriction lessens significantly in the transition from *H. erectus* to *H. sapiens*.

Greaves (1985) has suggested a general relationship between the post-orbital bar and the tooth row, whereas Dean (1986) was more specific in suggesting an angular relationship between the masticatory muscles and the dental wear facets they bring together. In both cases force generated at the anterior temporalis muscle insertion (on the posterior surface of the catarrhine post-orbital bar, sometimes overriding the ophryonic groove posterior to the posterior surface of the supraorbital ridge) would presumably have a role in shaping the superolateral and lateral portion of the orbits and supraorbital tori. It would be useful to know if the superolateral corner of the orbit comes under more strain in species where the anterior temporal line (the attachment of the temporal fascia) approaches the lateral segment of the supraorbital torus.

Hylander *et al.*'s (1991a and b; Picq and Hylander, 1989) results contradict various aspects of Endo's (1966, 1970; Endo and Adachi 1988) highly publicized dry skull model of mastication and study results. Endo characterized the brow

as a single rigid beam resisting vertically oriented strain caused by the down-pulling masticatory muscles and dental compression (especially from powerful incision) moving upward through the bony plates covering the paranasal sinuses. Given Endo's special emphasis on humans apart from non-human primates, many theories of supraorbital development began to ignore the morphology seen in other primates. Wolpoff (1980b) describes the development of large brows in *Homo* as due to the use of the incisors as a "third hand". This view is also referred to as the "teeth as tools" hypothesis. Rak (1983) accepted Endo's overall schema but questioned it (1986) when confronted with the horizontal extension of "classic" neandertal nasal bones. These nasal bones lie in a horizontal plane with no structure superior to them. This questioned theories suggesting that high anterior occlusal loads were transferred superiorly to the supraorbital torus. Rak's biostructural "infraorbital plate" model of the Neandertal midface was then questioned by Trinkaus (1987) and Demes (1987). Demes (1987) diagrammed the midface schematically as a tube that undergoes torsion during powerful unilateral chewing. Preuschoft *et al.* (1986), Greaves (1988), and Rosenberger (1986) idealized strain distribution in the primate face via other geometrical structures.

Apparently, the brow ridge, if it can be referred to as a single unit, is not an epigenetic result of masticatory or any other behaviors. The question still remains as to what

determines the observed pattern of variation. Not all primates exhibit brow ridges. They are primarily confined to the longer faced cercopithecids and hominoids. Building from Moss' functional matrix hypothesis (Moss and Young, 1960), Shea (1985, 1988) and Ravosa (1988, 1991a and b) have proposed a "spatial model" for the presence or absence of primate brow ridges. Shea and Ravosa contend that across primates there is a strong correlation between klinorhynchy (i.e., tilting of the face inferiorly in relation to the vault), an anterior positioning of the orbits, and strong supraorbital tori development.

The general morphology of the brow in *H. erectus* has been described by many students as a "continuous bar" (Weidenreich, 1943; Le Gros Clark, 1978; Macintosh and Larnach, 1972; Jacob, 1976; Wood, 1984). This is true for the segments of the brow found over the orbits, but in virtually every case where it is preserved the superciliary ridges grade inferiorly to glabella. Glabella itself is usually somewhat posteroinferiorly depressed in *H. erectus*.

The brow is noticeably different from this condition in earliest *H. sapiens*. It is broken up into the medial glabellar segment (i.e., both superciliary ridges joined at glabella) and the lateral brow ridge (supraorbital torus proper) at the supraorbital notch/depression (SON in Figure 2.2). As viewed from the superior aspect (see Figure 2.3), the superciliary ridges of the glabellar segment are in the frontal plane whereas the entire lateral segment has rotated

posteriorly. Thus, the angle between the lateral segment and the frontal plane (see Figure 2.3) in *H. sapiens* is greater than that seen in *H. erectus*.

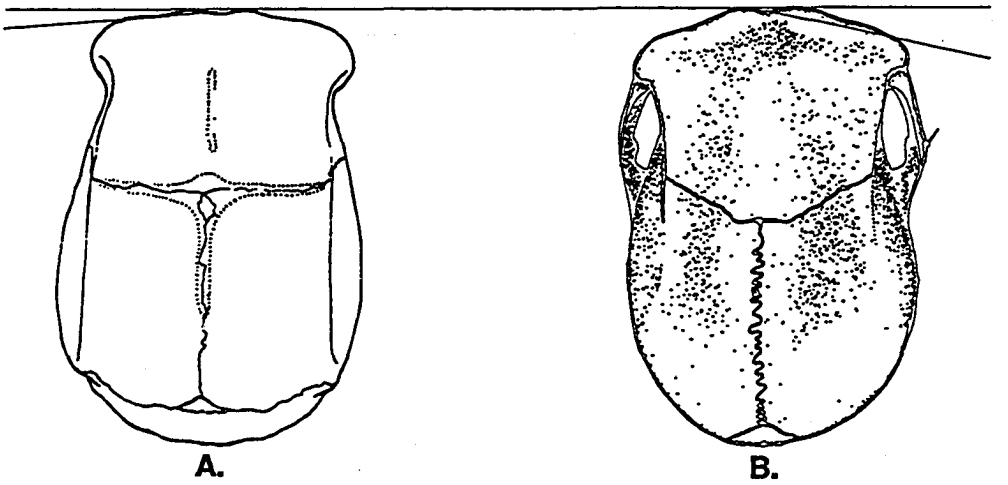

Figure 2.3 Superior View of skull: A: *H. erectus* (Solo 11, modified from Santa Luca [1980]) and B: *H. sapiens* (aboriginal Australian from Brown [1989]). The angle is drawn between a line representing the frontal plane and a line connecting glabella and the superolateral corner of the brow ridge (i.e., landmark C2.2 below).

From a frontal view the superciliary ridges, beginning above the supraorbital notch, in most cases rise well above the highest point of the lateral segment. The high point at the lateral end of each superciliary ridge is also the anterior terminus of a bulging "frontal boss" seen on the frontal squama. This rounding appears to be a superior expansion due to a convex projection of the orbital cone superiorly. The convex frontal bone portion of the orbital roof is under the frontal lobes and this projection combined with relatively large frontal lobes (compared to *H. erectus*), and their adjacency to the anterior cranial base,

appear to produce this effect, "orbital bosses" on the frontal squama. It is also possible that this effect is due solely to a changed ossification pattern of the two metopic halves of the frontal bone. Since these structures seem to closely follow the contour of the roof of each orbital cone, I would prefer to refer to them as "frontal bosses" rather than frontal tubers. The frontal bosses have a great deal to do with the loss of the ophryonic groove in "archaic" *H. sapiens*. Character number one is a test as to how diagnostic the glabellar segment is of *H. sapiens*. From visual observations it appears to be the most diagnostic character studied in this thesis project.

In modern humans the lateral brow segment (the 2/3's of the brow beginning just above and running laterally from the supraorbital notch) may not protrude anteriorly between the frontal squama superiorly and the orbital rim inferiorly at all. The brow is often less apparent in the most brachycephalic Asians and Central/Northern Europeans (Enlow, 1990; Peterson, 1987). Therefore, while the brow components discussed here are less pronounced in some mesocephalic and all brachycephalic populations, they are nevertheless present and discernible. Brachycephaly is not apparent in the record of early *H. sapiens*, therefore all the major components of the brow are strongly differentiated.

Along with the advance of the glabellar segment in earliest *H. sapiens*, the frontal poles have come to overlie the orbits on an enlarged anterior cranial base. The

increased size of the frontal poles and their increased association with the anterior cranial base (Grimaud-Hervé, 1991) combined to lessen post-orbital constriction laterally and there is a loss of the ophryonic (post-supraorbital torus) groove superiorly in earliest *H. sapiens*. It is interesting to note the position of the frontal sinuses and the trend for their medial edges toward the midline (often only a thin septum separates them in modern humans) as the frontal poles move over the orbits and take position over the ethmoid plates.

The role of the sinuses in the evolution of the human bony face is discussed in Chapter 3.

Character 1: The Glabellar Segment

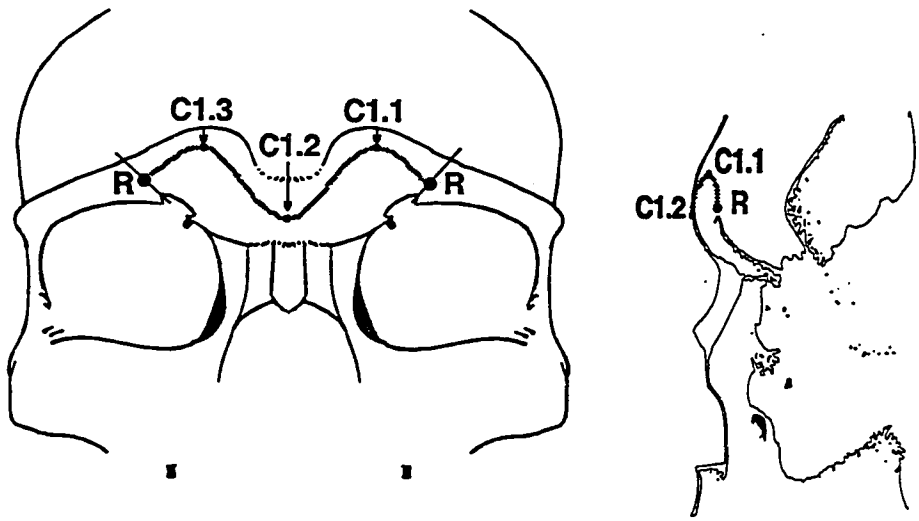

Figure 2.4a The glabellar segment in *H. sapiens sapiens.* (R = registration point, C = curvature maximum landmark, C1.2 = glabella). Figures are not actual size but approximately to scale. Both views are aboriginal Australian. (Frontal view at right modified from Russell [1983]; lateral view at left modified from Brown [1989]).

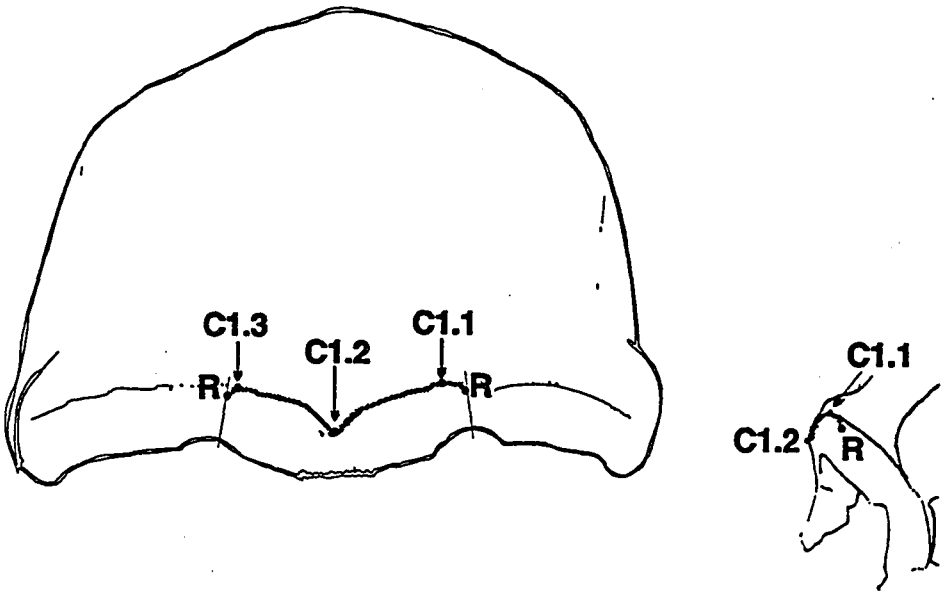

Figure 2.4b: The mid-glabellar segment in *H. erectus*. (Frontal view at right is Solo 11, lateral view at left is Zhoukoudian 12, both modified from Santa Luca [1980].)

The glabellar segment is the medial portion of the brow found between the supraorbital notches. The paired bossed arches on either side of glabella (the medial one third of the brow, medial to the supraorbital notch) in *H. sapiens*, are called superciliary ridges. Their greatest projection, just above and lateral to glabella, causes a furrowing in the area of glabella (especially in males where they tend to be more pronounced) when the extra-ocular muscles (orbicularis oculi, procerus, corrugator supercilii) contract the skin inferiorly.

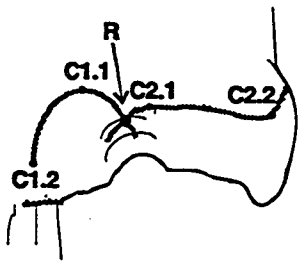

Figure 2.5 Intersection of glabellar and lateral brow ridge segments: R is shared registration point. See text for discussion of landmarks.

Thus, the glabellar segment consists of both superciliary ridges joined at glabella. The intersection of the glabellar segment with the lateral segment (discussed below) occurs in the supraorbital depression was taken as the endpoint for both curves (i.e., the lateral registration points of the glabellar segment and the medial registration points of the lateral brow segment are at the point of overlap between these two ridge curves as shown in Figure 2.5). In modern humans, just lateral to or coincident with this area is the supraorbital foramen or notch (the structure is variable). In fact, Santa Luca (1980), labeled it the supraorbital "fissure" in his study of the Solo material. While the associated nerve and artery were undoubtedly present, the supraorbital foramen/notch complex is not always apparent on fossil *H. erectus* or "archaic" *H. sapiens* crania (i.e. the three segments of the brow are truly continuous).

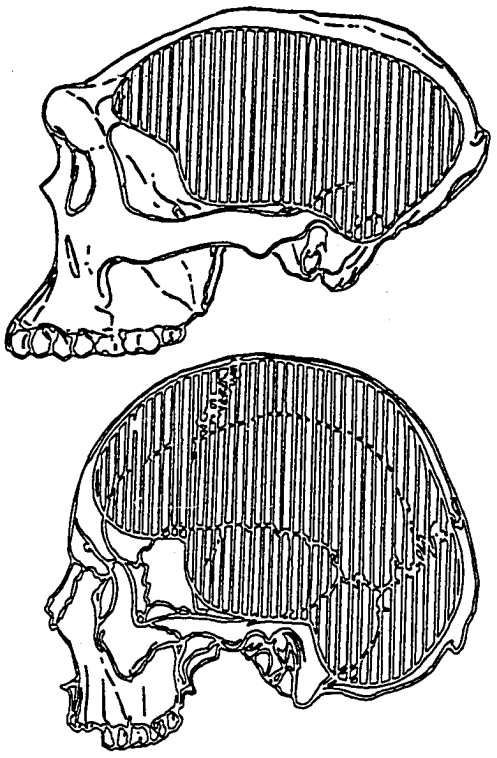

Figure 2.6 Spatial Relationship of Brain and Orbit: *H. erectus* (above) has frontal lobes that only slightly override the orbit in a highly restricted anterior cranial base. Anterior cranial base forms much of the orbital roof in *H. sapiens*. (Reconstruction of Sangiran 4 [above]. Modern Austrian male [below]. Both adapted from Weidenreich [1943].)

The separation between these two portions of the brow becomes more obvious in *H. sapiens* as, seen superiorly, the glabellar segment moves anteriorly and the lateral segment rotates posteriorly (see figure 2.3). The advance of the glabellar segment may be due to a change in the relationship of the frontal lobes and the orbital cavities and the remainder of the anterior cranial base. In *H. erectus* the orbital cavities are almost entirely anterior to the frontal poles of the brain. Only a small amount of the frontal cortex sits over the posterolateral portion of the orbital

roof in the anterior cranial fossa. Endosteal dural markings on *H. erectus* fossils suggest that the frontal lobes do not extend over the central ethmoid plates (just posterior to the glabellar segment). Irrespective of the external frontal squama morphology, the frontal lobes come to overlie and surround the olfactory bulbs entirely in both "archaic" and anatomically modern *H. sapiens*. Weidenreich (1951) noted that because of this architectural difference the Chinese and Indonesian *H. erectus* (including Solo) show lack or underdevelopment of the crista galli and frontal crest (superior sagittal sinus attachment). The large central gap between the frontal lobes must have been split by a dural-enclosed stalk of the olfactory bulbs extending anteroinferiorly to the cribriform plate. Weidenreich noted that this beaked frontal/ophthalmic tract and diminutive crista galli/frontal crest morphology was associated with a depressed cribriform plate in all Chinese and Indonesian *H. erectus*, including Solo: "The absence of these features is characteristic of the anthropoids. In the three great apes the lamina cribrosa is at the bottom of a deep oval pit sunk in the floor of the anterior cerebral fossa" (Weidenreich, 1951:251; *cf.* Grimaud-Hervé, 1991). In earliest "archaic" *H. sapiens* the frontal lobes appear rounded and globular. A strong crista galli and frontal crests are apparent (e.g., on Bodo) and the frontal lobes sit in nearly the same plane as the cribriform plate.

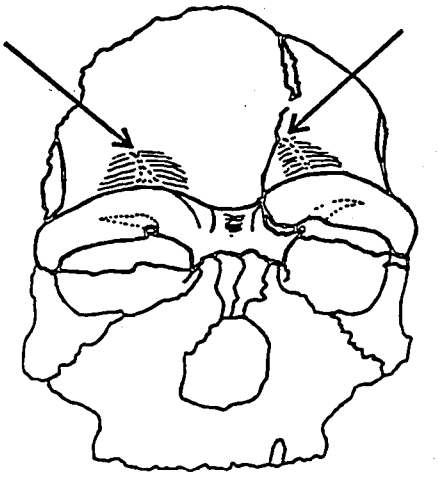

Figure 2.7 Orbital Bosses in *H. sapiens*: A rounded elevation on the frontal squama extends from the frontal bosses (marked by arrows) to the curvature maximum overlying supraorbital notches. This elevation mirrors the convexity seen on the anterior cranial base/orbital roof (Seen here on the Arago craniofacial fragment. modified from Spitery [1984]).

Along with the movement of the inferior plane of the frontal poles parallel to the cribriform plate, they move anteriorly becoming appressed on the endosteal surface of the pneumatized supraorbital torus. Because of the position of the frontal lobes in earliest *H. sapiens* the anterior frontal squama is thrust superiorly. This virtually eliminates the post-toral sulcus, a characteristic feature of *H. erectus* (also referred to as the ophryonic groove). The orbital bosses are also found to be more convex superiorly in *H. sapiens*. This superior convexity also appears on the portion of frontal bone over orbits, i.e., the roof of the orbital cone, and is transferred to the brain. The frontal bosses, like the parietal tubers, are also ossification centers in the two fetal/infant metopic bones. Thus the orbital boss convexity on the frontal squama

extends posterior from the intersection of the glabellar segment and the lateral brow segment (approximating the supraorbital notch) to the frontal boss points in both "archaic" and anatomically modern humans. In the most brachycephalic modern humans there is vertical flattening seen between these bosses along with a similar vertical flattening on the upper scale of the (posterior-most in Frankfurt orientation) occipital. This appearance of frontal bossing appears related to the glabellar segment morphology but is itself posterior to the ridge curve traced in this study.

The outer surface of the glabellar segment itself (on the ridge) undergoes a massive build-up of bone across the transition. The ethmoidally derived frontal sinus (Cave and Haines, 1940; Cave, 1961; Ward and Brown, 1986), often of massive proportions, is present directly behind the superciliary arches in "archaic" *H. sapiens*, usually extending laterally well past the superciliary arches, in most cases narrowing as it moves into the lateral segment. It is also present albeit relatively smaller, in both *H. erectus* and anatomically modern *H. sapiens*. The configuration of the sinus in modern humans is like that of "archaic" *H. sapiens*, and although not tested, is assumed to be absolutely smaller (vs. relatively) in volume. Internally to the *H. erectus* brow there is ample room for a frontal sinus cavity without producing any forward projection of the superciliary ridges as seen in *H. sapiens*. Conversely,

Weidenreich (1943) noted that large superciliary ridges could be found in Australian aboriginals with little or no frontal sinus. In general, the larger the frontal sinus, the more anteriorly placed the glabellar segment will be as compared to the lateral segment. The configuration of Sangiran 17 in this area is unusual for both *H. erectus* and *H. sapiens*.

Character 2: The Lateral Brow

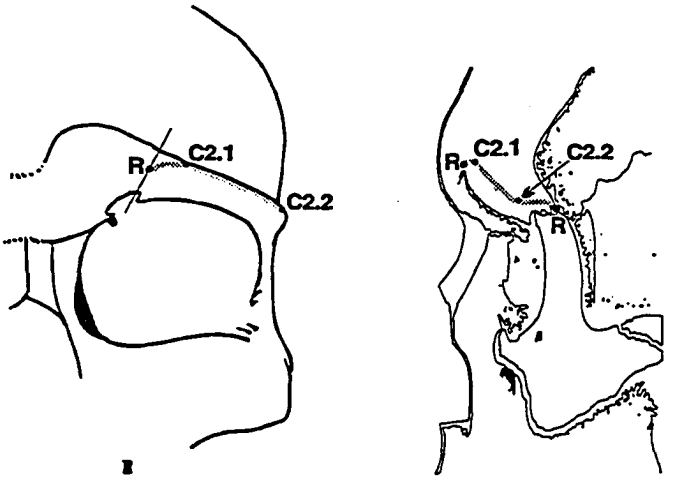

Figure 2.8a The Modern Lateral Brow Segment: Frontal view of the left lateral segment (above left). Left lateral view of same (above right; modified from Russell [1983]).

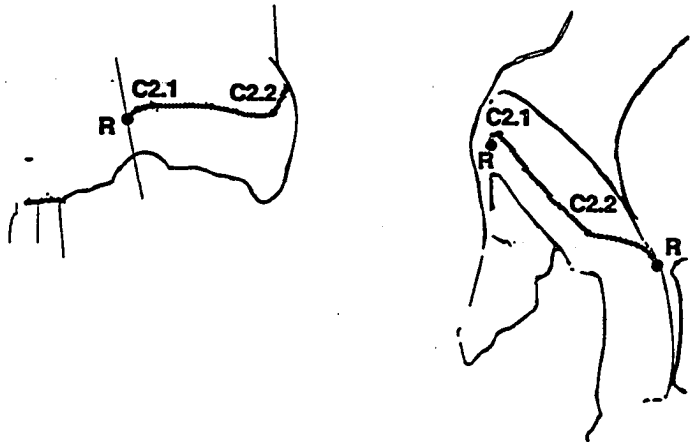

Figure 2.8b The left lateral segment in *H. erectus:* Frontal view of left supraorbital torus of Solo 11 (above left) and left lateral view of Zhoukoudian 12 orbital area (above right) both adapted from Santa Luca (1980).

The lateral brow segment as defined here begins at the intersection of the glabellar and lateral ridge curves (usually within the supraorbital notch) and ends at the posterolateral-most limit of the frontozygomatic suture. Just as the depression of the supraorbital notch served as an ending point for the glabellar segment, it was the starting point for this character (see Figure 2.5). The two curves share endpoints in the well of this notch. The lateral segment has been described most often as a continuous bar in *H. erectus,* but this is not always the case, especially on the earliest African specimens, KNM-ER 3733 and 3883. My preliminary idea was that this might be an adult male feature in earliest *H. erectus,* but published pictures (Day, 1986) of the sub-adult male, KNM-WT 15000, show that the lateral segment drops off in a fashion similar to 3733 and 3883. In modern humans this area varies from no thickening of bone, to a slight crescentic ridging over the

mid-lateral segment (similar in overall shape to the superciliary ridge), to a corner piece that makes nearly a 90 degree turn from the frontal plane to the sagittal at landmark C2.2. When this area has a dorsally flattened roof, this robust anterolateral corner of the frontal squama is referred to as the supraorbital trigone. While rare in modern humans, a highly developed lateral brow segment and even a supraorbital trigone can be found in living aboriginal Australians, southwest Pacific islanders, and other dolichocephalic modern humans.

Landmark C2.2 is also very strongly present in *H. erectus* and early *H. sapiens*. This landmark, defining the superolateral corner of the lateral brow segment, is often just anterior to the anterior-most point of origin of the anterior temporalis muscle. When strongly present the lateral segment of the brow will give the anterior temporalis muscle a strong anteroposterior component. In "archaic" and modern humans there is a tendency for the lateral brow and the lateral rim of the orbit to rotate posteriorly (e.g., Figure 2.3 in superior view and when viewing the skull in *norma lateralis* more of the medial wall of the orbit can be seen). Taken together in the superior view, the lateral-most portions of both lateral brow segments will resemble "handlebars" on each side of the skull. At present the biomechanical forces acting on this complex region are not clear (Picq, pers. comm.).

In less robust modern females there will be very little thickening of bone here and the entire orbital rim may be in the frontal plane (i.e., the lateral rim is not posteriorly positioned versus the medial rim). Also in such cases, small or gracile people with weak brows, the frontal sinus may not extend very far laterally into the lateral brow segment. Opposingly, the lateral brow segment in earliest *H. sapiens* is fully pneumatized in virtually all known cases.

Character 3: The Temporal Line

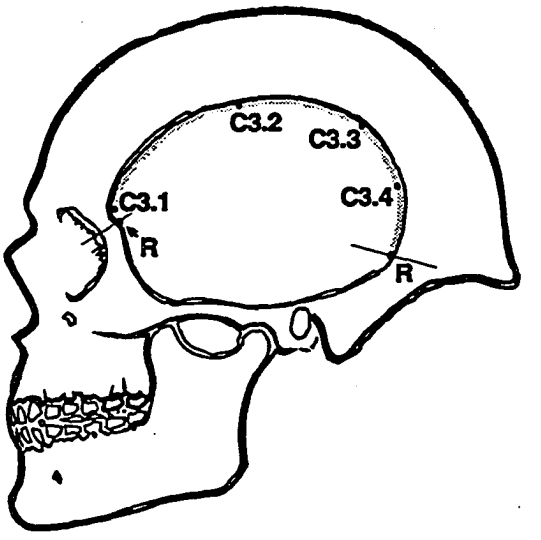

Figure 2.9a: Temporal line in *H. sapiens* (modified from Le Gros Clark [1978]).

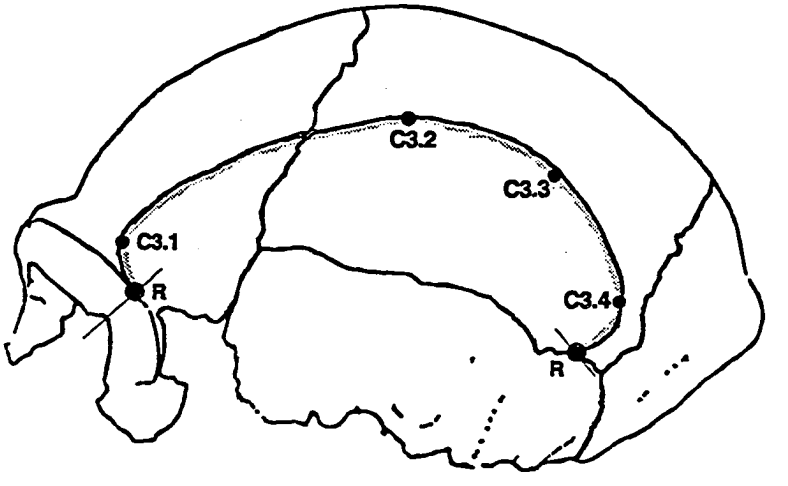

Figure 2.9b: Lateral view of the temporal line in *H. erectus* (Zhoukoudian 12 after Santa Luca [1980]).

Tracing commenced at the point on the superior temporal line closest to the frontozygomatic suture and continued posteriorly to the intersection with the squamous suture. Although the separation between the muscle and fascial boundaries were not always clear along the whole excursion

of the temporal line (often coincident), in all cases the superior-most temporal line was used. The build-up of bone posterior to the posterior portion of this line in Chinese and Indonesian *H. erectus* was referred to as the "angular torus" by Weidenreich (1943), but has since been identified on African specimens as well (Rightmire, 1990; Bräuer and Mbua, 1992).

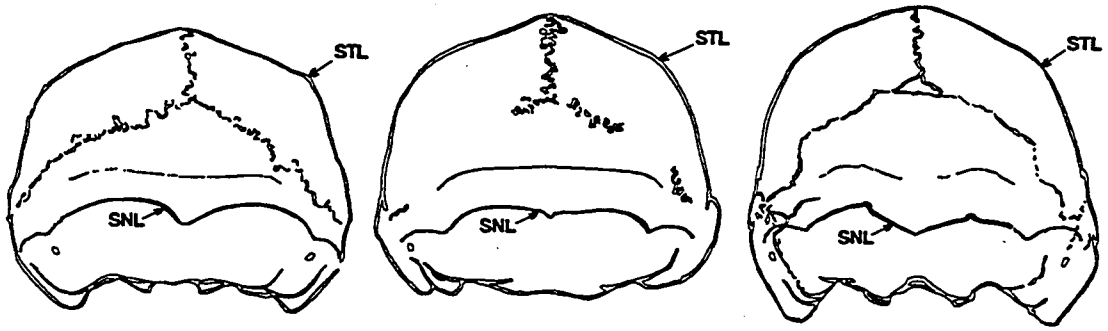

Figure 2.10 Temporal Line Gabling and Nuchal Tori in Asian *H. erectus* skulls: From left to right Sangiran 4, Zhoukoudian 12, and Solo 11. STL = Superior Temporal Line, SNL = Superior Nuchal Line (modified from Weidenreich [1951]). Asian *H. erectus* skulls typically display sharp angulation at temporal line. This line divides the flattened lateral walls and the dorsal surface of the vault.

The superior temporal line is the attachment site for the temporal fascia. Acting as a capsule it concentrates a great deal of the force of the temporalis muscle at its margin. While there is no ridging of bone here in most *H. erectus* (see Sangiran 51 for a notable exception; Sémah *et al.*, 1990) this line does correspond to the border, something like a gable, between the dorsal and sagittal surfaces of the skull. While the side of the vault may tilt somewhat medially in its gentle slope from inferior to superior, the entire lateral surface of the vault is in a

parasagittal aspect whereas all of the vault medial to the temporal lines is in a dorsal orientation. Thus landmarks 3.2 and 3.3 correspond to curvature maxima in a coronal cross-section plane (as seen in character 4, the coronal suture). This gabling is strongest in the Sangiran specimens, but is also clearly present in other Asian *H. erectus* (Lantian, Zhoukoudian, Hexian, and Solo) and OH 9. Such strong gabling is not present in earlier African *H. erectus* (nor in the Ternifine parietal) or early *H. sapiens* from Africa or Europe. The height of the temporal line (above the Frankfurt plane) gives the posterior view whatever steepness is seen to the gabling. The location of landmark 3.2 in both species is correlated strongly with this height.

Posteriorly along the temporal line landmark 3.3 is intimately related to the position of euryon, or the parietal boss in *H. sapiens*. Expansion of the parietal lobes caused the emergence of this bossing. This is what gives modern skulls their pentagonal appearance in posterior view. While the widest portion of the posterior vault in *H. erectus* is found at the mastoid (the primitive condition for Hominidae), euryon is somewhat protuberant in *H. erectus*. This point is only the midpoint along a coronal arc in earlier hominin species. The widest point is on the temporal squama in early *H. sapiens* and the parietal boss in modern *H. sapiens*.

It has long been noted that the posterior edge of the temporal line in the Indonesian and Chinese *H. erectus* evidences a ridging of bone Weidenreich (1940, 1943) named the "torus angularis". The angular torus has been suggested as a synapomorphy of an Asian lineage apart from the main stem of *H. sapiens*. In this view the African, or perhaps European, Early Pleistocene forebears of *H. sapiens* have been referred to as *H. ergaster* (Groves and Mazák, 1975; Wood, 1992; see Chapter 4) or *H. leakeyi* (Clarke, 1990). While the angular torus does appear to have a high frequency in the Far East and Southeast Asia. Rightmire (1990) and Hublin and Braun (1992) have suggested that even in combination with other far-eastern features the limits of variation that can be reasonably expected in a species with more than a million year tenure are not exceeded.

Because of the strong relief of the posterior temporalis muscle and its fascial insertion in *H. erectus* landmarks 3.3 and 3.4 has a louder signal (higher curvature) than in *H. sapiens*. There is not much relief on either side of landmark 3.2 in *H. erectus*. The increasing height of the temporal squama (the entire skull becomes shorter anteroposteriorly and higher superoinferiorly) in modern humans gives landmark 3.2 a louder signal in modern humans. However, many moderns had an extremely rounded posterior edge to this line. On these individuals landmark 3.4 was prominent.

There is one interesting difference in this region that was not measured by this study. There seems to be an

inferior-ward depression in the temporal line at or just posterior to the coronal suture in "archaic" and modern *H. sapiens* (e.g. Broken Hill, Petralona). The anterior edge of this depression seems to mark the posterior edge of the anterior temporalis muscle. Thus this depression may mark the transition between the anterior and posterior temporalis muscles.

Character 4: The Coronal Suture

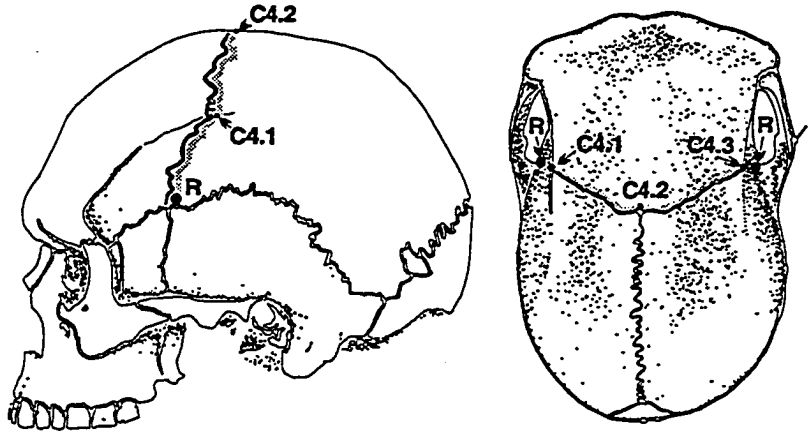

Figures 2.11a The Modern Coronal Suture: Running from pterion to pterion, curvature maxima were found roughly at stephanion and bregma along the modern human coronal suture (aboriginal Australian skull, modified from Brown [1989]).

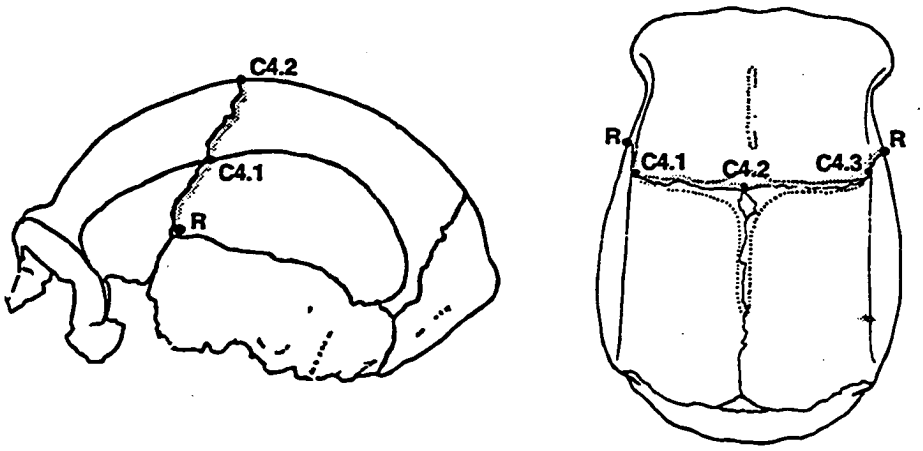

Figure 2.11b The Coronal Suture in *H. erectus*: as seen on a left lateral view of Zhoukoudian 12 and a superior view of Solo 11 (modified from Santa Luca [1980]).

The coronal suture was traced from left anterior pterion to right anterior pterion (anterior pterion would be the anterior part of the H crossbar formed by the sphenoparietofrontal suture). The gabling of the vault provided by the temporal lines was most evident in *H. erectus* but the effects of this line influence the overall shape in even the most brachycephalic modern humans. The intersection of the temporal line and the coronal suture, stephanion, proved to be at (or very close to) landmarks 4.1 and 4.3. Bregma was at or very close to a strong curvature maximum (landmark 4.2) at the top of this roughly semicircular curve.

The curvature reading (from the CrvStat program described below) at (or near) bregma would be larger if there was significant mid-sagittal keeling. It has been suggested that Asian *H. erectus* specimens have the strongest keeling. However, an isolated bregmatic eminence (a lesser

form of keeling) is found in most "archaic" and many modern humans (Bräuer and Mbua, 1992). It is more common in relatively dolichocephalic than brachycephalic individuals. Weidenreich (1943) thought that sagittal keeling occurred under a high stress regime, and caused an accelerated closing of the sagittal and metopic sutures, but no evidence exists to support such a claim. If keeling can be associated with loading that occurs during masticatory, prehensile, or another form of repetitive loading while the suture is open (the keeling is usually at or about the suture), it may even be the case that this suture stayed open relatively longer in *H. erectus* than in *H. sapiens*. Such a build-up might be due to stress transferred to the sutures from the surrounding bony plates via muscular or behavioral activities. Weidenreich (1941, 1943) suggested just the opposite, but for him sutures "allowed" shifting of bones. Thus, sutures (and sinuses) were a liability under the greater muscular strain that would be applied to an *H. erectus* skull over that of a modern human. It is clear that sutures can act as joints, but such movements allow for effective dissipation of local strain as evidenced by the extreme case of contrecoup fractures. It would seem that the increasing thickness of cranial bones in geriatric modern humans, lacking the torsional abilities of sutural joints (i.e., as with non-reinforced concrete their skulls can withstand compression but are more brittle), dissipate such forces over a wider area. Perhaps the uniformly thickened

areas of the *H. erectus* and some "archaic" *H. sapiens* vault represent such a post-closure process. It may be such that hormonal control over the timing of sutural closure is related to the tendency to robusticity Hublin (1986; Hublin and Braun, 1992) sees in the Far East. As a growth area sutures are of secondary importance; much more of adolescent and adult remodeling of the skull occurs by cortical shifts (see Enlow, 1990), often associated with sinus expansion. Appositive sutural growth is more likely a secondary reaction to the stretching apart and repositioning of bones during growth.

Character 5: The Superior Nuchal Line

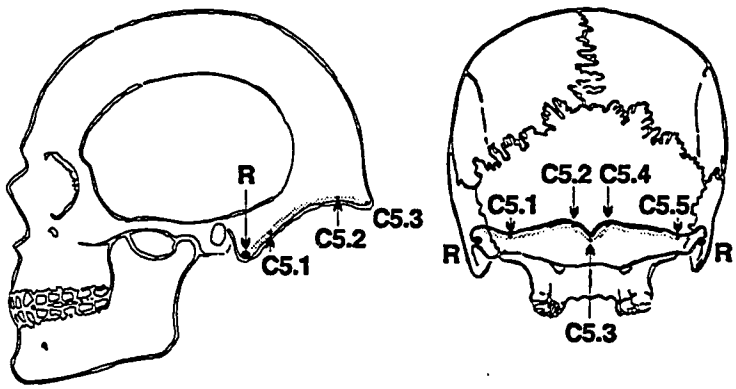

Figure 2.12a The Modern Superior Nuchal. (Left lateral view modified from Le Gros Clark [1967] and posterior view modified from Le Gros Clark [1978].).

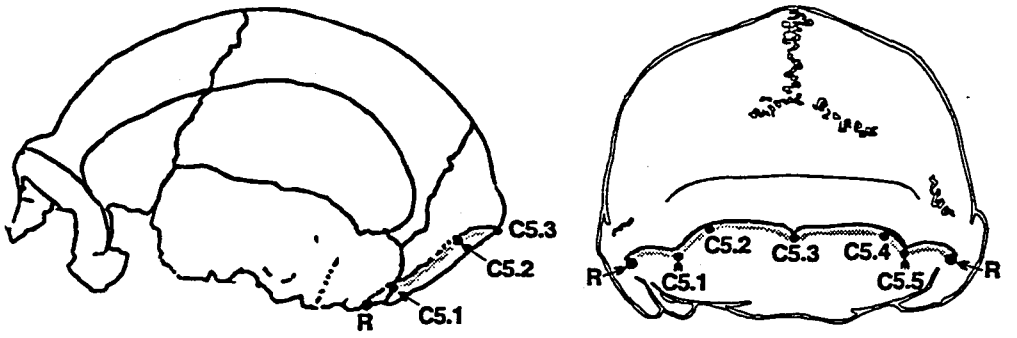

Figure 2.12b The Superior Nuchal Line in *H. erectus*. (Left lateral view is Zhoukoudian 12 modified from Santa Luca [1980]. Posterior view modified from Weidenreich [1951].).

The superior nuchal line, like the superior temporal line, is a fascial line demarcating the superior margin of the nuchal musculature. Tracing began at the lateral border of the splenius capitus scar on the mastoid. This registration point was usually just posteromedial to the digastric groove, in the vicinity of asterion. The superior nuchal line continues medially superior to the semispinalis capitus scar to inion. In *H. sapiens* inion is coincident with the external occipital protuberance, a feature rarely found in *H. erectus*. Landmarks 5.1 and 5.5 correspond to the border between the splenius capitus and semispinalis capitus muscle insertions. Landmarks 5.2 and 5.4 correspond to the most posterior bulge of the splenius capitus muscle scar on either side of inion (landmark 5.3).

In *H. erectus* inion and opisthocranion are usually coincident. Thus the superior nuchal line, posteriorly, marks the separation of the nuchal and occipital planes, i.e. this line is roughly the vertex of the two occipital scales. Modifications of this character may represent

another major shift at the origin of *H. sapiens*. Opisthocranion is usually on the flattened upper occipital scale in all *H. sapiens* from the earliest known fossils (see below).

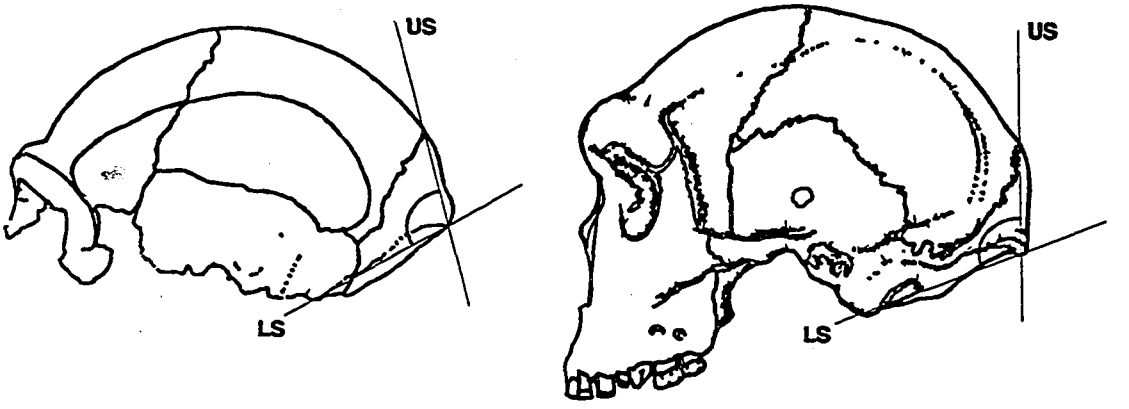

Figure 2.13 Inferior Rotation of Nuchal Scale across the "*erectus-sapiens*" transition: Zhoukoudian 12 (on left, modified from Santa Luca [1980]). Broken Hill, archetypal "archaic" *H. sapiens* (on right (modified from Santa Luca [1980]). US = upper occipital scale (chord from lambda to inion); LS = lower occipital scale (chord from registration point, R, on superior nuchal line [see Figures 2.12a and b] to inion). Not to scale.

It has long been observed that in lateral view the angle formed by the upper and lower occipital scales in *H. erectus* is more acute than that in earliest *H. sapiens* (Stringer, 1984; Hublin, 1986). Actually, the lambda-inion-opisthion angle is not much greater in *H. sapiens*, however the movement of the lower scale, the nuchal planum, inferiorly (and concurrent shortening of the nuchal planum) gives the appearance of tremendous difference. In earliest *H. sapiens* through to modern people the nuchal planum is almost parallel to the Frankfurt plane and the upper scale is nearly perpendicular to the Frankfurt horizontal. It is not

clear whether the Neandertals underwent a reversal of this trait or if the upper scale was just extended posteriorly [i.e., the chignon]. The latter appears more likely.

The horizontal orientation of the nuchal planum allows for more concentrated use of ligamentum nuchae, as opposed to stressing the broader band of nuchal musculature and fascia in support of the head. At the superosuperficial end of this ligament in *H. sapiens* there is a localized, round, insertion point; this arrangement produces the robust inferiorly oriented external occipital protuberance. Rightmire (1990) notes that only *H. sapiens* possesses a true external occipital protuberance. Some of the Solo specimens show a protuberant inion, but it does not stand out from the overall robust (laterally as well as centrally) superior nuchal line. Further, because the nuchal planum is not inferiorly rotated, the nuchal musculature and associated osteological structures appear to have been oriented more posteriorly than in *H. sapiens*. *H. erectus* specimens show an enlarged torus beginning at the level of, or just above, inion. This torus continues laterally for 2-3 centimeters. Opisthocranion is located centrally along this torus. With the inferior rotation of the nuchal planum in *H. sapiens*, opisthocranion comes to lie superior to inion.

Above the nuchal torus in *H. erectus* the upper occipital scale can slope back as part of a continuous arc with the parietal outline (as seen in lateral view). The Solo specimens appear superficially similar to *H. sapiens* in this

region. The swelling of the medial torus at inion combined with some swelling at lambda give the upper occipital scale an appearance of flatness. Most of this is exostotic growth. The inner contour is similar to other *H. erectus* specimens, with the occipital poles and inion coincident. The inferior rotation of the nuchal plane in *H. sapiens* allows endinion and inion to more nearly approximate. The superficial similarity of the Solo specimen's occipital region drops away entirely when the orientation of the nuchal planum is observed. It is not horizontally oriented, parallel to the Frankfurt horizon, as in *H. sapiens*.

The earliest "archaic" *H. sapiens* crania show a vertical (almost 90 degrees from the nuchal planum) upper occipital scale with a horizontal lower scale (e.g., Broken Hill, Petralona, Salé), viewed from the Frankfurt orientation. This contrasts greatly with the 60-75 degree from vertical orientation of the upper scale in *H. erectus*. The occipital poles (and usually opisthocranion externally) sit well above inion in *H. sapiens*.

The relationship of the two occipital scales has often been discussed in relation to kyphosis of the cranial base (Huxley, 1863; Boule and Vallois, 1957; Le Gros Clark, 1960). The correlation is partly artefactual from observations of lateral cephalograms. The actual architectural relationship here has been challenged. Increased levels of cranial base *sensu stricto* (anterior to the foramen magnum) bending about sella have been observed

in modern humans and are assumedly less bent in great apes, australopiths, *H. habilis*, *H. erectus* (Maier and Nkini, 1984), and Neandertals (Laitman *et al.*, 1978, 1979, 1992; Laitman and Heimbuch, 1982; Laitman, 1985; but see Frayer, 1992b). However concentration on defining kyphosis as the "pituitary angle" (sella is the vertex of this supposed basal bending) does not belie any known specialized growth process or phylogenetic trend (Biegert, 1963), This angle may be an indication of such a process, and it has been correlated to the position of the larynx (Laitman, 1985; but see Houghton, 1993). It is an artefact of the ease of measurement of this angle with our prevalent x-ray technology.

In 1917 D'Arcy Thompson (1961:320) was pointed out that anthropologists' overdependence on the facial and basicranial angles ignored data that could offer a fuller description. For example, with Thompson's coordinate deformations it becomes clear that the upper arc (sagittal suture) of the parietal bone outstripping that of the lower arc (squamosal suture) in *H. sapiens* and not in *H. erectus* is also correlated with the inferior rotation of the nuchal planum. This feature of the parietals apparently undergoes some reversal in Neandertals. There will be more discussion of this topic in Chapter 4.

Similarly, until more data has been analyzed, phylogenetic scenarios relating cranial base flexion and the orientation of nuchal planum to the evolution of speech or

brain enlargement should be offered cautiously. While the cranial capacity of the Broken Hill specimen doesn't exceed that of several Asian *H. erectus* specimens, the sphenoid clivus is flexed inferiorly and the nuchal planum is nearly parallel to the Frankfurt horizontal (Pycraft *et al.*, 1928). The expectation here is that a major shift in the *Bauplan* (architecture) of the skull has occurred in the earliest *H. sapiens.* As with the glabellar segment, there has been no intermediate form found as yet. It is expected that the quantification of this character in this study will obviate arguments over how significant this shift really was.

C. Methods

Although it is intuitively obvious that line tracings of the major surface features of the skull, ridge curves (see figure 2.12), convey a great deal of information visually, when this project began it had not been demonstrated that there was biologically useful information in these 3D space curves. In fact, there is no literature on this subject (Bookstein, pers. comm.). For this reason there is no statistical machinery for making shape comparisons between homologous ridge curves. The attempt to fill this void began with my need to find a sensible way to capture, average, and compare ridge curves.

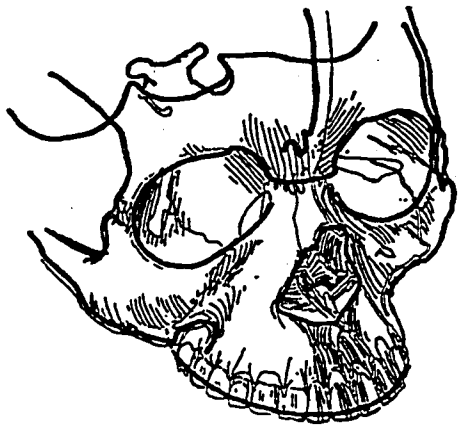

Figure 2.14 Ridge Curves of the Skull: Because they are the foci of curvature in their surface neighborhood, the edges of many structures can best be captured (collected as coordinate data) and represented as space curves (heavy lines, modified from Bookstein and Cutting, 1988).

Data Collection Hardware and Software

I used an electromagnetic hand-held sensor, the Polhemus (Colchester, VT) 3SPACE 6D TRACKER (TM), to collect the data for this project. The 3SPACE records data with six degrees of freedom (xyz coordinates and orientation) but only the xyz data are saved to disk. Since each space curve was analyzed in isolation, the orientation information was not saved. The magnetic source for this device is mounted under the surface of a non-ferrous table and specimens are placed atop it. The pencil-like stylus has 3 coils internally. The reference frame for the data collecting session is established at power-on by taking three registration points atop the digitizing table, the origin, a positive x reading, and a positive y reading. The offset of the stylus' sharp aluminum tip from the three sensor coils is compensated for during this calibration (by firmware) as well. Two digitizing

tables were used. Most of the specimens were digitized on the table that ships with the 3SPACE TRACKER (it is waist height, wooden, non-ferrous, shielded, weighted and balanced). However, for travel purposes, a smaller plastic table was purchased from Mira Imaging (Salt Lake City, UT). When the magnetic source was repositioned in the Mira table the firmware calibrated script had to be edited.

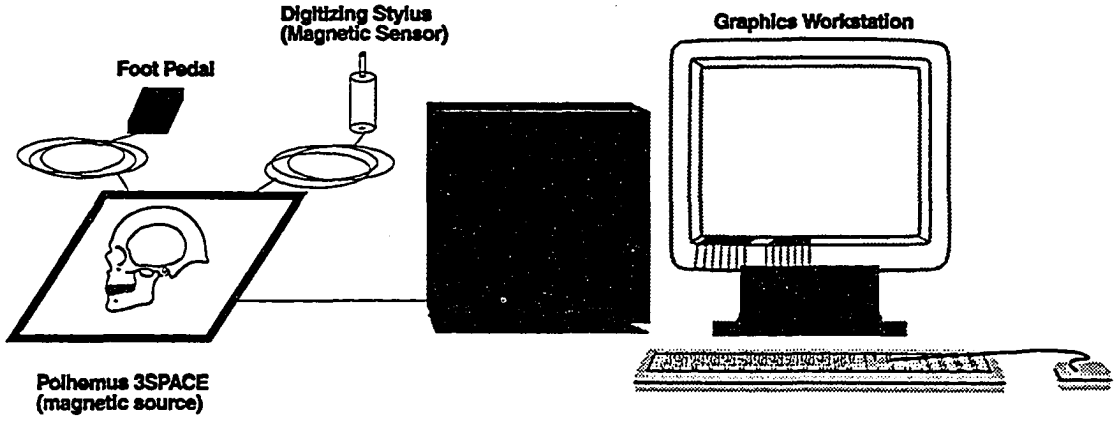

Figure 2.15 3SPACE Digitizing Workstation.

The 3SPACE records full rigid-body motion information and these data can be used to produce a real time display. I used a software interface called TableTop (Karron © 1990), written by Daniel B. Karron, Department of Applied Science, New York University. TableTop displays a grid representing a sheet of graph paper that is affixed to the digitizing surface. TableTop can set the 3SPACE TRACKER to single point mode to record a "landmark" or continuous point mode (records a point with approximately every 0.33 mm movement of the stylus) to record a "line". Data is captured when the user depresses a foot pedal, a second click ends data

acquisition. The program can use a direction the stylus points in to select the point-of-view. Up to 8 points-of-view can be saved during a single digitizing session. It is often useful to switch between points of view when digitizing a single curve if it undergoes a lot of torsion. The ability to change the point of view is also useful when overlying landmark and space curve data are collected. Inspection of very dense data from multiple points of view and distances is necessary to avoid user error as well as machine malfunction.

TableTop was written and primarily run under the UNIX operating system on a Silicon Graphics, Inc. (Mountain View, CA) IRIS GT workstation. To take the digitizer into the field I ported TableTop to DOS. The display of the DOS version required hardware support for the Silicon Graphics Graphic Library (GL). This was supplied as firmware with the Pellucida (Mountain View, CA) IBM PC-compatible graphics adapter card. Two sine-wave correcting power conversion units (220 to 110 Volt) were required to operate this equipment in Europe.

The analysis of the ridge curve data, the search for homologous landmarks along the ridge curves, began with visual observation of the data. Each ridge curve was visualized in a program called RidgeWatch (Cutting © 1992) to identify potential curvature maxima. An example of a single nuchal ridge curve, CMNH 962, is shown in Figure 2.16b, the average CMNH ridge curve in Figure 2.16c.

(a)

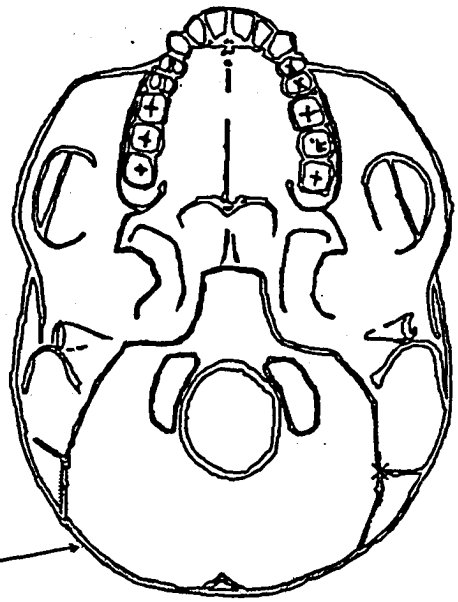

(b)

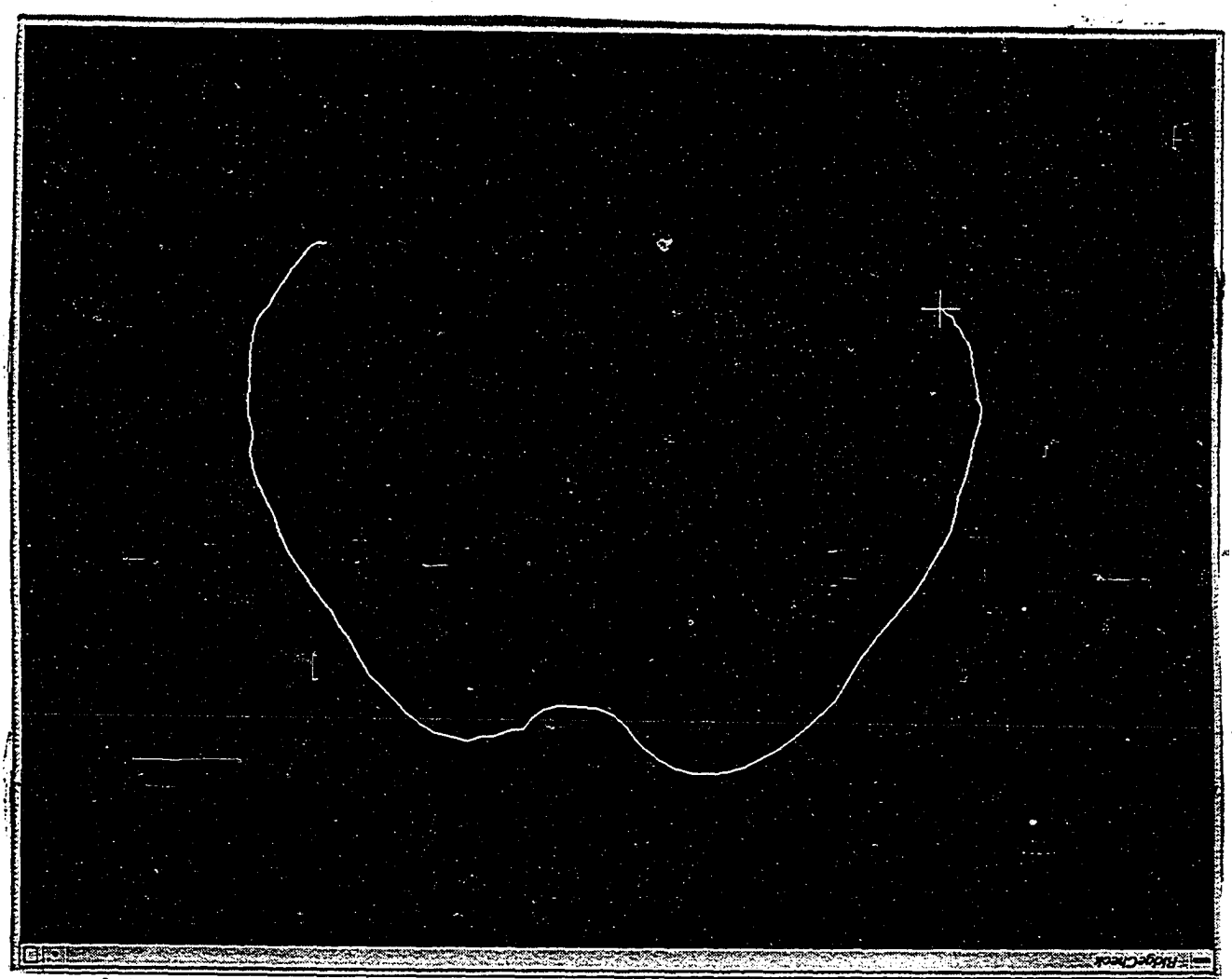

(c)

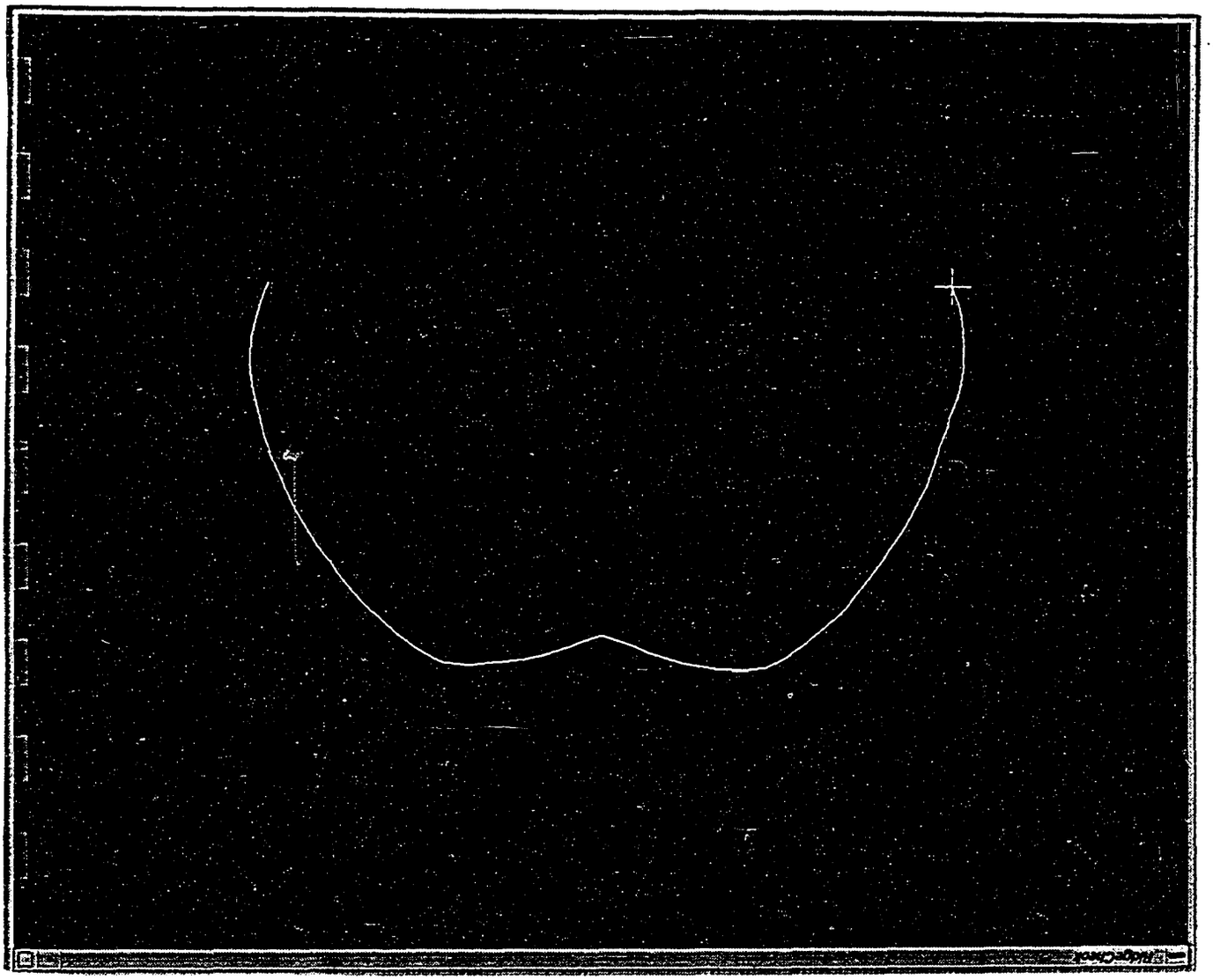

Figure 2.16 3SPACE hand digitized data: (a) Inferior view of the superior nuchal line (SNL) shown as thick gray line. (b) CMNH 962 SNL and (c) average CMNH SNL.

A visual survey of the entire sample of ridge curves gave an indication if these curvature maxima were present on every curve (potentially homologous). The curvature readings at every point along each curve was computed and sometimes the curvature maxima were found to actually lie one or two points laterally to the point suggested by visual inspection.

Geometric Landmarks

In the present case the particular space curves (i.e., 3D line tracings) being analyzed are five ridge curves found on the adult hominin skull (see Figure 2.14). Ridge curves are usually the edges of bony structures with biomechanical, physiological, epigenetic, or morphogenetic properties, such as those given for the choice of "Characters" in this study. Many if not most ridge curves are along muscle attachment sites or the edges of foramina. Such areas stand out visually in their bony neighborhood because they are the focus of local curvature changes. These inpocketings and tori stand out geometrically as well because perpendicular lines running from the traced ridge curves over the adjacent smoother surfaces to the ridge curves would show increasing levels of curvature (less flatness) as they approach these "ridges."

Traveling along a ridge curve the curvature is found to vary the same way as the surface curvature leading up to a ridge curve. The curvature steadily increases approaching a maximum then decreases after it is passed. Many such curvature maxima on ridge curves, such as those shown in the previous section on characters, are found homologously among "normal" individuals of a given species, and thus should be amenable to other landmark techniques. However, the methods used here are novel, and an analysis of landmarks located along space curves is unprecedented (Bookstein, pers. comm.).

To date, morphological treatment of curves has been on plane curves (2D) captured from photographs or video input. These studies have been limited primarily to closed outline data and the assumptions behind their use may make them inappropriate for a 3D problem (Olshan *et al.*, 1982; papers in Rohlf and Bookstein, 1990). Most of these techniques attempt to graphically or numerically represent the curvature data along the curve or in the shape of the area enclosed by the curve, such as median axis (Daegling, 1992). However, except perhaps for the notion of shape coordinates (Bookstein *et al.*, 1985), none of these techniques are easily extensible to space curves. Thus, the best place to begin is with standard landmark theory.

Bookstein (1991) defines three types of biological landmarks. Type I landmarks, e.g., traditional cephalometric landmarks, most of which have been recognized because they occur at the juxtapositions of tissues. Most have been chosen because a caliper, goniometer, or other mechanical measurement device can be registered on these points on either the original specimen, a photograph, or an x-ray film. The endpoints of the curves traced in this study are Type I landmark registration points. The utility of curvature (and torsion) maxima landmarks (e.g., on 2D outlines, space curves, or surface patches) is a major topic of interest to the "New Morphometrics" (Rohlf and Bookstein, 1990). It is intuitively clear that Gaussian curvature maxima (Hilbert and Cohn-Vossen 1990:173), if homologous

between specimens, could be treated in much the same way as Type I landmarks, thus Bookstein (1991) terms them Type II landmarks. Type III landmarks are the points along a an important edge (e.g. orbital foramen, nuchal torus) spanning Type I and/or Type II landmarks (more on this below).

While some of the traditional Type I landmarks happen to be curvature maxima (on some specimens), Type II curvature landmarks demarcate the salient geometry of the skull. The Type II landmarks discussed in this study were only accepted if they could be reliably found across the entire sample. Curvature information was obtained from the raw space curve xyz data. Tests were also done to see if the location of torsion maxima would compare across this study's sample of 5 curves, but their locations were extremely variable. Their relative positions along segments between curvature maxima varied so widely they were deemed useless. Thus, for the purposes of this study only Type II curvature extrema were used. There are several ways to determine the curvature at each point along a space curve.

Most discussions of curvature along space curves begin with the representation seen in Figure 2.17

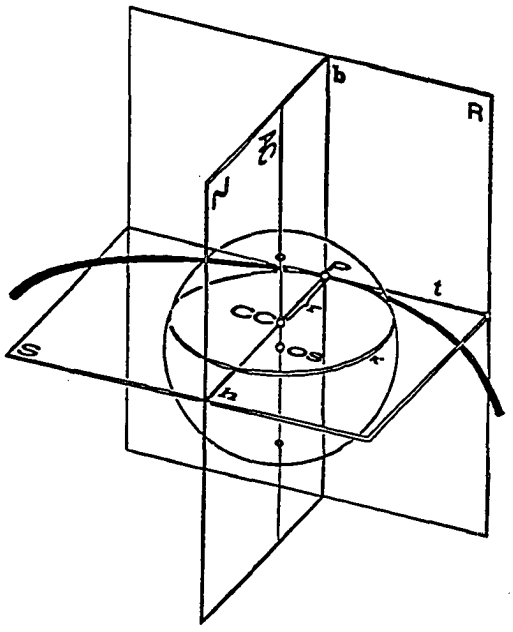

Figure 2.17 The Moving Trihedron: is a coordinate system that is relevant to each point at which curvature is calculated. It is demarcated by the right-handed orthonormal triplet t, b, and h. P = point under consideration, S = osculating plane, N = normal plane, R = rectifying plane, t = tangent, h = principal normal, b = binormal, κ = circle of curvature, r = radius of curvature, AC = axis of curvature, CC = center of curvature, OS = center of osculating sphere (after Hilbert and Cohn-Vossen [1990]).

The curvature of points along a space curve can be found by fitting a circle, called the *osculating circle*, to a triplet of points, one on either side of the point at which curvature is to be found. The osculating circle lies in a plane, the *osculating plane*. Curvature, κ, can be calculated as the inverse of the radius, r, of the osculating circle.

$$\kappa = \frac{1}{r}$$

Equation 2.1: Curvature.

If the three sample points are collinear curvature is 0. Nearly collinear points will produce a large circle as the radius approaches infinity. It follows that large osculating circles will have a small curvature.

Curvature values at each point on a space curve can be computed using standard differential geometric methods. Curvature can be calculated at any point along a spline. Therefore, the xyz space curve data were expressed as a "best fit" cubic spline. Such a spline has values that change as a function of parametric arc length, t, in the general equation for a cubic spline, shown here:

$$p = at^3 + bt^2 + ct + d$$

Equation 2.2 Cubic Spline.

where p is the raw space curve coordinate data, x, y, or z. Each set of coordinates (x, y, or z) must be substituted for p separately to solve for the constants a, b, c and d of the spline.

For a given arc length, t, of the original space curve data a "best fit" cubic spline may found with the regression (same equation used for y and z data):

$$\underset{a_x, b_x, c_x, d_x}{\arg\min} \sum_i \left(x(t_i) - (a_x t_i^3 + b_x t_i^2 + c_x t_i + d_x)\right)^2$$

Equation 2.3: Regression for x coordinates of Best Fit Cubic Spline.

Using the xyz data of the raw space curve, this regression has an overdetermined number of data points which allows solution for coefficients a, b, c, and d. This is

done separately for x, y, and z and can be calculated by single value decomposition (Press *et al.*, 1988; Rohlf, 1990). Using the spline polynomial curvature can be obtained for this xyz data.

The best fit is where the differences in these coefficients between the cubic spline polynomial and the actual curve data are minimized. These can be found at t = 0 first, then at the position at the end of the fitting distance, t=D. D is a linear approximation of the arc length (i.e., it is a sum of the straight line distances between each point along the raw space curve):

$$D=\sum_{i=1}^{n}\sqrt{(x_i-x_{i-1})^2+(y_i-y_{i-1})^2+(z_i-z_{i-1})^2}$$

Equation 2.4 Sum of Linear Arc Length.

At any point on the original curve data can be assigned an arc length distance, t, along the fitted segment. By substituting t into the best fit cubic spline equation and treating it as the midpoint along a segment of a cubic spline, curvature at that point can be computed as:

$$|K|=\frac{|x'\times x''|}{|x'|^3}$$

Equation 2.5: Curvature of a Fitted Span (Lipschutz, 1969).

Where x' is the first derivative, with respect to t, of equation 2.2 which for, the first point on the spline, t=0, is simply cx, cy, cz. And, x" is the second derivative of equation 2.2 which for t=0 equals bx, by, and bz.

Best fit cubic splines were found for all the space curves with a program, CrvStat (Cutting © 1992). CrvStat finds the best fit spline along any portion of, up to but not exceeding, the total arc length of the actual raw space curve data. The fitted spline is centered about the midpoint of the raw space curve data. CrvStat assigns t values (arc length) to the space curve coordinates along the best fit spline and solves for curvature (and torsion) at any point of the original space curve that resides within the selected fitting span.

The Type II landmarks used in this study exhibit extremely high curvature relative to other points along the curve (a local curvature maximum). By changing the fitting distance (arc length t of the polynomial function in Equation 2.4) the relative curvature at each maximal point can be made to stand out from the others. At fitting distances that are too low there is too much noise. At higher fitting distances curvature readings will change smoothly from point to point, but if the fitting distance is too long the fitted section will not include the maxima landmark(s) of interest. Because maxima were more easily identified by scanning the curvature readings, the longest fitting distance possible (that includes candidate maxima points) was always used.

Once isolated, the maxima are checked against a graphical representation of the curve. This visual check can also spot areas where curvature appears high but may perhaps

be too close to the end of the curve to get a curvature reading at a high fitting distance. Curves from all three samples were compared to find maxima that were homologous across the entire study population. This constitutes the first computer-assisted search for three dimensional geometric landmarks of the human skull. An endeavor that should have attendant importance to systematic, anatomical, and medical morphometrics.

All of the landmarks were found across the entire sample but they were not equally easy to detect. Fitting distances were varied to make the curvature landmarks identified visually stand out amongst the reading for curvature at other nearby points.

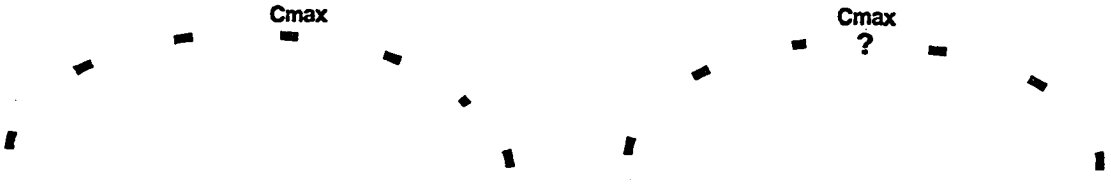

Figure 2.18 Curvature Maxima with incomplete data. The curve on the right is missing a point that is an obvious curvature maximum. One of the two points on either side of the gap has the higher curvature reading and was chosen as the maximum point.

Sometimes it was found visually that the curve flattened out on either side of what was obviously a curvature maximum when this area of the curve was viewed across the whole sample. The reason for this situation could be that the morphology is different on the specimen at hand. However, in a case like that seen in Figure 2.18, density of point

capture is a problem. The curvature maxima were determined on the raw, unresampled data. Thus, if the actual maximum point was not captured one on either side had to be chosen. In all cases one of the two points had at least a slightly higher curvature reading. Curves were not splined and resampled in order that morphological information that was not captured would not be created during the isolation of these maxima. It is hoped that with devices that capture finer data (less precise than more recent Polhemus, Inc. devices, the 3SPACE Tracker used in this project captures points approximately every 0.33 mm but if the stylus is moved quickly across the surface data gaps of up to 0.5 mm can occur), the need to choose points that are not "obvious" maxima will be obviated. Another option would be to "manufacture" a true curvature maxima landmark with software.

Briefly, the following discussion describes problems (or the lack thereof) in isolating each of the Type II landmarks located for this study. All three landmarks on the glabellar ridge curve were extremely easy to isolate on all specimens. Point 1.1 and 1.3 are the tops of the superciliary arches while point 1.2 approximates glabella. Both points on the lateral brow are very strong on all specimens surveyed. Point 2.1 is the turn laterally from the supraorbital notch and point 2.2 indicates the turn of the superolateral-most point on the brow in the frontal plane to the sagittal plane. Point 3.1, the anterior-most border of the temporalis

muscle was easily found in the modern human sample due its steep rise here (especially in meso- to brachycephalic skulls), but it was more difficult to isolate this point in *H. erectus*. As discussed in the section on character 2, landmark 3.2 was easier to find in *H. sapiens* because of superoinferior height and landmark 3.3 was easier to find in *H. erectus* because of the posterior robusticity of the temporalis muscle attachment site. Landmarks 3.1 and 3.3 approximate stephanion and euryon, respectively. The intensity of both indicate how strongly temporal muscle gabling has affected vault morphology. Landmark 4.2 approximates bregma. It stood out in those *H. erectus* and transitional specimens evincing mid-sagittal keeling, and was very clear in the modern human sample as the top of the typical meso- and dolichocephalic pentagonal contour. However this point would be expected to be more difficult to locate in more brachycephalic groups because the top of the head tends to be flatter. It should be noted that the coronal suture is not a true ridge curve, it is more like a Type I line (as opposed to landmark) of tissue intersection. It is expected that this line would not be found reliably by an algorithmic search of the skull surface data, i.e. a ridge curve would not be present. However, a visual scan for the coronal suture (i.e. a line) would find it wherever it is present and unfused. The hominin vault, in general, shows very few foci of curvature, a problem for geometric studies of this region.

Space Curve Statistics

Comparative analysis of Type II landmark positions, whether isolated along space curves or from a differential analysis of points making up the surrounding surface patch, across the *H. erectus/H. sapiens* transition, could be done by traditional landmark techniques as discussed in chapter 1. However one of the goals of this study was to see if ridge curves, themselves extended foci of curvature in their anatomical region, could add biologically useful information to comparisons of cranial form. A major stumbling block here was that no means for comparing the landmark data between Type I and Type II landmarks along a ridge curve was available to this study.

The interlandmark data in the raw space curves, as collected, is not directly comparable point by point. When tracing curves the 3SPACE digitizer was set to continuous point collection mode. The point density recorded along the curve is uneven between tracings of the same curve. However, as was seen in the previous section, it is possible to generate a spline function representing the raw space curve data. Such a spline best preserves the shape of the original curve and the interlandmark segments could be resampled at equidistant arc length intervals so that all could be represented with the same number of coordinates. Resampled space curves would be of different sizes but this should not be an insurmountable issue in an analysis of shape. It is

assumed that the resampled interlandmark points could be treated as "pseudo-landmarks".

Pseudolandmarks carry shape information only as part of the segment they span. These homologous segments were made comparable across the study by resampling them to have an equal number of Type III landmarks. Bookstein (1991) also describes these landmarks as Type III or "deficient" landmarks. Unlike the Type II landmarks on a ridge curve, deficient landmarks do not occupy three dimensionally unique positions on the skull. Type III landmarks do express curvature and torsion gradients. Curvature and torsion generally increase or decrease smoothly across segments of pseudolandmarks up to a Type II landmark and then grade in the opposite direction following it. Thus, pseudolandmarks are points along curvature or torsion continua between Type II landmarks. Because spans of pseudolandmarks do not exhibit abrupt changes in curvature and/or torsion they are deficient in the coordinate in the direction of the tangent line, and thus comparisons can be made between pseudolandmark segments that ignore tangent data. This cannot (and should not) be done with comparisons of the position of Type I and II landmarks. The goal of resampling the raw curves' interlandmark segments to contain uniform numbers of equidistantly space pseudolandmarks was to assign a vector to their positions and find differences in these

positions within a statistical analysis (see "Chi squared Distances" below).

It was deemed necessary to resample the raw space curves in order to make statistical comparisons of the interlandmark segments. The xyz positions of the raw space curve points in the interlandmark segments could be used to define a cubic spline function. Resampling the space curves in each interlandmark segment to have equidistantly spaced pseudolandmarks, by incrementing arc length, t, (see Equation 2.2) requires a piecewise cubic spline.

A piecewise cubic spline maintains first but not second order continuity across a joint (or node) to the next segment. First order continuity is maintenance of the tangent across the joint; second order continuity is maintenance of curvature. However, whether the goal is a smooth representation of the data or equally spaced data, the family of cubic splines occupy the lowest degree space (polynomial) capable of representing a twisting space curve with inflection points (Rogers and Adams, 1976).

A piece-wise cubic spline is of the same polynomial form as a best fit cubic spline (see Equation 2.2). Discrete arc length positions, D (see Equation 2.6), of the raw space curve points are normalized to a new span of t=0 to t=1.0. The number of points desired are divided into 1.0. Given a starting and ending t, there will be a separate cubic spline for each coordinate (x, y, and z) for each segment. The

midpoint of this segment is the resampled point, the pseudolandmark.

If the beginning and endpoints, t_1 and t_2, of all the piecewise cubic spline segments are known, then a, b, c, and d can be solved from an overdetermined matrix applied separately to x, y, and z, as was the case for the best fit spline (Rogers and Adams, 1976). P', the tangent vector of each splined segment, is equal across joints, and it is the first derivative of the cubic spine equation:

$$P' = 3at^2 + 2bt + c$$

Equation 2.6 First Derivative of a Cubic Spline (Tangent Vector).

thus, at $t=0$, $P'=c$. The second derivative, curvature, must also be equal across joints for a spline to have second order continuity.

D is used to calculate the desired t. A substitution of t produces the coordinates xyz for the joints (of each piecewise spline segment) which become pseudolandmarks.

Averaging Space Curves

In terms of a statistical analysis, aside from resampling to produce homologous interlandmark segments spanned by homologous Type III landmarks, another use of both the landmark and interlandmark raw curve data would be to generate an average (Cutting *et al.*, in prep.). This study compares both Type II and Type III landmarks on the unresampled curves to average curves.

An average ridge curve would be useful in describing the within-sample variability from which it derives. However, perhaps most interesting would be comparisons with homologous curves of "unknown" affinities (i.e. expressing species, ontogenetic, or pathological differences). The interlandmark segments on the unknown curve would also need to be resampled to contain the same number of equidistantly spaced Type III landmarks as on the average curve to which it is compared. In this study the "unknown" ridge curves are those captured from non-Caucasian and transitional (fossil) hominin forms.

In brief, average curves were used for statistical comparisons here by matching a curve segment to the average at the endpoints (1 and n) by rotation, translation, and scaling to some notion of best "fit" with the Procrustes (least squares) algorithm (Rohlf, 1990; Rohlf and Slice, 1990). Once fitted, the distances between homologous Type II landmarks on both curves (i.e. not the endpoints) were then summed and squared as one curve was rotated about the other. At the point where this error was minimized these sums of squares distances would be summed with those of the homologous Type III pseudolandmarks. The same comparison would be carried out within each sample between the resampled curves and their average. Chi square probabilities would be computed from these sums of squares figures and used to discern affinities among the "transitional" specimen curves.

The production of both samples' average curve, *H. sapiens* and *H. erectus*, for all 5 characters was undertaken after curvature maxima had been isolated from the raw unresampled curves. In short, the method used to produce an average has two major steps; the construction of an "arc length average" and a "final average." Each point along the final average curve is the average of points intersected at set intervals along the arc length average on the splined sample curves.

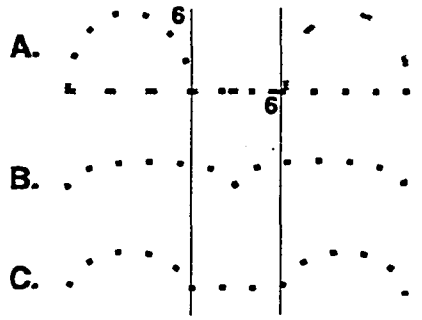

Figure 2.19 Problems of Averaging Space Curves by Arc Length: Averaging two curves by arc length, part B, results in an average space curve that dilutes the shape data carried in the 3 different segments of the two original curves. Points along curve 1 in part A are denoted as black dots; points along curve 2 in part A are denoted as gray dashes. Part B shows arc length average, used as a "rough estimate" in this study. Part C shows an average that preserves more of shape information carried in curves 1 and 2 in part A. .

Figure 2.19 illustrates the problem that necessitates the use of a two step process. Point number 6 of the curved segment on the thin black line is being averaged with point six of the thick gray line in the straight area that both lines share. And the same can be said for the curved area of

the second line (thick gray line). When averaged by arc length alone (point 6 on both lines are the same arc distance from the beginning of the curve), the curved areas at the ends of both curves are averaged with points in the straight area that both curves share. The arc-length average curve shown in the middle of Figure 2.19, shows that the shape "signal" from both curves has been "averaged" into the middle, previously straight segment. Thus not only are the curvature maxima defused but the truly homologous straight middle segment (shared by both curves) is lost in the arc-length average. The bottom average shows the reduced curvature "signal" at both ends and the maintenance of the shared straight segment in an average that is more useful for a shape analysis.

Arc length averaging does decrease the amplitude of a random variation in a sample of raw space curves, but by spreading out the variation its local character is lost. Actually, to obtain nearly the same average as that at the bottom of Figure 2.19 cutting planes could be set up as normal planes to an endpoint to endpoint chord as seen in Figure 2.20. The intersection points of these cutting planes with the raw space curves are averaged to give a new average point location.

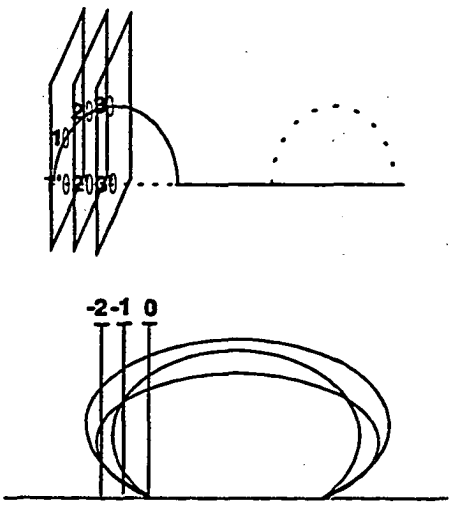

Figure 2.20 Averaging Space Curves by Perpendicular Planes.

The portion that is averaged at the top of Figure 2.20 is like that in the first and last of the three segments in Figure 2.19. What can be seen clearly is that as the slope of line 1 (as opposed to 1') increases, the intersection of point 1 (as opposed to point 1') becomes more a function of where the cutting plane is placed. Because of this, as with the arc length average, this portion of the curve is misrepresented in the average in terms of the shape data it carries. The bottom portion of Figure 2.20 shows several curve segments that all qualify as "ears". To effectively sample them with perpendicular planes normal to the shared endpoint-to-endpoint chord the chord must be extended laterally. However doing so produces double-hits at either end of the ears, over-representing the curves' shape data. Going too far laterally risks the cutting planes assuming an orientation parallel to the curves.

Both averaging methodologies, by arc length and perpendicular cutting planes, show failure on curve morphologies that are commonly encountered along ridge curves taken from the skull or the rest of the body. A combination of the two approaches was employed so that the failings of both methods could be overcome. An arc length average is used as the baseline for cutting planes that can then be guaranteed to sample the original raw space curve data from a useful orientation.

The Arc Length Average

An arc length average is constructed from all the curves sampled. This procedure requires at least 3 non-collinear points on all curves to be averaged. Two are the endpoints and the third must be a Type II curvature maxima landmark. Beginning with the second curve, its endpoint-to-endpoint chord is rotated, scaled, and sized to fit an endpoint-to-endpoint chord the first curve in the sample. (Assignments of numbers is arbitrary.) Then a one variable Procrustes fit (Rohlf, 1990) is used to minimize the error term, a sum-of-squares distances, between all curvature maxima landmarks. It is only a one variable fit because the curves are tacked down at the endpoints (only rotation about the endpoint-to-endpoint chord is possible). This error term is the sum of squares between homologous curvature maxima landmarks on the two curves. The movement matrix found is applied to all the points on the ridge curve between each pair of landmarks

(i.e. the final rotation matrix is applied to the first curve). Therefore two interlandmark segments have to be fit in a sample with two endpoints and one curvature maxima, three segments if there are two curvature maxima, and so on. This procedure is done recursively until all interlandmark segments of the sample curves are in the same coordinate space (Cutting *et al.*, in prep.).

The resulting arc length average of these data is akin to that shown in the middle of Figure 2.19 and it exists within the new reference frame determined by the first curve in the sample. In this procedure interlandmark segments are separately scaled and translated. Some rotation occurs at each landmark node (non first or second order continuity), but this is trivial (Bookstein, pers. comm.; Cutting *et al.*, in prep.). The rough average must also undergo a discrete approximation to D (total arc length/number of points desired) in order to obtain the pre-specified number of equidistantly spaced points for each interlandmark segment (i.e. it is resampled). The number of points chosen per interlandmark segment is based on the lowest common denominator of all the curves in the original unresampled set of curves. These points will serve as the location for the normal cutting planes needed to produce the final average.

Final Average

The arc length average is used to generate a more useful average that preserves more of the original curves' shape data. For reasons described in the comparison between averaging space curves by arc length and perpendicular planes (see "Averaging Space Curves" above), the original curves are *cut* by normal planes at each desired subdivision along the arc length average, as shown in Figure 2.21. The xyz coordinates of at the intersections with all of the sample curves are averaged. This average point becomes a pseudolandmark for that segment of the final average.

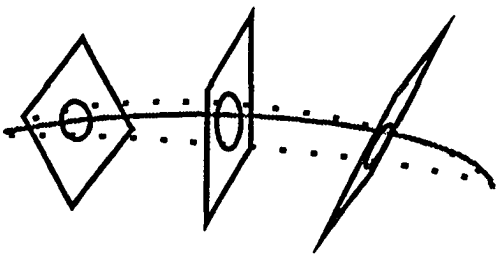

Figure 2.21 The "Two Step" Average: The solid gray line is the arc length or "rough" average. It was found by averaging points found at equal arc lengths along the other two curves. It is used to position normal or "cutting" planes at specified arc lengths. Any points intersected by these planes along the sample curves are averaged.

The equation of the plane perpendicular (normal) to the arc length average at each subdivision is computed at evenly spaced intervals (of predetermined length D) along each interlandmark segment. These normal cutting planes act as a perpendicular bisector of the raw space curve data.

This procedure was implemented in a program, RidgeAverage (Cutting © 1992). RidgeAverage makes a piece

wise cubic spline approximation of each raw curve that is to be averaged. These splined curves can be used to generate the rough average and then a final average (Cutting *et al.*, in prep.). RidgeAverage also resamples raw space curves. The raw space curves were resampled for comparisons to the average curve to determine the validity of a chi square test.

Chi squared Statistics

The statistical comparison of space curves in this study began with the best fit of each transitional curve to an average, then the distances between the corresponding pseudolandmarks and Type II landmarks were squared, summed and used in a chi square evaluation of affinity. The connections between the two curves may be thought of as a "ribbon" expressing their degree of similarity. There are several alternative means of fitting the two compared space curves, all of which will affect the point-to-point distances recorded by the ribbon statistic.

The method used, that of registering curves along the chord between their endpoints, was not obvious at first, but was taken as the standard procedure after the distances obtained by a Procrustes (least squares) fit at the centroid were shown not to be diagnostic of the shape differences between the two curves (Dean, 1991). The problem with a least squares fit is that registration at the centroid makes no assumptions about homology or shape (see Figure 2.22).

More importantly the distances obtained are extremely sensitive to outlier points (Rohlf and Slice, 1990; Slice *et al.*, 1992).

The procedure used to find the rungs of the "ribbon" matches curves at their endpoints, minimizes the sum of squares distances between curvature maxima landmarks, then sums these distances with those between homologous pseudolandmarks. The minimization involves first matching the average curve ($\bar{C}$) and the specimen curve (C_i) along their endpoint-to-endpoint chords. Curve C_i is translated, scaled to the same size as $\bar{C}$ (i.e. based on the identity of the endpoint-to-endpoint chord), and rotated to best fit. This rotation is about the chord connecting the shared endpoints and ends at the angle where the distances between homologous curvature maxima (pre-specified Type II landmarks) are minimized. Sum of square distances are then calculated between homologous pseudolandmarks (Type III landmarks) and added to the inter-landmark distances to produce a total sum of squares statistic, here called T.

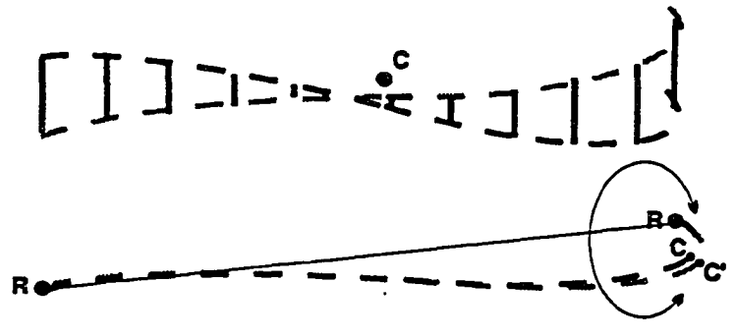

Figure 2.22 Various Space Curve Registration Techniques. In top example, a Procrustes fit, both curves have been registered at the centroid (C, large black point). In the bottom example, an endpoint chord match, the compared curve (light gray dashed line) is spun around the average curve (dark black dashed line). The axis of rotation is the shared endpoint chord, R-R (R = registration point, large black points). Rotation is ended at the point of minimum distance between curvature landmarks on the curve (C and C', small black points).

All of the matrix manipulation necessary to fit and spin the two curves has been done with the MatLab program DAVIDME3.M (Marcus © 1992; see Appendix A). The sum of squared distances were first calculated for all of the resampled curves (C_{ei} and C_{si}, *H. erectus* and *H. sapiens*, respectively) from their averages ($\bar{C}_e$ and $\bar{C}_s$) for each sample, for all 5 characters.

The chi square (χ^2) model then is a function of distances between both homologous pseudolandmarks and Type II landmarks. The general chi square model assumes:

$$T = c\chi_d^2$$

Equation 2.7: Chi square model.

where T is the overall comparison statistic, c is a coefficient to be estimated, and d represents the degrees of freedom.

In this analysis x_{ijkl} is the distance between the i_{th} specimen (i=1,...,n_k) and the k_{th} species mean (k=1,2) for the j_{th} pseudolandmark or Type II landmark (j=1,...,n_l), for the l_{th} character, we compute:

$$T_{ikl} = \sum_{j=1}^{n_l} x_{ijkl}^2$$

Equation 2.8: T values: within-species sample sum of squares.

Using the method of moments $\frac{T}{c}$ is fitted to χ^2, with mean:

$$\mu_T = cd$$

Equation 2.9: Mean of T statistic.

and variance:

$$\sigma_T^2 = 2c^2 d$$

Equation 2.10: Variance of T statistic.

Setting the sample moments of T equal to our theoretical moments, gives sample mean and variance:

$$\bar{T} = \hat{c}\hat{d}$$

$$s_T^2 = \hat{c}^2 2\hat{d}$$

Equation 2.11: Mean and variance of T statistic.

so that the estimates are now:

$$\hat{c} = \frac{\overline{T}}{\hat{d}}$$

$$\hat{d} = \frac{2\overline{T}^2}{s_T^2}$$

Equation 2.12: Estimates for χ^2 components c and d.

Then $\frac{T_{kl}}{\hat{c}}$ will have an approximate chi squared distribution with $\hat{d}$ degrees of freedom for the transitional specimens if they represent one or the other species (i.e., species k for each character l).

An evaluation of the goodness of fit of the χ^2 model may be obtained from a p-p plot (Wilk and Gnanadesikan, 1968) of the observed versus expected (straight line between 0,0 and 1,0 on this plot) chi square probabilities. This plot compares the empirical cumulative distribution function of T_{ikl} for each species character to the cumulative distribution function of a χ^2 distribution with $\hat{d}$ degrees of freedom. The plots were created with the MatLab program PROBOUT.M (Marcus © 1992; see Appendix A). Plotting the expected $\hat{F}$ (based on the average) versus the observed F (based on the sample values) chi square outcomes (R versus S) is expected to produce an identity or p-p (probability-probability) plot with a slope of 1.0.

The Kolmogorov-Smirnov test can also be used to test for goodness of fit (Wilk and Gnanadesikan, 1968; Sokal and

Rohlf, 1981). A K-S (Kolmogorov-Smirnov) distance statistic was generated. It also measures this fit.

The K-S test statistic (D) is:

$$D = greatest|F - \hat{F}|$$

Equation 2.13 Kolmogorov-Smirnov Test Statistic.

If this test statistic is above the tabled 0.01 value (Rohlf and Sokal, 1981) then goodness of fit is rejected for the p-p plot with slope of 1.0. This would mean that the measurements made for that particular sample of ridge curves did not behave as would be expected of a random sample from a chi squared distribution. The significance level (α = 0.01) is used throughout this study, The ρ value, the probability of getting a larger KS statistic, is not given because it always exceeds the largest ρ<0.20 given in the table (Rohlf and Sokal, 1981:204). Thus, unless the Kolmogorov-Smirnov statistic is larger than the appropriate tabled value, the resulting statistic is considered "not significant" (abbreviated ns in the p-p plots in Chapter 3 and Appendix B).

If the chi squared model is appropriate for these data, then we may compare the transitional curves (each C_t) to the sample averages for each species ($\bar{C}_e$ and $\bar{C}_s$) for each character. The transitional $\frac{T}{\hat{c}}$ values will be approximately chi squared distributed with $\hat{d}$ degrees of freedom. The corresponding tail probability for this comparison is the

probability that a more extreme curve than C_t occurs by chance.

Species Attribution

One major underlying assumption in this study is that there are only two hominin species present in the Middle Pleistocene. Thus it should be possible to attribute the characters found on the transitional fossils to one of the two species. It is, however, possible that a transitional specimen will not be similar to either species average (as seen in a number of cases). A chi square function in the MatLab program PROBUNK.M (Marcus © 1992; see Appendix A) determines this probability. Of course a species assignment is only justified if the distribution of the T statistic has been accepted as having a chi squared distribution.

Each of the transitional specimens and six non-Caucasian skulls (labeled AMNH in chapter 3, see Section A of this chapter for more details) were then compared to the averages of both species and were reported by the (right) tail probabilities of each within-sample chi square. Greater affinity to either average curve is expressed by a higher probability, and disaffinity by small probability.

The AMNH non-Caucasian specimens give an estimate of the level of variability for each character within anatomically modern *H. sapiens*. Thus, it is assumed that for a given character the AMNH specimens would exhibit higher empirical probabilities (affinity) for the average ridge curve

generated from the CMNH Caucasian sample than with the *H. erectus* average. If there is significant overlap, i.e. the AMNH specimens show high affinity with the *H. erectus* average, the character is not deemed useful for diagnosing anatomically modern *H. sapiens* affinities.

Finally, a probability ratio, PR in chapter 3 (*H. sapiens* empirical probability/*H. erectus* empirical probability), was calculated as another indication of affinity (Bookstein, pers. comm.). If there is little or no overlap of the AMNH specimens in this statistic, it provides a numerical criterion for diagnosis. This statistic is consistent in most regards with a direct examination of the probabilities. It may however be misleading when both probabilities are vanishingly small, and attribution is made to one category based on the probability ratio in isolation of this fact. In most cases a probability ratio of 1.0 or higher indicates *H. sapiens* affinities, below 1.0 indicates the opposite. Based on all the PR's in this study and my conclusions it appears that allocation of a specimen to *H. sapiens* should only be made where the PR > 2.0 and diagnostic assignment to *H. erectus* should only be made where the PR < 0.5. It would be useful, perhaps, to develop an empirical criterion based on this ratio and digitizing error.

The interpretation of results where the empirical probabilities are significant (α = 0.01) in both or neither category is problematic. Either case might indicate that homology cannot be judged from the character. An ordination

of the data by principal coordinates (Marcus *et al.*, in prep.) may provide an additional perspective.

Summary: The Chi Square Model

The methodology and assumptions behind the chi square model used in this study (discussed above in detail) are summarized briefly here. Chi square values were computed for each raw curve in the *H. sapiens* and *H. erectus* samples with respect to the average curve for each sample. The plot of the cumulative distribution function (cdf) of a chi square distribution (i.e., left tail probability) versus the empirical cdf (which is a step function) is expected to produce a probability-probability (p-p) plot with a slope of 1.0. The K-S (Kolmogorov-Smirnov) distance statistic was used to test this fit. The mean and variance have already been calculated during the fit of the chi square model.

The K-S statistic was unacceptably large in only one of these comparisons, that for the *H. erectus* nuchal torus. The p-p plot suggested an outlier specimen (Sangiran 4) and the analysis was rerun without it. The following statistics are provided in the next chapter: K-S statistic and criteria related to fitting a chi square model, i.e., mean, variance, c (estimated coefficient for chi square), and degrees of freedom, d.

Methodological Improvements

Increased precision of the data collection device would likely solve the problem highlighted by Figure 2.18, that of

determining a point among the raw data set to assign as the curvature maximum. Another means of determining the exact Type II landmark coordinates would be to spline the raw curve data and solve for the curvature maximum. An error term between this ideal curvature maximum and the closest point actually collected would give a measure of precision. There is a legitimate reasons for not wanting to smooth the data. Solving an equation for the coordinates of the curvature maximum, even though the answer is based on actually collected data, is nonetheless manufacturing data. This, however, can be controlled for by testing the effect on the space curve's shape of spline-generated points, perhaps through the error term just mentioned or by comparing orthogonal polynomial coefficients for unsmoothed and smoothed data.

Other manipulations of the raw space curve data might also prove useful. Only seemingly undeformed specimens and casts (or the parts digitized) were used in this study. Thus there was no control or correction for postmortem deformation of space curves digitized from fossils nor was there any mirroring for missing data (i.e., bilaterally symmetric missing data). Some curves could be corrected for obvious deformations (e.g., clean breaks and folds) with merely a translation of misplaced pieces of the curve. Mirroring and unwarping techniques have been explored by Kalvin *et al.* (1992) and Bookstein and Cutting (1991; Bookstein, 1991; Koenderink, 1990). These techniques would

not only be useful for studying specimen morphology, but rather as an aid for reconstruction.

Other descriptors of the data contained in the Type III pseudolandmarks could be added to the analysis undertaken here. Orthogonal descriptions of the line, such as Legendre Polynomial coefficients recursively describe the major linear, quadratic, cubic, etc., features of an entire space curve (or planar curve) or one or more interlandmark segments. Standard statistical techniques could be applied to these shape-encoding coefficients (Bookstein, pers. comm.).

Lastly, the interpretation of the chi square probabilities is actually a reflection of relationships to the average in multidimensional space. Preliminary tests showed that these distances are not well represented by single point statistics (e.g. the chi square test used here) and perhaps principal coordinates analysis and cluster analysis might be a better way to visualize the relationships of all specimens under consideration. This approach might also give a clearer picture of the distance between the *H. erectus* and *H. sapiens* means and the multidimensional nature of sample overlap (Marcus *et al.*, in prep.).

III Results

"You and Plato appear to be deadly enemies -- he with his deference of the good and the end, you with your physicalistic mockery of final causes. But you share a certain picture of philosophical progress, on account of which you will both be unable to accept either my methods or my results. You share a disdain for the appearances and a determination that true philosophic, or, in your words, scientific, discourse must be about a solid changeless realm beyond the shifting and indefinite terrain of *nomos* or human interpretation ."

Aristotle to Democritus (345 BC)

"Although the metaphysical cannot be investigated directly by the methods of science, its results may be."

George Gaylord Simpson (1949)

"Even if you're on the right track, you'll get run over if you just sit there."

Will Rogers (1935)

Overview

The major new contention of the methods of this thesis is that information can be found along interlandmark segments of biologically significant ridge curves in space. This chapter presents results of this analysis and brief interpretations. The overall pattern of results suggests that, where two or more forms differ, the methods used can successfully judge affinities of homologous space curves. Possible enhancements to the methodology, as used here, were discussed at the end of the previous chapter.

The results for all 5 characters (actually 7 since two are bilaterally present and each side was treated separately) are presented here. The test for the appropriateness of the chi square model is shown for Character 1. These data for characters 2-5 are in Appendix

B. The results from each character is followed by a verbal description of the results. This section is followed by a discussion of the phylogenetic implications for each character. A summary of all the results ends the chapter. The phylogenetic results are discussed in terms of the evolutionary model discussed in Chapters 1 and 2 (i.e., that *H. sapiens* may have had an early to middle Middle Pleistocene origin). A summary discussion of the impact of these data and other issues raised in this thesis and other workers ideas surrounding the *H. erectus/H. sapiens* transition follows in Chapter 4.

Glabellar Ridge Curve

The p-p plot and K-S statistic for the *H. erectus* sample are given in Figure 3.1. The p-p plot and K-S statistic for the *H. sapiens* sample are given in Figure 3.2. The T values, empirical probabilities, and chi square model probabilities for both samples are given in Tables 3.1 and 3.2. T is the sum of squares of differences between a particular specimen's curve and the average curve; $T = c\chi^2_d$, where d is degrees of freedom and c is a constant. Tests of the chi square model for characters 2-5 appear in Appendix B. The use of the Probability Ratio (PR) is explained in Chapter 2.

Figure 3.1 *H. erectus* Glabellar Ridge Curve Sample p-p Plot.

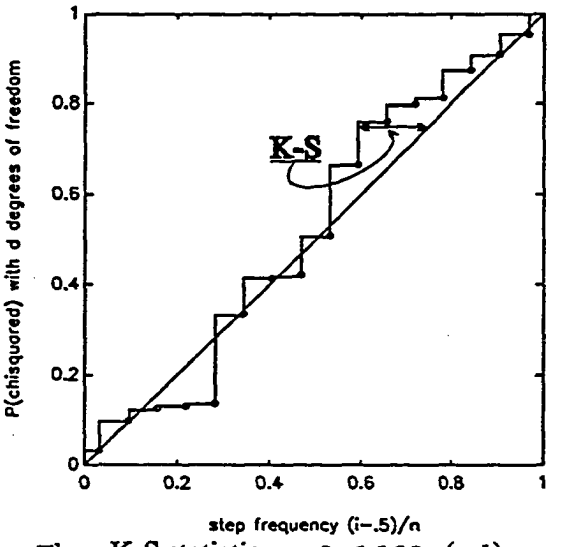

The K-S statistic = 0.1663 (ns[1]).

Table 3.1 *H. erectus* glabellar ridge curve intrasample data (N = 16).

The mean of T = 4.2988, variance = 4.5620, c = 0.7284, and d = 3.1314.

Specimen	T	Emp. Prob.	χ^2 Prob.
Zhoukoudian 1966	0.6555	0.0312	0.0316
Solo 7	1.2058	0.0938	0.0978
Solo 12	1.3899	0.1562	0.1251
Solo 10	1.4276	0.2188	0.1309
KNM-ER 3883	1.4646	0.2812	0.1366
KNM-ER 3733	2.6401	0.3438	0.3358
Sangiran 17	3.1096	0.4062	0.4146
Zhoukoudian 3	3.1578	0.4688	0.4224
Zhoukoudian 11	3.7181	0.5312	0.5096
Zhoukoudian 12	4.9144	0.5938	0.6655
Lantian	5.8749	0.6562	0.7600
Solo 5	6.3739	0.7188	0.7995
OH 9	6.5446	0.7812	0.8116
Solo 11	7.6130	0.8438	0.8737
Solo 4	8.4966	0.9062	0.9102
Zhoukoudian 10	10.1948	0.9688	0.9544

[1]This K-S statistic is "not significant" because it does not exceed the tabled α = 0.01 (ρ<0.20; see Chapter 2, page 70, for more discussion).

Figure 3.2 *H. sapiens* Glabellar Ridge Curve Sample p-p Pot.

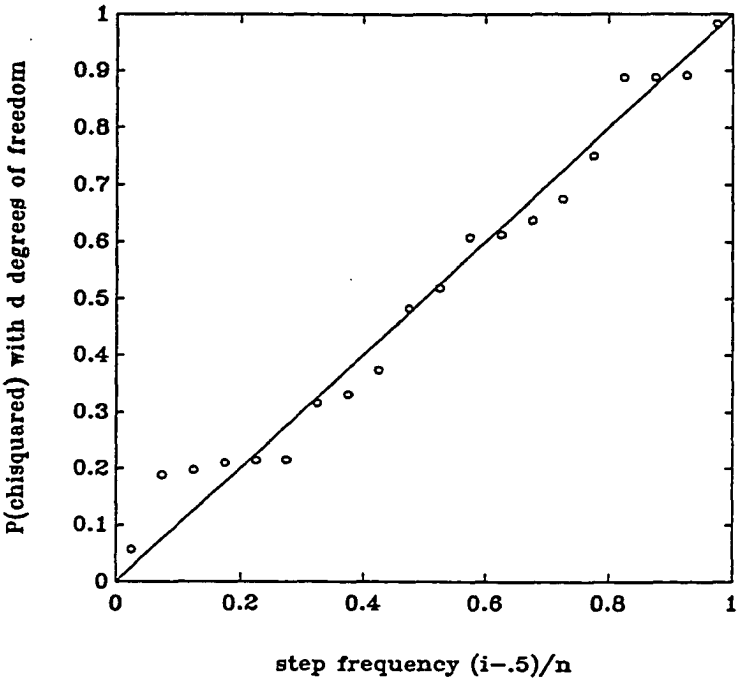

The K-S statistic = 0.1634 (ns).

Table 3.2 *H. sapiens* glabellar ridge curve intrasample data (N = 20).

The mean of T = 7.4307, variance = 44.6095, c = 3.0017, and d = 2.4755.

Specimen	T	Emp. Prob.	χ^2 Prob.
CMNH 681	0.2282	0.0250	0.0568
CMNH 1157	0.6595	0.0750	0.1884
CMNH 2584	0.6880	0.1250	0.1970
CMNH 920	0.7327	0.1750	0.2105
CMNH 1273	0.7458	0.2250	0.2144
CMNH 514	0.7492	0.2750	0.2154
CMNH 560	1.0998	0.3250	0.3164
CMNH 2401	1.1556	0.3750	0.3317
CMNH 881	1.3141	0.4250	0.3736
CMNH 1759	1.7736	0.4750	0.4834
CMNH 667	1.9402	0.5250	0.5190
CMNH 919	2.4102	0.5750	0.6080
CMNH 883	2.4394	0.6250	0.6130
CMNH 1253	2.5908	0.6750	0.6380
CMNH 630	2.8362	0.7250	0.6754
CMNH 856	3.4240	0.7750	0.7508
CMNH 2860	5.1651	0.8250	0.8880
CMNH 2048	5.2365	0.8750	0.8882
CMNH 962	5.1674	0.9250	0.8917
CMNH 939	9.1540	0.9750	0.9830

The "Unknown" (Un) non-Caucasian (AMNH in the table, N = 6) and transitional fossil (listed by site in the table, N = 5: Arago, Bodo, Kabwe, Petralona, Saldanha) glabellar brow ridge line tracings were compared to the *H. erectus* mean ridge curve (He in the table, N = 13) and the Caucasian *H. sapiens* mean ridge curve (Hs in the table, N = 20).

Table 3.3 Findings: Glabellar Ridge Curve.

The He d = 4.2988, c = 0.7284. The Hs d = 2.4755, c = 3.0017.

Specimen	Un-He T Statistic	Un-He χ^2 Prob.	Un-Hs T Statistic	Un-Hs Emp χ^2 Prob.	PR[2]
AMNH 1439 M Chin	8.5966	0.0235	11.3079	0.2133	9.1
AMNH 1440 F Chin	10.3836	0.0083	13.5849	0.1506	18.1
AMNH 2382 M WAfr	10.7346	0.0068	14.1234	0.1386	20.4
AMNH 2386 F WAfr	9.5150	0.0139	17.0494	0.0881	6.3
AMNH 8173 M Aust	8.3077	0.0278	17.6854	0.0797	2.9
AMNH 8175 F Aust	8.4822	0.0251	12.0233	0.1913	7.6
Arago	2.6209	0.5084	23.4688	0.0321	0.1
Bodo	14.2666	0.0008	16.9223	0.0898	112.3
Kabwe	15.3827	0.0004	19.3948	0.0610	152.7
Petralona	13.3719	0.0014	3.1874	0.6941	495.8
Saldanha	2.2553	0.5876	18.3423	0.0720	0.1

Description of Results

There is no sample overlap in this case. All of the non-Caucasian specimens show clear-cut affinities with the Caucasian average curve and none exhibit significant affinity with the *H. erectus* average ridge curve (note that all of the AMNH PR's are > 2.0). Among the "transitional" specimens, Arago and Saldanha show stronger affinities with the *H. erectus* mean. The other three transitional specimens,

[2] PR, Probability Ratio, is discussed on page 72, Chapter 2.

Bodo, Kabwe, and Petralona, show strongest affinities with the *H. sapiens* average.

The *H. sapiens* sample was, unexpectedly, more variable than the *H. erectus* sample (see variance in Tables 3.1 and 3.2). Judging from the other characters, it seemed that the *H. erectus* sample should be much more variable because it was drawn from a larger geographic and temporal span. However, despite this unexpected pattern of variability, all 5 transitional specimens showed greater affinities with the modern sample than any of the non-Caucasian specimens showed with the *H. erectus* average.

It is important to view results from the chi square model used in terms of populational affinities. For this character, the morphology detected on any of the non-Caucasian AMNH specimens would be likely to occur in the *H. erectus* population in fewer than 279 out of 10000 individuals (based on the highest chi square probability, AMNH 8173). Compare this to a greater than 320 out of 10000 likelihood that all of the transitional specimens could be observed in the *H. sapiens* population, including the Arago and Saldanha specimens (based on the lowest chi square probability, Arago).

Other presence/absence features also show affinities between these two specimens and *H. sapiens*. The glabellar segment, composed of both superciliary ridges joined at glabella, houses the medial portion of the frontal sinuses. Another salient portion of the glabellar-orbitofrontal

region (i.e., upper face and anterior vault) is not detected by this ridge curve. All 5 transitional specimens exhibit rounded projections, or frontal bosses, posterior to the two lateral curvature maxima on either side of glabella (see Figure 2.7).

The anterior projection of glabella is another major feature of this curve. The Arago specimen shows very little anterior projection at glabella. Judging from the cast used and published pictures it seems possible that the Arago 21 fronto-facial fragment could be diagenetically flattened (anteroposteriorly) in this region. This would effect a greater resemblance with *H. erectus*. The Arago specimen shows weak indications of the superiorly swelled glabellar ridging, moreso on the frontal squama than on the ridge curve itself. This superior swelling is weaker on Saldanha but the anterior projection is stronger than in Arago. Judging from the cast and pictures the Saldanha frontal does not seem to have been diagenetically deformed.

I have examined the original fossil Kabwe and Petralona skulls and casts and pictures of the Bodo fossil. All three specimens appear undeformed in this region. Therefore the data strongly support the attribution of Bodo, Kabwe, and Petralona to *H. sapiens* in terms of glabellar morphology. However, the measure given here shows the least support for *H. sapiens* affinities of Arago and Saldanha.

Phylogenetic Implications

This analysis shows that this region underwent a dramatic change in morphology across the *H. erectus/H. sapiens* transition. Apparently, in earliest *H. sapiens*, this portion of the brow advanced anteriorly along with the now anteriorly projecting frontal lobes. The change in position of the frontal lobes is indicated when they come to fully overlie the anterior cranial base (orbital cones, especially) and ethmoid complex, and lie underneath bilateral frontal bosses, parallel to variably present midline keeling (see Chapters 2 and 4 for a fuller discussion).

One feature, discussed earlier in this thesis but worthy of further consideration, is pneumatization. Most often in *H. erectus* the frontal sinus, if present, is limited to two small bulbs underlying, just deep to, the glabellar segment with a rather thick bony septum separating the right and left air cell. The lateral brow segment is not highly pneumatized in *H. erectus*. Of all the *H. erectus* specimens, the Solo specimens show the largest frontal air cells, but according to Weidenreich (1951), none invades the lateral brow segment. Conversely, the frontal cell pneumatizes much of the lateral brow segment in virtually all early *H. sapiens* and, although the robusticity of the lateral brow segment varies, pneumatization into the lateral brow is the rule rather than the exception in most groups of living people (Tillier, 1975; Stringer *et al.*, 1979).

It should be noted that Sangiran 17 has a shape that is exceptional for this curve (see Appendix B). Just lateral to a depressed glabella, this specimen exhibits two protruding, semi-hemispheric frontal air cells that project anteriorly but not superiorly. Thus, the glabellar curve remains flattened superiorly as in other *H. erectus*. In transitional and modern forms, where the glabellar segment protrudes, the lateral portion of the brow sweeps back, posteriorly. The Sangiran 17 lateral brow does not sweep back, it is relatively straight across (see Figure 2.3). This assertion is supported by the relatively high degree of similarity seen between the left lateral brow of Sangiran 17 and the *H. erectus* average (see Appendix B), especially superiorly. The frontal bossing above the orbital cones (see figure 2.6) is also not present on Sangiran 17. Instead, a well defined ophryonic groove separates the depressed frontal squama from the brow.

The entire facial skeleton of *H. sapiens* is heavily pneumatized, and the overlying bone appears relatively thinner than in the larger facial skeletons known for *H. erectus*. There are very few specimens of *H. erectus* preserving the relevant facial skeleton, and not all have been X-rayed, fewer have been CT-scanned or visualized in any way that might obtain a careful estimate of paranasal sinus volume. It is possible that the actual volume of the sinuses does not change in anatomically modern *H. sapiens* over that of *H. erectus*. It may be the case that the same

size sinuses are filling a smaller face. Given the size and known pneumatization level of some of the early *H. sapiens* craniofacial specimens, this seems unlikely. In any event, the most obvious areas that are reduced in size and become virtually hollow sinus cavities in *H. sapiens* are the malar, zygomatic process of the maxilla, and the maxilla itself.

There has been much discussion of the functional and adaptive roles which sinuses play, especially in the Neandertals (Tillier, 1975; Stringer, 1979; Ward and Brown, 1986; Franciscus and Trinkaus, 1988). It does appear that there is a basic relationship between the volume of the paranasal sinuses and the functioning of these spaces during respiration and, perhaps less importantly, phonation (Taylor, 1981; DeLong and Getchell, 1987). Although we will likely never know their precise function, if the sinuses were indeed enlarged in early *H. sapiens* we can be sure their morphology as functional spaces (Moss and Young, 1960) was constrained by natural selection. The fact that some minimum paranasal air volume is conserved is evidence by two craniofacial syndromes, Crouzon and Apert, involving congenital synostoses. In these individuals a greatly reduced maxillary sinus is found correlated with a vastly expanded frontal sinus. The frontal sinuses, especially around the glabellar prominence, expand greatly, giving this area and the nasal bones below a "beaked appearance" (Tessier, 1986; Van der Meulen *et al.*, 1990; Cohen, 1986).

Whether or not the frontal air cells (and other facial sinuses) have dramatically increased in volume, the trend seen is for the curvature maxima, C1.1 and C1.3, over each one to move medially (as shown in Figure 2.4a-b) from their lateral position in *H. erectus* to modern *H. sapiens*.

Right Lateral Brow Ridge Curve

The "Unknown" (Un) non-Caucasian (AMNH in the table, N = 6) and the transitional fossil (listed by site in the table, N = 5: Arago, Kabwe, Petralona, Saldanha, Steinheim) right lateral brow ridge line tracings were compared to the *H. erectus* mean ridge curve (He, N = 9) and the Caucasian *H. sapiens* mean ridge curve (Hs in the table, N = 20).

Table 3.4 Findings: Right Lateral Brow Ridge Curve.

The He d = 5.6722, c = 0.2847. The Hs d = 3.0594, c = 0.9540

Specimen	Un-He *T* Statistic	Un-He χ^2 Prob.	Un-Hs *T* Statistic	Un-Hs Emp χ^2 Prob.	PR
AMNH 1439 M Chin	0.3542	0.9662	2.9871	0.3818	0.4
AMNH 1440 F Chin	1.2708	0.5734	3.7526	0.2771	0.5
AMNH 2382 M WAfr	0.4376	0.9446	1.0018	0.7980	0.9
AMNH 2386 F WAfr	0.9809	0.7153	0.9223	0.8177	1.1
AMNH 8173 M Aust	0.7386	0.8305	2.6357	0.4402	0.5
AMNH 8175 F Aust	0.1379	0.9969	2.0802	0.5468	0.6
Arago	3.1225	0.0757	1.8420	0.5979	7.9
Kabwe	5.7144	0.0021	7.9596	0.0413	19.7
Petralona	9.6358	0.0000	13.3395	0.0031	>31.0
Saldanha	4.0451	0.0224	6.3356	0.0879	3.9
Steinheim	14.0447	0.0000	19.7927	0.0001	>2.5

Description of Results

It appeared from a visual survey of the material that there might be clear separation of the supraorbital torus (the lateral brow ridge in this study) between the two species. Especially promising were the large lateral torsion

points, or the "handle-bars" of the brow (see Chapter 2, Character 2, page 58), present on most *H. erectus* and some "archaic" *H. sapiens*. However this feature seems to be very weak in the earliest Lake Turkana *H. erectus* and anatomically modern *H. sapiens*. The overlap in this feature between species is highlighted by the strong affinities the non-Caucasian modern specimens show to both samples (note the majority of the AMNH PR's < 1.0). Therefore no affinities are ascribed for this character.

Both Petralona and Steinheim show low affinities with either average. The phylogenetic implications of this character are discussed with the results from the left side in the following section.

Left Lateral Brow Ridge Curve

The "Unknown" (Un) non-Caucasian (AMNH in the table, N = 6) and the transitional fossil (listed by site in the table, N = 4: Arago, Bodo, Kabwe, Petralona) left lateral brow ridge line tracings were compared to the *H. erectus* mean ridge curve (He, N = 13) and the Caucasian *H. sapiens* mean ridge curve (Hs in the table, N = 20).

Table 3.5 Findings: Left Lateral Brow Ridge Curve.

The He d = 4.7246, c = 0.6481. The Hs d = 7.1083, c = 0.1766

Specimen	Un-He T Statistic	Un-He χ^2 Prob.	Un-Hs T Statistic	Un-Hs Emp χ^2 Prob.	PR
AMNH 1439 M Chin	5.9749	0.0867	0.7158	0.7833	9.0
AMNH 1440 F Chin	1.9638	0.6592	0.9530	0.6236	1.0
AMNH 2382 M WAfr	4.7259	0.1763	2.4295	0.0587	0.3
AMNH 2386 F WAfr	5.6283	0.1060	1.2943	0.4069	3.8
AMNH 8173 M Aust	2.5080	0.5299	1.0001	0.5916	1.1
AMNH 8175 F Aust	5.6313	0.1059	0.5050	0.9037	8.5
Arago	1.8349	0.6910	4.6189	0.0005	0.0
Bodo	3.7407	0.2969	2.1423	0.1010	0.3
Kabwe	4.6163	0.1872	5.1538	0.0001	0.0
Petralona	4.7660	0.1725	4.5685	0.0006	0.0

Description of Results

As with the right lateral brow ridge curve there is overlap in the affinities of the non-Caucasian moderns to either average curve (note two AMNH PR's are approximately 1.0 [equivocal affinity] and one is below 1.0 [*H. erectus* affinity]). This overlap was not as inconsistent as on the right side, however there were some other oddities. The affinities shown for the Arago, Kabwe, and Petralona specimens are the opposite of the right side. A possible explanation for the Arago specimen could be differential deformation on one or both sides, but this would not hold for the latter two skulls. No affinities are indicated by the lateral ridge curve alone.

Phylogenetic Implications

When this study began it was hypothesized that the lateral brow ridge would demonstrate two characterizable morphologies. However, there was a great deal of overlap found between the two samples for this character.

In terms of the within-sample variation, the data in Appendix B show that KNM-ER 3733 and 3883 are the two most different from the *H. erectus* average (lowest chi square probabilities); a fact which may offer partial support for Wood's (1992) contention that these Early Pleistocene African specimens may not belong in *H. erectus sensu lato*, but rather in a different species *H. ergaster* (see chapter 4 for more discussion). However, it is also possible that the morphology in these early African specimens is merely primitive for the species as a whole. It may be that approximately 0.5 million years of within-lineage (anagenetic) evolution beginning with forms like KNM-ER 3733, 3883, and WT 15000 could have resulted in the changes, especially in the supraorbital region, that allow OH 9 and the Asian *H. erectus* material to appear so similar (Rightmire, 1990).

It should also be mentioned that the variability in lateral brow ridge (i.e., the supraorbital torus proper) morphology is deserving of more study. The lateral brow measurements of Smith and colleagues (e.g., Smith and Ranyard, 1980; Smith *et al.*, 1989b) cannot discern the morphological dissociation of the brow that occured across the *H. erectus/H. sapiens* transition. Perhaps a single space curve tracing of the entire brow ridge (glabellar and lateral segment), along with some indication of surface curvature intensity along the brow, would provide a better morphological measure of this complex area.

Right Temporal Line Ridge Curve

The "Unknown" (Un) non-Caucasian (AMNH in the table, N = 6) and the transitional fossil (listed by site in the table, N = 2: Petralona, Steinheim) right temporal line tracings were compared to the *H. erectus* mean ridge curve (He, N = 10) and the Caucasian *H. sapiens* mean ridge curve (Hs in the table, N = 20).

Table 3.6 Findings: Right Temporal Line Ridge Curve..

The He d = 2.5709, c = 34.9315. The Hs d = 2.5073, c = 61.3600.

Specimen	Un-He T^2 Statistic	Un-He χ^2 Prob.	Un-Hs T^2 Statistic	Un-Hs Emp χ^2 Prob.	PR
AMNH 1439 M Chin	318.5126	0.0189	191.4894	0.2910	15.4
AMNH 1440 F Chin	34.6407	0.7320	38.5113	0.8264	1.1
AMNH 2382 M WAfr	57.4469	0.5657	99.0887	0.5593	1.0
AMNH 2386 F WAfr	31.0026	0.7612	43.7423	0.8008	1.1
AMNH 8173 M Aust	227.2374	0.0647	158.9190	0.3681	5.7
AMNH 8175 F Aust	153.8286	0.1700	88.5859	0.6004	3.5
Petralona	194.3881	0.1000	143.5638	0.4106	4.1
Steinheim	281.5311	0.0312	205.0816	0.2636	8.5

Description of Results

Three of the non-Caucasian specimens show much higher than expected affinities with the *H. erectus* mean. None of the AMNH *H. sapiens* specimens can be allocated to *H. erectus*, but their affinities to *H. sapiens* are equivocal (note three AMNH PR's ~ 1.0, i.e., overlapping affinities). Thus on this basis the affinities exhibited by the transitional specimens cannot be weighted highly. On the basis of the chi square model, and without any phylogenetic implications, what can be safely said is that these two transitional specimens appear less extreme as members of the Caucasian sample than as members of the *H. erectus* sample.

Of the two transitional specimens, the Steinheim skull shows the least affinity with the *H. erectus* mean. The degree of similarity with the Caucasian average right temporal ridge curve is greater than for than that on the left side of the Petralona skull (see next section). In any event, both transitional specimens show clear *H. sapiens* affinities but because there is overlap in the non-Caucasian affinities it appears that this character can be given only moderate importance. Phylogenetic implications for this character are discussed with those of the left temporal line in the next section.

Left Temporal Line Ridge Curve

The "Unknown" (Un) non-Caucasian (AMNH in the table, N = 6) and the transitional fossil (listed by site in the table, N = 2: Kabwe, Petralona) left temporal line tracings were compared to the *H. erectus* mean ridge curve (He N = 8) and the Caucasian *H. sapiens* mean ridge curve (Hs N = 20).

Table 3.7 Findings: Left Temporal Line Ridge Curve.

The He d = 7.5200, c = 10.2429. The Hs d = 2.5884, c = 34.9115.

Specimen	Un-He T^2 Statistic	Un-He χ^2 Prob.	Un-Hs T^2 Statistic	Un-Hs Emp χ^2 Prob.	PR
AMNH 1439 M Chin	344.0350	0.0000	152.3950	0.1750	>1750
AMNH 1440 F Chin	129.3871	0.1028	28.8810	0.7813	7.6
AMNH 2382 M WAfr	78.4114	0.4179	56.0325	0.5785	1.4
AMNH 2386 F WAfr	53.6739	0.6855	121.9749	0.2583	0.4
AMNH 8173 M Aust	116.6244	0.1514	37.8885	0.7097	4.7
AMNH 8175 F Aust	151.9502	0.0497	62.2732	0.5379	10.8
Kabwe	251.9068	0.0013	173.4089	0.1331	102.9
Petralona	572.8123	0.0000	252.2074	0.0469	>469.0

Description of Results

The results are similar to those for the right side. Both transitional specimens show much stronger similarity with the modern human average. However, overlap, especially like that seen in the *H. erectus* affinities of AMNH 2386 (PR < 0.5), raises questions as to the weight that can be given to the transitional specimens' similarity with the modern human average.

Phylogenetic Implications

Given the species samples used here, this measure exhibited enough overlap in affinities of the non-Caucasian modern humans, especially AMNH 2386, between the *H. erectus* and *H. sapiens* average ridge curves to make the affinities observed for the transitional fossil specimens suspect. This ridge curve may carry too much uncorrelated morphology, i.e. noise. It represents much of the origin of both the anterior and posterior temporal muscles. Only a very small portion of the latter, the posterior-most, is related to the

hypothesized Asian *H. erectus* (*sensu stricto*) apomorphy, the angular torus (Weidenreich, 1943).

It had been expected that a strong "gabling" (structural edge between sagittal and dorsal surfaces of the skull) would be detected in the *H. erectus* sample over that of the *H. sapiens* sample. Some of this effect does seem to have been detected in the coronal ridge curve tracing (see below). In the temporal ridge curve it was assumed that running anteroposteriorly on the upper margin (i.e., the gable) landmarks C3.2 and C3.3 would project much further superiorly than would landmark C4.1 or C4.3 (stephanion). On visual inspection it appeared a higher (more superior) position of these landmarks would demonstrate *H. sapiens* affinities.

Future study of the segment(s) between C3.3 and C3.4 might elucidate more about the area of the angular torus, although a true robusticity index (i.e., strength of the toral marking) would require a very detailed analysis of the surface morphology of this region. An analysis of the segments between landmarks C3.1 and C3.3 might give more evidence of the proposed anterosuperior movement of landmark C3.2. Similarly an analysis of the segments between landmarks C3.2 and C3.4 might give more evidence of the proposed posterosuperior movement of landmark C3.3. This hypothesis could be directly tested via "shape coordinates" (Bookstein, 1991).

The anterosuperior movement of landmark C3.2, like the anterior projection and superior bowing of the glabellar ridge segment and the development of frontal bossing (discussed above), is expected to track the reorganization of the frontal lobes. Similarly, the posterosuperior movement of landmark C3.3 should track the growing prominence of euryon, the lengthening of the superior sagittal suture chord (relative to the squamous suture chord), and the development of the pentagonal posterior view characterizing *H. sapiens*.

All three of the transitional specimens sampled showed overwhelming affinities to the modern human average curve. Further study is merited that would, perhaps, lead to a better characterization of the effect of the temporalis muscle on the lateral walls of the skull.

Coronal Suture Ridge Curve

The "Unknown" (Un) non-Caucasian (AMNH in the table, N = 6) and the transitional fossil (listed by site in table, N = 6: Eliye Springs, Kabwe, Petralona, Reilingen, Salé, Swanscombe) coronal suture line tracings were compared to the *H. erectus* mean ridge curve (He, N = 13) and the Caucasian *H. sapiens* mean ridge curve (Hs in the table, N = 20).

Table 3.8 Findings: Coronal Curve.

The He d = 1.6989, c = 64.2016. The Hs d = 3.3957, c = 23.3648.

Specimen	Un-He T^2 Statistic	Un-He χ^2 Prob.	Un-Hs T^2 Statistic	Un-Hs Emp χ^2 Prob.	PR
AMNH 1439 M Chin	407.0073	0.0306	71.1787	0.4516	14.8
AMNH 1440 F Chin	487.2716	0.0160	37.9900	0.7205	45.0
AMNH 2382 M WAfr	251.6619	0.1083	145.7373	0.1300	1.2
AMNH 2386 F WAfr	748.2576	0.0020	88.8265	0.3423	171.2
AMNH 8173 M Aust	228.6146	0.1310	47.4329	0.6369	4.9
AMNH 8175 F Aust	555.1318	0.0093	45.4731	0.6539	70.3
Eliye Springs	55.7831	0.5698	449.5171	0.0004	0.0
Kabwe	57.7933	0.5596	339.5715	0.0034	0.0
Petralona	36.7768	0.6783	305.1144	0.0066	0.0
Reilingen	71.8085	0.4939	147.6293	0.1257	0.3
Salé	257.6492	0.1031	548.8889	0.0000	0.0
Swanscombe	301.2694	0.0721	252.7420	0.0180	0.3

Description of Results

While AMNH 2382 shows equivocal affinities, there is no overlap in this character (note all AMNH PR's > 1.0). All of the transitional specimens show clear affinities with the *H. erectus* average for this character. Both Swanscombe and Reilingen, which are thought to have several Neandertal or late "archaic" *H. sapiens* features (depending on the worker), show greater affinity with the modern average than the other transitional forms.

Phylogenetic Implications

One interpretation of the results from this character could be that all of the transitional specimens are plesiomorphic, assuming *H. erectus* presents the primitive condition. It would be useful to bring a mean curve for *H. habilis* into the analysis for more indication of the polarity. It is interesting to note the increased affinities of the Swanscombe and Reilingen specimens with the modern

human average. Perhaps this character records progress toward the modern condition in later "early" and "late archaic" populations, although without more evidence this statement should be made guardedly. From the point of view of the results obtained here, it also would be interesting to broaden the coronal suture curve sample across populations of "late archaic" *H. sapiens*.

Another character which shows similar variability is the presence of a vertical frontal squama. On the one hand, the Zhoukoudian cranial specimens show a protuberant prebregmatic eminence that appears vertical in lateral view. However, "early archaic" specimens, for the most part, do not show the vertical frontal seen in some later "archaic" and most modern human groups. Because this feature is not present in all modern human populations, its presence in any does not necessarily support the late or restricted origin of modern humans either.

Information on the variability of coronal suture shape, and that of the vault in general, is needed across all modern populations; there is a good deal of verbiage in the literature, mostly older texts, but very little quantification. For example, information on the relationship between postorbital constriction and frontal squama elevation would be useful. Many of the general relationships posited for the dolicho-meso-brachycephalic continuum (Weidenreich, 1941; Enlow, 1990) have not been demonstrated metrically.

Superior Nuchal Line (Nuchal Torus) Ridge Curve

The "Unknown" (Un) non-Caucasian (AMNH in the table, N = 6) and the transitional fossil (listed by site in the table, N = 7: Eliye Springs, Ndutu, Petralona, Reilingen, Salé, Steinheim, Swanscombe) superior nuchal line tracings were compared to the *H. erectus* mean ridge curve (He, N = 14) and the Caucasian *H. sapiens* mean ridge curve (Hs in the table, N = 20).

Table 3.9 Findings: Superior Nuchal Line.

The He d = 4.3421, c = 62.6186. The Hs d = 6.9551, c = 66.2133.					
Specimen	Un-He T Statistic	Un-He χ^2 Prob.	Un-Hs T Statistic	Un-Hs Emp χ^2 Prob.	PR
AMNH 1439 M Chin	428.50	0.1724	157.9591	0.9336	5.4
AMNH 1440 F Chin	953.20	0.0057	170.7828	0.9188	161.2
AMNH 2382 M WAfr	467.60	0.1366	274.8989	0.7579	5.6
AMNH 2386 F WAfr	862.20	0.0106	53.3090	0.9973	94.1
AMNH 8173 M Aust	700.60	0.0313	61.4035	0.9957	31.9
AMNH 8175 F Aust	326.80	0.3071	155.0844	0.9367	3.1
Eliye Springs	131.00	0.7645	720.7054	0.1411	0.2
Ndutu	214.40	0.5416	485.5790	0.3902	0.7
Petralona	434.00	0.1669	230.2105	0.8342	5.0
Reilingen	303.60	0.3477	393.7638	0.5409	1.6
Salé	1457.1	0.0002	269.8942	0.7668	3834.0
Steinheim	1803.0	0.0000	248.9834	0.8031	>8031.0
Swanscombe	1545.0	0.7000	497.4702	0.3728	0.5

Description of Results

As with the coronal suture, this character appears to have little overlap. Three of the non-Caucasian specimens (AMNH 1439, 2382, and 8175) show χ^2 probabilities > 0.1 of falling within the *H. erectus* sample, however, all three of these specimens also show greater affinity with the modern average curve (note no specimen shows a PR < 3.1, i.e., no overlap). The Salé and Steinheim specimens show definitively

stronger association with the *H. sapiens* mean curve (note PR > 3800 for both), but the Salé specimen may exhibit a congenital deformation in this area (Hublin 1985, pers. comm.).

The Ndutu PR ratio is equivocal. The Swanscombe and Eliye Springs PR's demonstrate *H. erectus* affinities. Judging from the KNM-ES 11693 cast of Eliye Springs that I used and photographs of the original, it seems possible that this cranium has been plastically deformed in this area. Therefore, interpretation has to be tempered. The Ndutu specimen may also be diagenetically deformed, through both plastic warpage and breakage. Overall the reconstructed Ndutu specimen appears to have similar dimensions, especially length and breadth, as in the Steinheim cranium (Clarke, 1990). However, pictures of the unprepared specimen show the vault, especially at the lateral ends of this ridge curve, having been severely flattened mediolaterally. This damage appeared to have been corrected in the reconstruction. It is clear on both the original find and the reconstruction that the nuchal planum is rotated inferiorly as in other "early archaic" *H. sapiens*, as was first noted by Clarke (1990). This makes its affinity with the *H. erectus* mean all the more puzzling. The role of deformation in this area is unknown since I have not observed the original specimen.

Reilingen and Swanscombe show the most affinity with the *H. erectus* average. It appears that the "en bombe" (a

reversal?) morphology present in the latter two is responsible. That is, Neandertals show levels of posterior occipital projection similar to *H. erectus*. However, Neandertals do not have the superior rotation of the nuchal-planum/torus/upper-occipital scale complex. Petralona, Salé, and Steinheim show clear affinities with the average modern curve. Unfortunately the effect of the elevation or inferior rotation of the SNL does not affect this analysis as strongly as length and width of the curve in the nuchal plane.

Phylogenetic Implications

The first and last segments of the curve (the first between the starting-point and point C5.1 and the last between the other endpoint and C5.5) outline the superior margin of both splenius capitus muscles. These segments, therefore, indicate how this muscle affects occipitomastoid morphology. Landmarks C5.2 and C5.4 represent the superior-most insertion points of both semispinalis muscle bellies. Landmark 5.3, inion, is affected by: the medial margins of both semispinalis muscles, the insertion of the trapezius muscle, and the (primary) attachment of ligamentum nuchae.

Together both segments (segment 1: end-C5.1, C5.4-end and segment 2: C5.1-5.3, C5.3-5.4) of this curve give an indication of the posterior versus mediolateral projection of the superior nuchal line in the nuchal plane. Posterior projection is the dominant component in *H. erectus* whereas, apart from the Neandertals, brachycephalization seems to

have made mediolateral projection a larger contributor to nuchal morphology from the time of the transition through to modern people. However, data for later Middle and Late Pleistocene "archaic" *H. sapiens* will be needed to test this proposition.

The nuchal ridge curve, as digitized, does not measure the orientation of the nuchal planum or the relationship of the upper and lower occipital scales. A ridge curve of half the superior nuchal line with the addition of a portion of the midsagittal chord from basion to lambda might better serve measure the orientation of the nuchal planum versus the rest of the skull. The Solo skulls are an example within the *H. erectus* sample where such a ridge curve would be useful. The Solo specimens show a more vertical upper occipital scale than in most other *H. erectus*. However, the nuchal planum is still highly elevated above the Frankfurt horizontal as in other *H. erectus*. Endocast evidence shows that while there has been brain expansion in the Solo population compared to most other *H. erectus*, however instead of an inferior rotation of the occipital lobes and cerebellum there is posterior expansion of the occipital lobes and an anterior shift of the cerebellum (Grimaud-Hervé, 1991), a Bauplan similar to other Indonesian and Chinese *H. erectus* (Holloway, 1980; Santa Luca, 1980). It appears that more substantial landmark and surface morphometric techniques could be profitably applied to the

study of the evolutionary changes seen across hominid basicranial and vault morphology.

Summary of Results

This section presents a brief review of the results with some discussion of how they relate to topics covered in Chapters 1 and 2. The circumvault features measured were a test of the theory that there was a shift in craniofacial architecture that occured across the *H. erectus/H. sapiens* transition. The evidence presented supports overall allocation of all the "transitional" specimens to "archaic" *H. sapiens* on the basis of glabellar brow ridge and superior nuchal line morphology, except for the measure of the glabellar ridge curve on Arago and Saldanha. Of this "early archaic" group, Saldanha and Bodo seem to present, overall, the most conservative morphology, whereas Arago seems damaged, somewhat less conservative, and perhaps evinces Neandertal features.

While the characters measured here suggest a major architectural change occured during the transition to earliest *H. sapiens*, late *H. erectus* did attain cranial capacities well within the range of earliest *H. sapiens*. However, brain size alone is not a very strong character. Late *H. erectus* populations preserve architectural features of the vault that include a superoposteriorly angled nuchal planum, constricted frontal lobes, and continuous supraorbital tori anterior to an ophryonic sulcus. In

distinction to these features, the earliest *H. sapiens* specimens show a more prominent glabellar brow ridge segment, loss of the ophryonic groove, development of frontal bosses, varying lateral brow morphology, somewhat variable but apparently different temporal line morphology, apparently no change in coronal suture shape, an inferiorly rotated superior nuchal line with prominent external occipital protuberance, and an inferiorly directed, weaker laterally than medially, nuchal torus . A summary table of the affinities of the transitional fossils based on characters 1, 3, 4, and 5 (i.e., the definitive, non-overlapping characters) appears below.

Table 3.10: Summary of Diagnostic Characters.
Codes: (+) = *H. sapiens,*(-) = *H. erectus, (blank) = missing.*

Specimen	Glabellar Prominence	Temporal Line	Coronal Suture	Superior Nuchal Ln.
Arago	-			
Bodo	+			
Eliye Springs			-	-
Kabwe	+	+	-	
Ndutu				-
Petralona	+	+	-	+
Reilingen			-	+
Saldanha	-			
Salé			-	+
Steinheim		+		+
Swanscombe			-	-

In sum, this morphometric analysis of the vault detected two prominently affected areas, the glabellar ridge segment and the nuchal torus. These results suggest that glabellar and nuchal changes are baseline apomorphies of the species *H. sapiens*.

Traditionally, these two characters have been associated with either the downward flexion, or kyphosis, of the anterior and middle cranial base areas (i.e., the pituitary angle) or other descriptors captured in *norma lateralis* projections or cross-sections. Traditionally, discussion of cranial base "kyphosis" has been restricted primarily to measurements of inferior flexion of the sphenoid clivus in *norma lateralis* versus the anterior cranial base. Changes in the posterior cranial base, and their relationship to the orientation and morphology of the upper and lower occipital scales have likewise been drawn from lateral views of the skull highlighting mid-sagittal landmark relationships, such as the coincidence of opisthocranion, inion, and endinion. The new morphometrics (Rohlf and Marcus, in press; Bookstein, 1991), especially the comparison of three dimensional representations of form, should make for a richer description of evolutionary changes that will add to current knowledge but allow a far more exhaustive approach to the data.

IV Discussion and Conclusions

"Following about 0.4 million B.P. we have a sampling of hominids from many parts of the world that are clearly not *Homo erectus* but yet do not resemble modern *Homo sapiens* either. ... **At a deeper level, however, the inclusion of these forms in *Homo sapiens* seems to reflect not only the myth of a restricted morphological space between *Homo erectus* and modern man,** into which paleoanthropologists have been reluctant to intrude another species, but also the generous liberalism we spoke of earlier, which makes excluding large-brained hominids from our own species seem somehow nastily discriminatory." (emphasis added)

Niles Eldredge and Ian Tattersall (1982)

"In fact, the recent populations included here seem, on another look, to be cranially rather homogeneous, with a limited dispersion of character into which some early upper Pleistocene specimens like Dali, Ngaloba, Qafzeh, or Border Cave--or even later ones like Afalou or Mladeč --might be introduced only with trepidation. This, I think, is a feeling my colleagues would share. **What we have lacked is a measure of the degree of likeness among all moderns, and a measure of the distinctness of the patterns considered above.** The search for such things calls for more rigorous numerical treatment ..." (emphasis added)

William W. Howells (1989)

"While the origin of *Homo erectus* appears to have been a cladogenetic event, no cladogenesis marks the appearance of archaic ***Homo sapiens*** **and there is no distinct boundary between these in either time or morphology."** (emphasis added)

Milford H. Wolpoff (1992)

"Don't let it end like this. Tell them I said something."

Pancho Villa's last words (1923)

Overview

Perhaps the most important goal of this project was to survey potential characters and add morphometric evidence to the debate over the *H. erectus/H. sapiens* transition. It was hoped that morphometric-assisted character identification

and discrimination might bring about better agreement on what significant morphological differences, if any, separate *H. erectus* and *H. sapiens sensu lato*. Such hard-nosed character analysis is necessary in order to "weight" characters. The robusticity of a character depends on the investigator's ability to observe, delineate, describe, and explain the etiology of the salient morphology. If transformations are vital to the character state, they must not contradict ontogenetic, functional, and phylogenetic (outgroup) information. Without such weightable assumptions behind characters the effects of homoplasy (convergence, parallelism, and reversal) will be rampant.

It is assumed that the characters analyzed for this thesis, as well as others discussed in this chapter, are of use to the debate on the origin of *H. sapiens*. The *H. erectus/H. sapiens* transition involves character transformations within and between two species. The issues surrounding Early and Middle Pleistocene *H. erectus* origin and evolution and later interaction amongst *H. erectus* derivatives in producing the *H. erectus/H. sapiens* transition are discussed in the first section of this chapter. The second section discusses the issues surrounding the origin of *H. sapiens* and this species' continued evolution through the Late Pleistocene. A summary of these ideas appears at the end of the chapter as well as in the thesis abstract.

Plio-Pleistocene Hominin Evolution

As was discussed in chapter 1, Leakey (1966, 1972) and Andrews (1984), called attention to the overall similarity between *H. habilis* and later anatomically modern *H. sapiens*. That these similarities are plesiomorphous was obvious to both, but that does not obviate the need to know about intervening populations, especially if there are any side-branches or qualitative leaps indicating another species. Wood (1984, 1991, 1992; Bilsborough and Wood, 1986) has discussed the problems of species identification in the Plio-Pleistocene. He currently proposes *H. habilis* (e.g. KNM-ER 1813) as an Early Pleistocene common ancestor for separate lineages of Asian *H. erectus* and African *H. ergaster*, the latter being the ancestor of *H. sapiens*. Wood finds various levels of support for this position from Hublin (1983), Stringer (1984), Groves (1989a), Clarke (1990), and Rightmire (1993).

The superior rotation and posterior projection of the occiput and the continuous supraorbital torus/ophryonic groove complex, seen clearly in *H. erectus*, is indicated but is not as robustly present in Olduvai *H. habilis*, i.e., OH 13, 16, 24 (Tobias, 1980, 1991). These features are also apparent in KNM-ER 1813 and in the brow region of SK 847 (Clarke, 1985). It would appear both specimens belong in *H. habilis* (*sensu* Wood, 1992), not *H. rudolfensis* or *H. erectus sensu lato*. Without further study, it would be premature to argue that the presence of advanced supraorbital morphology

and a superiorly rotated occiput alone support the inclusion of these specimens in *H. erectus sensu lato,* but the lack of this morphology seems a good argument for not including Stw 53 or KNM-ER 1470 in *H. habilis*. This "missing" morphology is all the more incongruous given that specimens like KNM-ER 1470 and 3732 (and perhaps 1590) are larger crania with relatively large brain volumes. Yet, there is less anterior projection of the brow, especially medially, of these two specimens than in the diminutive KNM-ER 1813 (Wood, 1991). In terms of the nuchal torus, visual comparison of the proportions in KNM-ER 1470 and Stw 53 show inion not as elevated and a shorter nuchal (lower occipital) scale than in KNM-ER 1813 or OH 24. The upper occipital scale is also rounded in KNM-ER 1470, as in earlier *Australopithecus*. Unlike OH 24, KNM-ER 1813, and *H. erectus sensu lato,* the lower occipital scale of KNM-ER 1470 and Stw 53 is proportionately short and inferiorly rotated, as in *Australopithecus.* Bromage's (1992) reconstruction of the midface of KNM-ER 1470 is also reminiscent of Stw 53 and KNM-ER 1805. These three specimens do seem to show a more superiorly positioned opisthocranion than inion, which is not typical for *Australopithecus*. Noting such differences, Wood (1992) assigns KNM-ER 819, 1470, 1482, 1483, 1590, 1801, 1802, 3732, 3891 and KNM-BC1 to a sister taxon of *H. habilis, H. rudolfensis*. On the evidence presented here KNM-ER 1805 and Stw 53 could also be allocated to *H. rudolfensis.* Wood does not comment on Stw 53; however,

Tobias (1991) and Clarke (1985) have suggested other features ally it with *H. habilis*.

Wood and Chamberlain (1986; Chamberlain and Wood, 1987) show clear support, including several synapomorphies, for the inclusion of *H. habilis* and *H. rudolfensis* in *Homo*. Wood (1992) has further posited that the overall morphology seen in the earliest African *H. erectus sensu lato* is unlike OH 9, or any of the extra-African *H. erectus sensu lato*, and therefore he assigns KNM-ER 730, 731, 806, 820, 992, 1466, 1507, 1648, 1808, 1812, 1821, 2592, 2598, 3733, 3883, 3892, and KNM-WT 15000 to *H. ergaster*. KNM-ER 992 was designated the type of *H. ergaster* by Groves and Mazák (1975). Wood (1984, 1985, 1991, 1992), like Leakey (1972) and Andrews (1984), has called attention to the special similarity that this subset of specimens shows to *H. sapiens* over the larger sample of specimens usually ascribed *to H. erectus sensu lato*.

Dividing the ancestry of African and Asian *H. erectus sensu lato* in the Early Pleistocene (or Pliocene?) from an *H. habilis*-like, common ancestor necessitates explanations of newly parallel characters. Bromage (1992) has recently documented one of the more robust synapomorphies of *H. erectus sensu lato*. He has shown that changes in craniofacial hafting in earliest *H. erectus* correspond to a major shift toward orthognathy and concomitant increasing vertical height of the face. The 30% increase in *H. erectus* orbitomeatal angle marks a clear divergence from *H. habilis*

sensu lato. Bromage (1992, pers. comm.) suggests there is a decrease in this angle from *H. erectus* to *H. sapiens*.

Mayr (1951), Leakey (1972), Santa Luca (1980), and Rightmire (1988, 1990), amongst others, have all strongly advocated the specific unity of African and Asian *H. erectus* samples. In making a case for the integrity of *H. erectus sensu lato*, Rightmire (1990) has called attention to the similarities between OH 9 and the Asian *H. erectus* specimens. Turner and Chamberlain (1989) agreed with Rightmire that OH 9 is properly assigned to *H. erectus*, a taxon defined for the Asian specimens. They conclude:

> "Overall, we are unconvinced that a case has been made for autapomorphies confined to Asian representatives of *Homo erectus* and for the exclusion of the African specimens from the hypodigm."

Bräuer and Mbua (1992) have shown that there is vast overlap in the features Andrews (1984), Wood (1984), and Stringer (1984) proposed to be apomorphies of Asian *H. erectus sensu stricto*. Bräuer and Mbua's (1992) survey of virtually the entire relevant fossil record shows that these characters do not separate either the whole or any part of *H. erectus* from "archaic" *H. sapiens*. Bräuer and Mbua make three very important comments on these characters: First, their appearance seems to be intercorrelated. Thus, they lend the most support to the identification of *H. erectus* based on combined use with the supraorbital and nuchal features described in this thesis. Second, the presence or absence of many of these features differs among authors.

Thus, better morphometric techniques are needed to choose among competing impressions. This highlights the need to discontinue allocating specimens to species via scoring techniques whereby presence of some number of characters from a list allows a positive identification; instead, discontinuous character states, or at least clearly characterizable population frequencies of a single character state that discretely indicate its presence or absence are needed. Third, and most importantly, many of the proposed Asian *H. erectus* apomorphies may be epiphenomena of other more diagnostic characters as opposed to primary characters themselves. Therefore, the architectural shifts between *H. habilis* and *H. erectus*, as well as between *H. erectus* and *H. sapiens*, need to be better described. This will result in better measurements documenting those character transformations.

As presented in chapter 1, the working hypothesis of this thesis has been that one set of apomorphies demarcates the origin of *H. erectus* and yet another set of features, also primarily corollaries of an increase in size and repacking of the brain, evidences earliest *H. sapiens*. The increase in size, over 1200 cc, in earliest *H. sapiens* seems to be paralleled at least in Solo skull V and Zhoukoudian skull 10 (Weidenreich, 1943). However, even these larger-brained individuals do not show the characteristic glabellar or nuchal morphology demonstrated here as characteristic for earliest *H. sapiens*.

The Origin of *H. sapiens*

An earlier Middle Pleistocene origin of *H. sapiens* suggests the earliest population displayed a morphology somewhere between OH 9 and Bodo and perhaps Saldanha, although both of these specimens may be very close to this ancestral morphotype. This localization of the earliest *H. sapiens* population can be contrasted to Wood's (1992) model of a Plio-Pleistocene divergence of *H. erectus* and *H. ergaster* and an Early through Middle Pleistocene gap in the record between *H. ergaster* and *H. sapiens* (and any intervening species). From this perspective there is no need to factor in characters seen in later Middle Pleistocene *H. erectus* specimens from Olduvai, Zhoukoudian, Hexian, Sangiran, and Solo. Unfortunately the paucity of European and African hominin fossils dated with certainty to the period between the later Early Pleistocene and early Middle Pleistocene is a major problem for all models.

If there was a cladogenetic event at the origin of *H. sapiens*, we are left with the question of where this population first arose, the geographical area analogous to that referred to by Wolpoff (1989a) as the "Garden of Eden." No species, not even modern humans, maintains uniform coverage of the earth's surface. All species utilize some ecozones more than others. Although this ecozone can shift about through time, at any one time its largest distribution will likely correspond to the species greatest density. This area may be referred to as a gene sink, referring to its

role as the place where the population shrinks back to in times of environmental stress (i.e., island biogeography *sensu* Wright, [1969]).

Foley (1989) suggests oscillations of Pleistocene glacial maxima and minima would have served to isolate hominin populations, including those within Africa. Any one of these could have given rise to an emigrating population as conditions ameliorated. Africa's role as the largest reserve of temperate to tropical habitat (Foley, 1987) makes it the most likely candidate in the Pleistocene. However, Multiregional (MR) advocates have suggested that more northerly sites such as Torralba and Ambrona, Atapuerca, and Zhoukoudian evidence continuous (including glacial maxima) habitation. Delson (1981; Delson and Brooks, 1988; Dean and Delson, in prep.) has suggested a possible role for glacial isolation of a northerly extra-African *H. erectus* population, most likely in southeastern Europe or southwestern Asia (i.e. the Paratethys basin between the Alps, Caucasus, Urals, Zagros, and Levantine ranges) as a possible source for the allopatric evolution of earliest *H. sapiens*.

It remains to be seen if the Dmanisi mandible, claimed to be later Early Pleistocene, is the first specimen from this region to evidence *H. erectus* features. There are also three famous archeological sites that have so far not offered any useful human skeletal material. From oldest to youngest: Olorgesaile, Vallonet, Kärlich, and Isernia (in

Kenya, France, Germany, and Italy, respectively) offer glimpses into the latest Early and earliest Middle Pleistocene. However, of those sites producing skeletal finds, two early Middle Pleistocene sites in Africa give the best current evidence of earliest *H. sapiens*. The advanced supraorbital and frontal morphology of the skull from the Middle Awash site of Bodo and the advanced mandibular morphology (e.g., vertical symphysis, incipient mental trigone, wide symphyseal and intercondylar breadth; *contra* Howell, 1960) of the Ternifine specimens make Africa seem the most likely place for the earliest *H. sapiens* population. However, the Mauer mandible does offer evidence for theories involving European populations.

A question important to the origin of *H. sapiens* is at what point, if at all, were the extra-African *H. erectus* populations, especially those in the Far East, genetically isolated from their African contemporaries, the progenitors of *H. sapiens* (see Figure 4.1)?

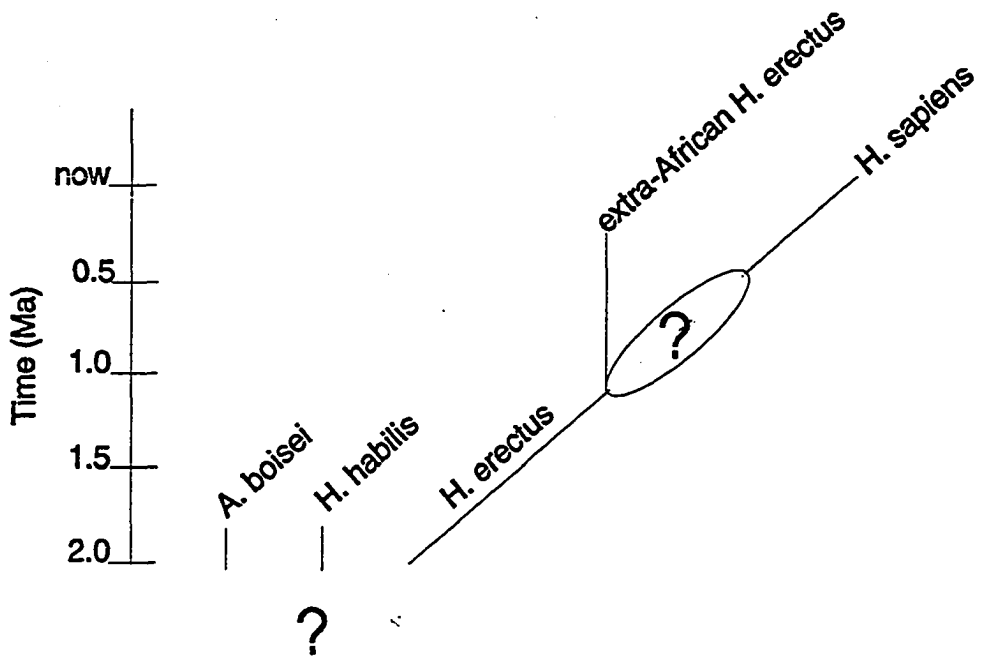

Figure 4.1 *H. erectus* Out of Africa: When was *H. erectus* genetically isolated from "archaic" *H. sapiens*?

The determination of when and where this isolation occurred depends on the characters used to mark the Middle Pleistocene origin of *H. sapiens*. The answer to this question also depends on how many migrations there were out of Africa by *H. erectus* populations? Given the well known Asian record for *H. erectus* it would seem that there was at least one window of opportunity in the late Early or early Middle Pleistocene for *H. erectus* populations to migrate to the Far East and at the same time possibly Europe. Turner (1992) suggests that carnivore-mediated scavenging opportunities may have precluded such migrations, at least to Europe, before the Middle Pleistocene.

If there were multiple migrations out of Africa, there may have been little contact between new and old inhabitants

of Eurasia, or perhaps there was continuous interchange. Dong (1989) and Picq (nd) have questioned the unity of Javan and Chinese *H. erectus*, raising the possibility of at least two immigrant waves of *H. erectus*. There is also unanswerable speculation (Thorne and Wolpoff, 1981; Li and Etler, 1992; Pope, 1992) as to whether there could have been gene flow between these regions before the late Middle Pleistocene appearance of earliest *H. sapiens* in China.

Both Li and Etler (1992) and Pope (1992) have recently pointed to the appearance of "modern" human features on the apparently "early archaic" *H. sapiens* crania from Dali, Jinniushan, and Yunxian. Pope (1992) suggests these populations may evidence the earliest appearance of *H. sapiens*. Li and Etler (1992) also suggest regional links between the morphology of the Yunxian specimens and Asian *H. erectus*, but prefer not to cite Asia as the site of origin for the earliest modern features, much less the earliest moderns humans. Instead, they suggest that a mosaic of different regional features eventually coalesced into the modern distribution.

Li and Etler (1992) claim that the Yunxian specimens demonstrate continuity of features with earlier and apparently contemporaneous Chinese *H. erectus* primarily on the basis of the preservation of vault and basicranial features. Judging from published pictures, both specimens appear highly crushed and deformed. It seems that diagenetic processes may have produced several of the features they

cite as regionally continuous. Interestingly the less crushed specimen, EV 9002, appears to have a significantly shortened lower occipital scale. This suggests that inion is positioned inferiorly (i.e., inferiorly rotated nuchal plane). Both specimens appear to show a horizontally oriented lower occipital scale. Along with the protruding glabellar region, overall, these specimens appear to evince "early archaic" *H. sapiens* morphology.

Pope (1991) details other proposed regional Asian features that would link *H. erectus* and *H. sapiens* populations across the later Pleistocene. Principal among these continuous features is the "incisura malaris" and low set maxillary buttress or infrazygomaticomaxillary margin (IZM). Only the latter is found in *H. erectus* but the former, according to Pope (1992), first appears in Chinese "archaic" *H. sapiens*. Pope (1992), claiming yes, and Li and Etler (1992), claiming no, disagree as to whether the IZM is low set in the two Yunxian specimens. The etiology of this feature needs to be better understood, judging from its variability in African "early archaic" *H. sapiens* such as Bodo (low) and Broken Hill (high). It is also variable among European "early archaic" *H. sapiens,* but later this feature fixes to be more uniformly low, sweeping anteroinferiorly from the malar, in Neandertals *sensu stricto*.

Pope (1992) emphasizes the narrow tympanomastoid fissure and thickened cranial bones seen in Dali, claiming its intermediacy between *H. erectus* and later *H. sapiens*.

However, both features have been shown to be variable within *H. erectus* and "archaic" *H. sapiens* by Bräuer and Mbua (1992). Pope judges Jinniushan to be more advanced than Yunxian or Dali because of its large cranial capacity (1390 cc) and thin cranial bones. However, its occipital, supraorbital, and midface morphology is consistent with "early archaic" *H. sapiens* elsewhere. On the one hand, Pope (1992) offers a tortuous account of mixed similarities amongst Jinniushan, Dali, and Maba. On the other hand, he notes similarities between Maba and Djebel Irhoud (an advanced "late archaic" *H. sapiens*) but fails to note that Maba is probably more similar in several of these features to other "late archaic" *H. sapiens* such as Zuttiyeh and Narmada. He admits straining to avoid the early claims of Neandertal status for the specimen despite the discontinuous glabellar and lateral brow segments and a frontal prominence, both of which he cites as evidence of Asian regional continuity.

A sophisticated morphometric analysis may be necessary to show the claimed continuity, i.e., homology, in various features between Chinese *H. erectus* and populations prevalent in contemporary eastern Asia. Given agreement on the *H. sapiens* status of the Yunxian, Jinniushan, and Dali specimens, perhaps the most interesting data presently available are that all are potentially contemporary with or perhaps slightly older than the youngest *H. erectus* late Middle Pleistocene specimens known from Zhoukoudian and

Hexian (Chen, and Zhang, 1991; Yuan *et al.*, 1991). This fact makes immigration of "archaic" *H. sapiens* from the west a more likely scenario than *in situ* evolution.

Like Li and Etler (1992), Wolpoff (1992a and b; Thorne and Wolpoff, 1991) and Tattersall (1992a and b) argue against the presence of Middle Pleistocene features unique to *H. sapiens*, anywhere, but for opposing reasons. Wolpoff has argued against the African origin of *H. sapiens* because he claims the earliest anatomically modern specimens (Late Pleistocene) in Africa and the near East do not present features consistent with living sub-Saharan Blacks. Of course this teleological argument could be applied to earliest African or European *H. sapiens*. Wolpoff (1989a) asks why, assuming MR continuity of racial features, they aren't present in the earliest members of our species in a particular region. Tattersall (1986, 1992a and b) argues that there are no *H. sapiens* features in Middle Pleistocene hominin material because there were several allochronic hominin species at this time, only one of which survives as modern humans.

I would suggest that the features characterizing *H. sapiens sensu lato* seem to be related to a *major architectural shift in the vault* with ramifications in most other portions of the skull. Lieberman *et al.* (1992; but see Houghton, 1993) note that the basicranial changes associated with modern vocal capabilities are first apparent on earliest *H. sapiens* specimens such as Broken Hill. Does the

origin of *H. sapiens* have any other correlates, especially cultural? It has been suggested that there is no lithic revolution associated with the Middle Pleistocene appearance of *H. sapiens* (Klein, 1983), but Delson *et al.* (1977) suggested there may be a correlation with the first appearance of "prepared core" technology. It is only much later that Middle Paleolithic industries appear amongst various groups of "archaic" and "modern" humans (Bar-Yosef, 1992a).

The Archaic to Modern Transition

As was discussed in Chapter 1, most of the OA versus MR debate has centered on the origin of anatomically modern *H. sapiens*. If one ignores "late archaic" *H. sapiens*, conveniently ignoring significant morphology and forcing their assignment to anatomically modern *H. sapiens*, debate can continue as to whether and where anatomically modern humans diverged from *H. erectus*. In such chaos calls to erect new species, such as for the "early" and "late archaics," will abound.

It is interesting to consider the uniformity of morphology among "early archaic" *H. sapiens* specimens noted by Bräuer (1984a) and Stringer *et al.* (1979). These include the similarities in supraorbital and nuchal tori morphology, described earlier. The malar is flattened in the frontal plane but the robusticity of the maxillary buttress and the height of its insertion into the maxilla vary widely. There

is a consistent depression seen, especially laterally along the mid-sagittal arc, between obelion and lambda among "early archaic" *H. sapiens* as well.

There is a trend toward parietal expansion between "early" and "late archaic" *H. sapiens* which ends in the modern human adult's pentagonal posterior view and the almost bizarre parietal tubers seen in most newborns. Modern frontal morphology ranges from the flattened frontal squama of some Australian populations, nearly equivalent to that seen in the earliest "archaic" *H. sapiens*, through the mid-sagittal frontal bossing of some Nilotic and Bantu African groups, to the vertical flat frontals and laterally placed frontal bosses of many northern European populations. Overall vault shape is quite varied in modern groups and ranges from extreme dolichocephaly through mesocephaly to the near turricephaly of the most brachycephalic Caucasian and Asian peoples (Enlow, 1990).

The presence of unique features of early *H. sapiens* have led Rightmire and Tattersall to propose one or more species of Middle Pleistocene hominin other than *H. sapiens*. It is my opinion, however, that a level of diversity consistent with that among modern *H. sapiens* appears early on in "early archaic" *H. sapiens*. It is likely that geographical gradients of features begin to occur in *H. sapiens* highlighted by the appearance of the Neandertals, other groups of primarily long-headed "late archaics", and eventually anatomically modern *H. sapiens*. It is likely that

each region's population underwent interchange with others through time, making it difficult to interpose another species once *H. sapiens* has appeared. The level of variation seen within *H. sapiens* is relatively greater than that seen between Early and Middle Pleistocene *H. erectus*, probably, in part, because of increased population densities, varied lifeways, and environments inhabited. However, the level of overlap among "early" and "late archaic" and anatomically modern *H. sapiens* groups argues for the integrity of a single species, *H. sapiens sensu lato*, since the earlier Middle Pleistocene.

Europe

When the relevant morphology is preserved, the earlier European specimens, such as those from Petralona, Apidima, Atapuerca, and Arago, have shown evidence of a trend toward later "classic" Neandertal morphology. The lower edge of the malar and zygomatic process of the maxilla (maxillary buttress) are uniformly low and swept back (i.e., in an oblique parasagittal plane more than a frontal plane). Further, in the earliest European "archaic" *H. sapiens* the nasal bones already appear more projecting than in other "archaic" *H. sapiens* and there is a Neandertal-like flattening of the adjoining maxilla producing a horizontal sill or ledge at the inferomedial margin of the orbit onto the projecting nasals. Although there is no evidence of true bunning in these "early archaic" specimens, I have observed

evidence of suprainiac notching on a broad, flattened upper occipital scale in Petralona, Steinheim, Reilingen, and Swanscombe like that of later Neandertals. These features foreshadow later Neandertal hyper-dolichocephaly, increased prognathism, and en-bombe vault morphology.

The most difficult aspect of accepting Neandertals as a subspecific grouping, or race, within *H. sapiens* is that many of the Late Pleistocene moderns who replace them are characteristically brachycephalic Caucasians and more similar to the earlier ante-Neandertals. The Neandertals are reported to have undergone a trend toward decreased cranial base flexion (cf Weidenreich, 1941; Laitman *et al.*, 1979, 1992; but see: Frayer, 1992b; Houghton, 1993). This feature would be considered a reversal if the morphocline could be seen to reverse from the earliest *H. sapiens*, especially so-called ante-Neandertals such as Petralona, Apidima, Swanscombe, Steinheim, and Reilingen. It is clear that most of the known "late archaics" outside of Europe, e.g. Djebel Irhoud 1, Omo 1 and 2, Laetoli 18, Narmada, and Maba, are more dolichocephalic than their anatomically modern successors. Bräuer (1992) and Hublin (1992) are both agreed, as opposed to earlier students of this material, that there are no Neandertal features on the Djebel Irhoud, Omo 1 and 2, Laetoli 18, Zuttiyeh, Narmada, or Maba specimens.

Most of the discussion of the fate of the Neandertals has been a debate over replacement versus hybridization. Bräuer (1982) proposed that both processes occured during

the transition. It is clear that modern features were introduced into Western Europe very rapidly. However, the combination of, on the one hand, orthognathic jaws and high frontal squama, and, on the other hand, projecting nasals and associated maxillary sills[1], reduced occipital buns, and suprainiac fossae in the Mladeč, Vindija and other Late Pleistocene central European specimens offer plausible evidence of hybridization (Smith, 1984; 1991). Interestingly, such combinations of features are not known from the earlier Late Pleistocene Neandertal or earliest anatomically modern specimens in the Levant (i.e., none display hybrid features).

There are highly dolichocephalic early modern peoples in central and western Europe after the demise (or at least the swamping) of the Neandertals who may be immigrants to Europe themselves, or the children of assimilated peoples (Bräuer, 1982; Smith, 1984; Graves, 1991). At the very least it seems clear that there have been large scale migrations of people bringing various anatomically modern features into Europe since the beginning of the latter half of the Late Pleistocene.

The Far East

There are now four nearly complete crania, Dali, Jinniushan, and two from Yunxian, that illustrate what seems

---

[1] The medial inferior edge of the Neandertal orbit continues anteriorly onto the maxilla and joins the nasal bones creating a sill in the horizontal plane.

to be a sudden late Middle Pleistocene appearance of "early archaic" *H. sapiens* in the Far East (Groves, 1989b). Pope (1992) counters this assessment by reporting that Jinniushan and Maba evidence "the first Asian instances of thin cranial bones and rounded orbits" due to the immigration of "archaic" *H. sapiens* or Neandertals. However, it would seem that such strong claims about such weakly described features need more explanation and documentation. The Jinniushan cranium is broadly similar to those from Dali and Yunxian.

The Maba specimen exhibits "late archaic" morphology (Habgood, 1992) comparable to that seen in the crania from Zuttiyeh and Narmada. In the Far East, the earliest documented anatomically modern humans, such as the Upper Cave specimens at Zhoukoudian (Kamminga and Wright, 1988), as with "early archaic" *H. sapiens*, seem to appear much later than in the West. Kamminga and Wright (1988) found no evidence of extant Asian regional features in the Late Pleistocene specimens from the Upper Cave at Zhoukoudian. In their PCA morphometric analysis of the virtually complete and well preserved "Old Man" (Skull 101) they found that this individual:

> "lies in an ambiguous position between Caucasoids on the one hand and sub-Saharan Africa/Australo-melanesians on the other."

While they question whether the Liujang (Wu, 1990, 1991; Wu and Olsen, 1985) skull is latest Pleistocene or Holocene (Pope, 1992 presents it as early Late Pleistocene), they do find its affinities consistent with living southern Chinese.

If it can be proven to be Late Pleistocene or older it could be the oldest specimen with visually and metrically demonstrable Mongoloid features. Along these same lines Kamminga and Wright (1988) note that the likely origin of the Ainu is hybridization between the rice farmers who arrived in Japan 2-3,000 BP and the aboriginal Jomon. The Jomon were contemporaries of the Upper Cave people and both the affinities of both groups with current Asian or extra-Asian groups are unclear. Like the Ainu, the origins of New World aborginals are still puzzling. New evidence (Hoffecker *et al.*, 1993) on the Late Pleistocene lithic sequence in the Beringian staging ground for the New World suggests that passage was not possible until about 12,000 BP.

Australasia

Habgood (1989a, 1992) and Rightmire (1991) have documented minimal support for the Australasian continuity hypothesis (Thorne and Wolpoff, 1981; Wolpoff, 1985) between Indonesian *H. erectus* and living Australoids. Habgood (1989a) accepts the diagnosis of the Willandra Lakes sample (Australia) as intermediate between the morphology seen in the Solo sample and that of extant aboriginal Australians. Both Habgood (1989a) and Brown (1992) call attention to the very great gap in the fossil record between Solo (Middle Pleistocene) and the earliest East Asian and Australian fossil record. However, Habgood (1992) also takes that gap as evidence that unlike other regions of Asia there was no

large wave of "archaic" *H. sapiens* into Indochina and Australasia (*contra* Picq, 1990); and, Brown (1992) notes, given the small sample, there does not seem to be as noticeable a difference between the known Late Pleistocene and mid-Holocene specimens as there is in the West.

Anatomically modern Australoids at Niah (Sarawak) and Tabon (Philippines) appear to date to over 30 Ka. The fully modern but extremely robust Willandra Lakes specimens could be as old as 45 Ka (Habgood, 1989a; Jones, 1992). Therefore it seems possible that Australia has been inhabited since the last third of the Late Pleistocene. There is no evidence of an Upper Paleolithic *coup de grace* being delivered to "archaic" populations with the arrival of modern populations in Australia. The parallels of immigrations into the Australian and Western European cul de sacs at the end of the Pleistocene were not lost on Birdsell's (1967) trihybrid theory. His theory of aboriginal Australian immigration patterns also has parallels with the North American large game overkill.

The maxillofacial morphology of aboriginal Australians and many other southeast Pacific Islanders should give pause to those who think that a reduced maxilla with an incisura malaris is a synapomorphy of anatomically modern humans. Hublin (1986; Hublin and Braun, 1992) suggests, this and other features of cranial robusticity may have a hormonal general correlation with overall robusticity. This problem is also encountered when interpreting the significance of

cranial vault thickness, which in and of itself, does not appear to be diagnostic of either *H. erectus* or *H. sapiens* (Bräuer and Mbua, 1992).

Africa

On the basis of the supraorbital and frontal morphology described in this thesis the Bodo skull shows clear affinities with other "early archaic" *H. sapiens*. However, it is easy to see why Conroy's (1980) visual inspection concentrated on the heavy malar of Bodo which he correctly judged more similar to Sangiran 17 than the Broken Hill 1 malar which is much reduced. (A morphometric test of this statement, however, is badly needed.) On the basis of vault and supraorbital morphology, both Bodo and Broken Hill clearly sort with "early archaic" *H. sapiens*. The Eliye Springs specimen described by Bräuer and Leakey (1986), while attributed to "late archaic" *H. sapiens* by them, was found to be intermediate between these two groups. Indeed, Bräuer *et al.* (1992) cite their expectations of continuity of "early archaic," "late archaic," and early modern populations with modern populations. This viewpoint is consistent with the model presented in this thesis, the "traditional" model. However, there is an inconsistency where Bräuer (1984a, 1992) appears to propose a polyphyletic origin for *H. sapiens* in Europe and Africa from separate developed *H. erectus* populations.

The African "late archaics," e.g. Florisbad, Laetoli 18, Omo-Kibish I and II, and earliest modern Africans such as Klasies River Mouth, Border Cave, Ishango, Boskop, and Gamble's Cave are a heterogeneous group that possesses mixtures of modern and "archaic" features. Rightmire (1978, 1981b) discusses and dismisses most potential San-like features in Florisbad, but Habgood (1989b) and Bräuer (1978) suggest general Negroid features are present on this skull. Although, Rightmire (1990) supports separation at the species level for "early archaic" *H. sapiens* as *H. heidelbergensis*, he also sees little significant difference between "early archaics" such as Broken Hill and "late archaics" such as Omo 2 (Rightmire, 1989). Rightmire (1989) also calls attention to Omo 1, Laetoli 18, and Eliye Springs as distinct from the "early archaics." Given that these writings occured over an extended interval it would be useful to know if a species distinction between the two Omo skulls was ever intended.

Rightmire (1976, 1979) found the Border Cave skull to be "closest to the Hottentot centroid" in a discriminant analysis with various representative modern sub-Saharan crania in contradistinction to De Villiers and Fatti (1982) and Habgood (1989b), but later dropped that position (Rightmire, 1984). Habgood (1989b), however, notes that the Border Cave skull shows features that are similar in general to all living sub-Saharan groups. For the most part the "archaic anatomically modern" sub-Saharan Africans were more

prognathic and dolichocephalic than living sub-Saharan Africans. Brauer (1984a) notes that anatomically modern people could be present by the early Late Pleistocene and that:

> "the mosaic-like pattern could ... have been the result of mixing between populations of the still little known 'late archaic" *Homo sapiens*' and early anatomically modern humans."

It is now clear that anatomically modern humans were present at Skhūl, Qafzeh, Omo-Kibish, and Klasies River Mouth during the last interglacial interval, between 130 and 75 Kyr (Day and Stringer, 1982; Vandermeersch, 1989; Rightmire and Deacon, 1991; Bräuer *et al.*, 1992; Miller *et al.*, 1992; Aitken and Valladas, 1992; Schwarcz and Grün, 1992). The Middle Eastern populations seem to use basic Middle Paleolithic industries much like those of their "archaic" contemporaries (Bar-Yosef, 1989, 1992a and b). Therefore it could be assumed that the first appearance of moderns is not associated with the major advance to Upper Paleolithic technology. However Deacon (1992; see also Shreeve, 1992) suggests there are some parallels between the Middle Stone Age Howiesons Poort industry known from Klasies River Mouth and Border Cave and the African Late Stone Age and European Upper Paleolithic.

Interestingly, as Habgood (1989b) notes, both the extreme OA and MR models predict great antiquity of skeletal features seen in living African populations. Habgood (1989b) supports Rightmire (1975, 1978) and Bräuer (1978) in

claiming that fossil crania demonstrating modern sub-Saharan affinities do not appear until the latest Late Pleistocene. Whatever the role of hybridization, it would now appear that all living modern humans trace some portion of their ancestry to either the known "archaic modern" people or closely related populations.

Summary

This thesis documents distinctive supraorbital and occipital morphology in earliest *H. sapiens*. The appearance of "early archaic" *H. sapiens* in Africa, and possibly Europe, likely occurred during the earlier Middle Pleistocene. As opposed to *H. erectus*, the supraorbital region in earliest *H. sapiens* shows a protruding glabella anterior to a frontal squama exhibiting bilateral frontal bossing. There is no ophryonic groove. The frontal sinus distribution appears to spread more laterally than in *H. erectus*, but overall craniofacial sinus distribution in *H. sapiens* needs to be quantitatively studied. The superolateral edges, or curvature maxima, of the glabellar portion of the brow are the start of a convexity which courses posteriorly on the frontal squama to each frontal boss, a convexity mirroring that of the roof of each orbital cone. The frontal lobes come to lie directly on the orbital roofs (i.e., superior frontal and ethmoid complex surfaces) level with crista galli. There appears to be a difference in the temporal line morphology, although coronal suture morphology is conservative in "early" *H. sapiens*. The occiput has rotated inferiorly as the shortened lower occipital scale now approximates Frankfort horizontal and the upper occipital scale approximates the coronal plane. The nuchal muscle scars are vertically oriented and weaken lateral to the strong external occipital protuberance.

This thesis began with three models of *H. sapiens* evolution. Although not all the characters are statistically significant, at least several documented major discontinuity between *H. erectus* (*sensu lato*) and the "transitional" fossils studied. On the one hand, this suggested a rejection of the extreme MR model of Wolpoff (1992b; Thorne and Wolpoff, 1991) which sees *H. sapiens* extending back to the earliest Pleistocene (see Figure 4.1), as well as the broader MR concept because of the number of, and degree of change implied by, the autapomorphies associated with earliest *H. sapiens*; evidence of sympatry of these populations with late surviving *H. erectus*, especially in Asia (Chen and Zhang, 1991), further supports the Traditional (TR) model (Howells, 1980; Howell, 1978; Delson, 1981). On the other hand, the generally close links between the "transitional" fossils and anatomically modern *H. sapiens* refute the extreme OA model of Tattersall (1986, 1992a, b) and Stringer (1991) which sees one or more extra species between *H. erectus* and (modern) *H. sapiens*. The OA version originally advocated by Bräuer (1982, 1984a) and the TR Model are the most compatible with the results of this analysis. Scenarios of *H. erectus* and *H. sapiens* evolution consistent with these results are discussed.

In most respects, Wood's (1992) separation of *H. habilis* (*sensu lato*) into *H. habilis* (*sensu stricto*) and *H. rudolfensis* seems appropriate. Given Bromage's (1992) reconstruction of KNM-ER 1470, KNM-ER 1805 and Stw 53 could

be allocated to *H. rudolfensis*. And, given the "advanced" brow and occipital morphology of Olduvai *H. habilis* (*sensu* Wood), KNM-ER 1813 and SK 847 (only on supraorbital morphology) can be allocated to this taxon. Wood's (1992) separation of *H. ergaster* from all later *H. erectus* as the ancestor of *H. sapiens* does not seem warranted. Assuming anagenetic continuity between the earlier population represented by KNM-ER 3733, 3883, and KNM-WT 15000 and the later one represented by OH 9, the question arises: when did the extra-African *H. erectus* populations, especially those of the Far East, become isolated from the progenitors of *H. sapiens*? While Delson (1981) suggested Europe as the possible site of origin for *H. sapiens*, key characters on the Ternifine mandibles, and especially the Bodo and Saldanha crania, evidence the earliest record of and most conservative morphology for this species in Africa.

Populations of "early archaic" *H. sapiens* may not have entered the Far East until the late Middle Pleistocene, and it is not clear if these populations ever inhabited Indochina and Australasia. Various clines of regional "late archaic" *H. sapiens* developed after the appearance of "early archaic" *H. sapiens*. These are best known from Europe (Neandertals), Africa, and the Near East. In the Far East, Maba and Narmada are specimens clearly attributable to "late archaic" *H. sapiens*. Morphology carried by anatomically modern peoples gradually replaced that seen in all "archaic" populations. There is evidence for hybridization of

Neandertals and anatomically modern *H. sapiens* during this time in Europe (Smith, 1984, 1992a; Graves, 1991).

It is likely that other lesser known or currently unknown late "archaic" groups also demonstrated trends toward certain geographically characteristic features which do not survive widely in any living population. That is, there may be several Neandertal-like populational clines in the late Middle and early to middle Late Pleistocene of which we are as yet unaware. Only a few visual comparisons or morphometric tests have been attempted to examine the differences between various "archaic" and modern *H. sapiens* for the characters discussed in this chapter (e.g. Albrecht, 1992; Waddle, 1992; Stringer, 1989a, c, 1992a, b; Stringer *et al.*, 1984; Bräuer *et al.*, 1992).

Figure 4.2 Various Current Theories on the *H. erectus/H. sapiens* Transition.

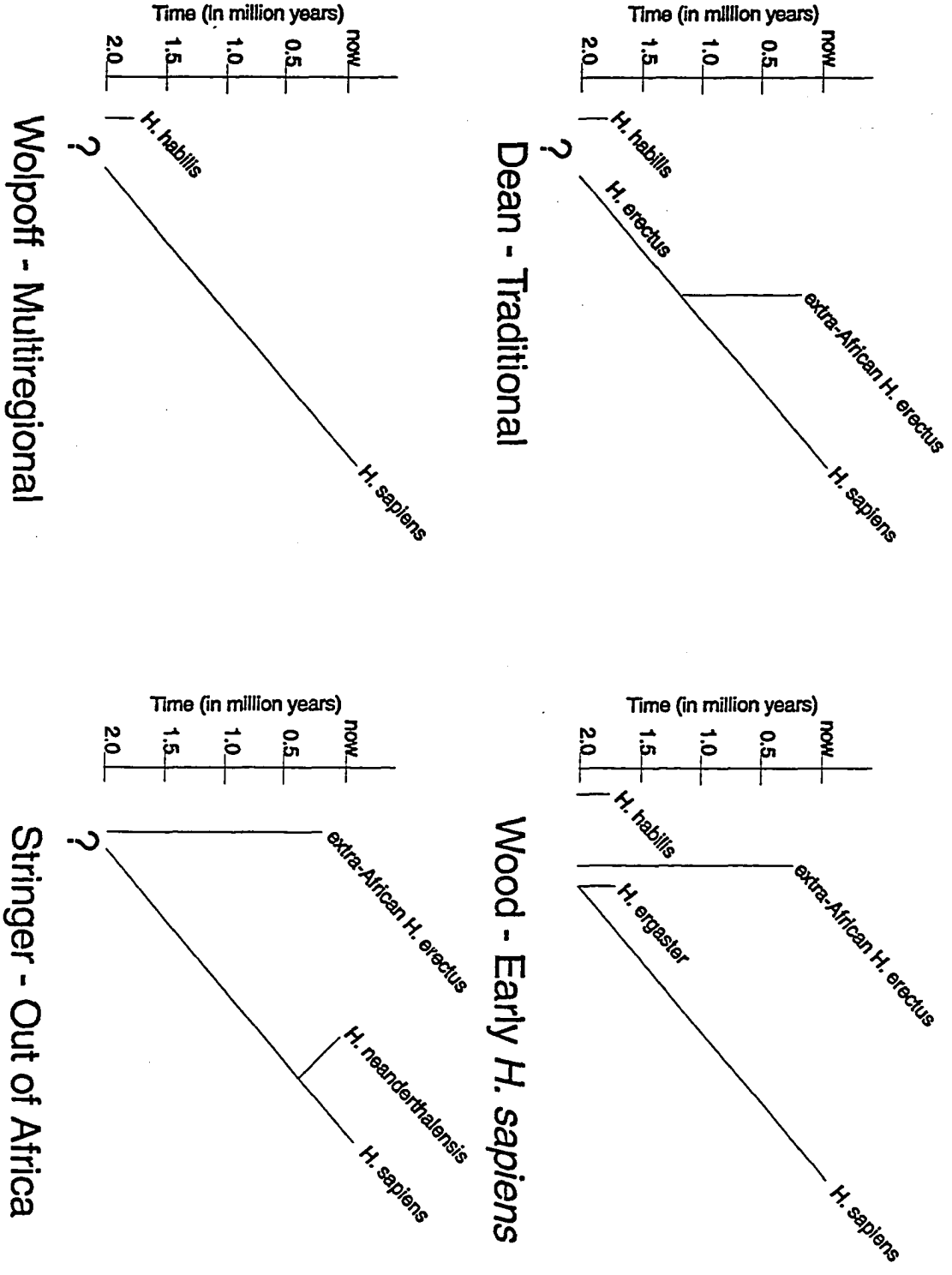

The identification of new geometrically salient osteometric landmarks and their use in space curve statistics or other morphometric techniques offers a new means by which to compare the variation seen within and between hominin species. While agreement about the underlying assumptions defining character states is vital to systematic discussions, the quantification of morphology should offer a new level of confidence in character state attribution. In fact, the use of computer vision and the "New Morphometrics" (Rohlf and Marcus, in press) in systematics offers new opportunities for the identification and morphometric quantification of character states and the potential to resolve many debates on character states that are currently tangled on visual presence/absence characters mustered in favor of theoretical prejudice.

Appendix A - The Software

Overview

The following software was used to compare the transitional and non-Caucasian space curves to the *Homo erectus* and *H. sapiens* averages. The addition of a principal coordinates module to allow ordination of interspecimen distances is in preparation (Marcus *et al.*, in prep.). These programs are available via ftp from Dr. Leslie F. Marcus (Internet: LAMQC@CUNYVM) directly and through the Internet/USENET Morphometrics Bulletin Board, MORPHMET-L (Internet: MORPHMET@CUNYVM). The three main programs listed here run under MatLab™ (MathWorks, Inc.). Versions of MatLab are available for most PC and workstation platforms.

Information on the 3D digitizing program, TableTop (Karron © 1990), is available via Internet electronic mail from Dr. Daniel Karron (karron@nyu.edu). The software used to determine curvature, CrvStat (Court Cutting © 1992), and generate average space curves, RidgeAverage (Court Cutting © 1992), will be described further by Cutting *et al.* (in prep.).

MatLab Programs Used For the
Chi Square Analysis of Ridge Curve Affinities.

By: Leslie F. Marcus, Ph.D
Department of Biology
Queens College and Graduate Center, CUNY
Department of Invertebrate Zoology
American Museum of Natural History
Central Park West @ 79 Street
New York, NY 10024

Internet: LAMQC@CUNYVM

Five files (directory listing below) are used to compute the chi squared probabilities, etc.:

```
DAVIDME3.M       1193   7-30-92   4:49a
DAVID5  .M       4388   8-22-92   7:31p
PROBOUT2.M       1673   8-18-92  11:36a
PROBUNK .M       1016   7-30-92   4:50a
CHISQPRB.M         53   7-22-92   5:01a
```

DAVIDME3.M is the main program for comparing one form to several others. It calls DAVID5.M, where most of the computations are done. Note that the distance between the endpoint landmarks is standardized to the first form entered.

PROBOUT2.M is the program that fits the chi square model to the T's. It calls chisqprb - a function to compute chi squared probabilities. It also produces a p-p plot and Kolmogorov-Smirnov test of the model.

PROBUNK.M is the program that finds the chi squared probabilities (right tail) for comparing "unknown" forms to an average form.

```
% DAVIDME3.M
% By Leslie F. Marcus, July 29, 1992 4:50 PM
% Program to recall david5 several times and put results in
%  array for further processing
['Input the file name for the mean specimen by name'
 '      xxxhe.avg for Homo erectus                  '
 '      xxxhs.avg for Homo sapiens                  '
 'Note syntax:   load  filename.avg                  '
 '               X=filename;                         '
 '               return                             ']
keyboard
xyz0=X(:,2:4);
nruns=input('Number of specimens - ')
hlmark0=input('give array of landmark indices within [ ] -
')
hlmark1=hlmark0;
findsq=ones(nruns,1);
for ifin=1:nruns
      david5
      findsq(ifin,1)=sumdsq;
```

```
end
findsq
[' Note dsquares will be named for species, rename for
feature']
choose=input('Comparison to: 0 for H. sapiens; 1 for H.
erectus ')
if choose==0
   save hsdsq.dat findsq /ascii
elseif choose==1
   save hedsq.dat findsq /ascii
end
choose2=input('If transitional specimen(s) type 1, anything
else otherwise')
if choose2==1
   if choose==0
      save tr_sdsq.dat findsq /ascii
   elseif choose==1
      save tr_edsq.dat findsq /ascii
   end
end
```

```
% DAVID5.M
% By Leslie F. Marcus
% August 22, 1992
% Program to attempt to find alignment of landmarks for
xyz0an
% and xyz1ing data give matrices for further analysis called
% xyz0an and xyz1ing latest one allows different numbers of
% points and landmarks for each specimen DAVIDME3.m will
take
% in the mean specimen and landmark array.
clg
com='Input the array specific individual=xyz1'
keyboard % make data arrays equal to xyz1
xyz1=X(:,2:4);
[n0,m0]=size(xyz0)
[n1,m1]=size(xyz1)
xyz00=xyz0-ones(n0,1)*xyz0(1,:); % moves objects so one end
at 0,0,0
xyz10=xyz1-ones(n1,1)*xyz1(1,:);
choose0=[1 n0]; % endpoints
choose1=[1 n1];
xyz0ends=xyz00(choose0,:); % arrays of endpoints
xyz1ends=xyz10(choose1,:);
```

```
[v0,d0,u0]=svd(xyz0ends); % to find rotation angle for
arrays
xyz0r=xyz00*u0; % rotated to 0,0,0 - xlen,0,0
[v1,d1,u1]=svd(xyz1ends);
xyz1r=xyz10*u1;
len0=xyz0r(n0,1);
check00=sqrt((xyz0(1,:)-xyz0(n0,:))*(xyz0(1,:)-
xyz0(n0,:))');
check01=sqrt((xyz1(1,:)-xyz1(n0,:))*(xyz1(1,:)-
xyz1(n0,:))');
check0=sqrt(xyz00(n0,:)*xyz00(n0,:)'); % ref chord value
check1=sqrt(xyz10(n1,:)*xyz10(n1,:)'); % unknown chord value
len1=xyz1r(n1,1);
xyz1r=xyz1r.*xyz0r(n0,1)./xyz1r(n1,1); % standardizes
unknown to xlen
len10=xyz1r(n1,1);
com=['chord lengths and x axis lengths - should be the same
'
     '  orig   proj check  final
']
check=[check00 len0 check0 len0
       check01 len1 check1 len10]
% hlmarks=input('Give the arrays of landmark indices']
% at this point refer to or input two arrays of indices for
% the landmarks one called hlmark0 and the other hlmark1
% com='Input the two sets of landmark indices as hlmark0
% and hlmark1'
% keyboard
[dum,nlm]=size(hlmark0);
xyz0lm=xyz0r(hlmark0,:); % arrays of landmarks for two
objects
xyz1lm=xyz1r(hlmark1,:);
diff=xyz0lm-xyz1lm;
com='Initial sum of squares between landmarks before
rotation'
ss0=sum(diag(diff'*diff))  % sum of squared differences
between objects
pause
ji=0;
xyz1te=ones(nlm,3);  % just making space
xyz1te(:,1)=xyz1lm(:,1);
xyzr=[xyz0r
      xyz1r];     % concat of files to find plotting limits
xyzmin=min(xyzr)
xyzmax=max(xyzr)
```

```
subplot(221)
  v=[xyzmin(1,1) xyzmax(1,1) xyzmin(1,2) xyzmax(1,2)];
  axis(v)
  plot(xyz0r(:,1),xyz0r(:,2),'w')
  hold
  plot(xyz1r(:,1),xyz1r(:,2),'r')
  hold off
  xlabel('x ')
  ylabel('y ')
  title('Rotated to end Pts')
subplot(222)
  v=[xyzmin(1,3) xyzmax(1,3) xyzmin(1,2) xyzmax(1,2)];
  axis(v)
  plot(xyz0r(:,3),xyz0r(:,2),'w')
  hold
  plot(xyz1r(:,3),xyz1r(:,2),'r')
  hold off
  xlabel('z ')
  ylabel('y ')
subplot(223)
  v=[xyzmin(1,1) xyzmax(1,1) xyzmin(1,3) xyzmax(1,3)];
  axis(v)
  plot(xyz0r(:,1),xyz0r(:,3),'w')
  hold
  plot(xyz1r(:,1),xyz1r(:,3),'r')
  hold off
  xlabel('x ')
  ylabel('z ')
  title('Rotated to end Pts')
pause
%keyboard
for j=0:.05:2*pi,    % 0 to 2*pi radians in increments of .05
   xyz1te(:,2)=cos(j)*xyz1lm(:,2)+sin(j)*xyz1lm(:,3);
   xyz1te(:,3)=-sin(j)*xyz1lm(:,2)+cos(j)*xyz1lm(:,3);
   diff=xyz0lm-xyz1te;
   ss=sum(diag(diff'*diff));
%j,ss
%pause
   if ss<ss0;
     ss0=ss;
     ji=j;
   end;
end;
com='Final sum of squares at angle ji'
ss0
```

```
ji
pause
xyz1te(:,2)=cos(ji)*xyz1lm(:,2)+sin(ji)*xyz1lm(:,3);
xyz1te(:,3)=-sin(ji)*xyz1lm(:,2)+cos(ji)*xyz1lm(:,3);
xyz1bf=ones(n1,3);
xyz1bf(:,1)=xyz1r(:,1);
xyz1bf(:,2)=cos(ji)*xyz1r(:,2)+sin(ji)*xyz1r(:,3);
xyz1bf(:,3)=-sin(ji)*xyz1r(:,2)+cos(ji)*xyz1r(:,3);
clg
xyzr=[xyz0r
      xyz1bf];
xyzmin=min(xyzr)
xyzmax=max(xyzr)
subplot(221)
  v=[xyzmin(1,1) xyzmax(1,1) xyzmin(1,2) xyzmax(1,2)];
  axis(v)
  plot(xyz0r(:,1),xyz0r(:,2),'w')
  hold
  plot(xyz1bf(:,1),xyz1bf(:,2),'r')
  hold off
  xlabel('x ')
  ylabel('y ')
  title('Rotated to Land Marks')
subplot(222)
  v=[xyzmin(1,3) xyzmax(1,3) xyzmin(1,2) xyzmax(1,2)];
  axis(v)
  plot(xyz0r(:,3),xyz0r(:,2),'w')
  hold
  plot(xyz1bf(:,3),xyz1bf(:,2),'r')
  hold off
  xlabel('y ')
  ylabel('z ')
  title('Rotated to Land Marks')
subplot(223)
  v=[xyzmin(1,1) xyzmax(1,1) xyzmin(1,3) xyzmax(1,3)];
  axis(v)
  plot(xyz0r(:,1),xyz0r(:,3),'w')
  hold
  plot(xyz1bf(:,1),xyz1bf(:,3),'r')
  hold off
  xlabel('x ')
  ylabel('z ')
  title('Rotated to Land Marks')
  pause
if n0==n1;diff=xyz0r-xyz1bf;
```

```
    %dsq=diag(diff*diff');
    %dist=sqrt(dsq);
    %sumdsq=sum(dsq)
    sumdsq=sum(diag(diff'*diff))
end;
```

```
% PROBOUT2.M
% By: Leslie F. Marcus, PhD
% August 18, 1992
% This is a MATLAB translation of the program PROBDSQ.SAS
% The file in the next line must be the appropriate file
% containing all of the appropriate ribbon dsq values for
% erectus or sapiens
% cdata dsq; infile 'c:\matlab\david\finaldsq.dat';
choose=input('Type 0 for H. sapiens, 1 for H. erectus or 2
for transitional ')
if choose==0
    load hsdsq.dat
    X=hsdsq;
elseif choose==1
    load hedsq.dat
    X=hedsq;
else load trdsq.dat
    X=trdsq;
end
[n,p]=size(X)
if n>1;
        mn=mean(X)
        var=(X'*X-mn*mn*n)/(n-1)
        d=2*mn*mn/var;  %* degrees of freedom for chi-square
*/
        c=mn/d;         %* constant in FL Bookstein
formula*/
        chisq=X/c;
        % probability of chi squared values
        % to be added and plotted;
        n, c, d, chisq
        parms=[n c d]
        pause
        prob=chisqprb(chisq,d); % probabilities from above
*/
        prob=sort(prob);
        pause
        clg
```

```
        steprob=[.5/n:1/n:(n-.5)/n];
        ['Empirical Prob.  Chi-square Prob.']
        [steprob' prob]
        pause
        KS_stat=max(prob(2:n,:)-steprob(:,1:(n-1))')
        pause
        axis([0 1 0 1])
        axis('square')
        dum=[0 0
             1 1];
        plot(steprob,prob,'ow',dum(:,1),dum(:,2),'-w')
        xlabel('step frequency (i-.5)/n')
        ylabel('P(chisquared) with d degrees of freedom')
        if choose==0
        title('p-p plot for sapiens data')
                save hsncd.prm parms /ascii
        elseif choose==1
        title('p-p plot for erectus data')
                save hencd.prm parms /ascii
        end
end
```

```
% Program PROBUNK.M by Leslie F. Marcus July 29, 1992 4:07
pm
% This program computes tail probabilities for sapiens and
% erectus, where c and d values come from files hsncd.prm
% and hencd.prm from respective runs of probout.m
choice=input('Type 0 if use last H. sapiens, tr_sdsq.dat, 1
if you will supply dsq')
if choice==0
   load tr_sdsq.dat
   dsq=tr_sdsq;
 else
     dsq=input('Give the dsq value for the unknown compared
to H. sapiens - ')
end
load hsncd.prm
  hsncd
  c=hsncd(:,2)
  df=hsncd(:,3)
chisq=dsq/c;
prob=1-chisqprb(chisq,df);
['unknown-sapiens']
 dsq ,df, prob
```

```
choice=input('Type 0 if use last H. erectus, tr_edsq.dat, 1
if you will supply dsq')
if choice==0
   load tr_edsq.dat
   dsq=tr_edsq;
 else
     dsq=input('Give the dsq value for the unknown compared
to H. erectus - ')
end
load hencd.prm
  hencd
  c=hencd(:,2)
  df=hencd(:,3)
chisq=dsq/c;
prob=1-chisqprb(chisq,df);
['unknown-erectus']
 dsq ,df, prob
```

```
% CHISQPRB.M
% By: Leslie F. Marcus, Ph.D
% July 22, 1992
function P = chisqprb(X2,v)
P = gamma(v/2, X2/2);
```

Appendix B - The Data

Overview

This chapter presents the intrasample data for the 4 characters, for both *Homo erectus* and *H. sapiens*, not shown in Chapter 3. These data indicate the validity of the chi square model used to test the affinities of the "transitional" specimens. The right and left side lateral brow and temporal line ridge curves have been treated separately, therefore there are six character sections to follow.

Right Lateral Ridge Curve

The *H. erectus* sample for the right lateral ridge curve had an N = 9. The mean = 2.9186, variance = 5.5685, c = 0.9540, and d = 3.0594. The K-S statistic = 0.1738. (acceptable with α<0.01).

Figure B.1 *H. erectus* Right Lateral Ridge Curve Sample p-p Plot.

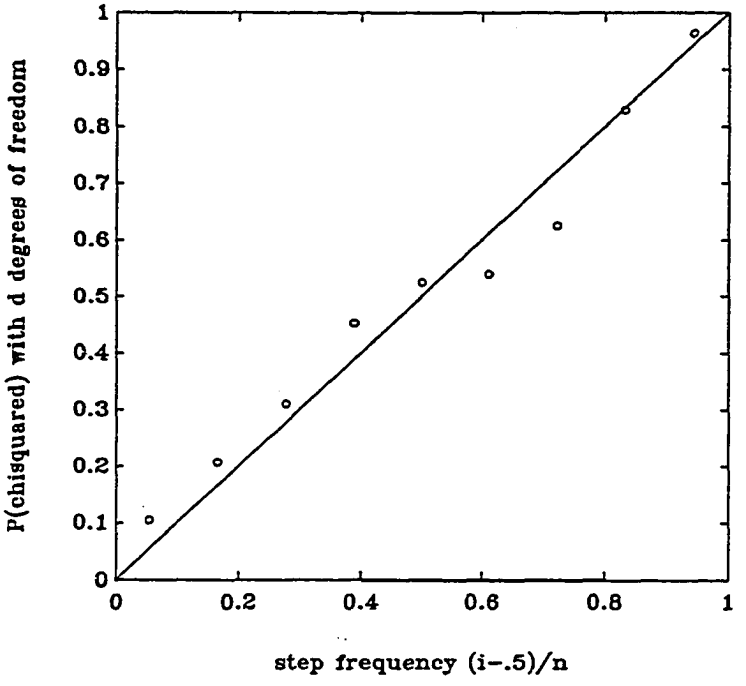

Table B.1 *H. erectus* right lateral ridge curve intrasample data			
Specimen	T	Emp. Prob.	χ^2 Prob.
KNM-ER 3733	1.5139	0.0556	0.1053
KNM-ER 3883	1.0723	0.1667	0.2073
Solo 10	2.1725	0.2778	0.3105
Solo 11	0.6342	0.3889	0.4516
Solo 12	5.1053	0.5000	0.5246
Solo 4	2.6432	0.6111	0.5393
Zhoukoudian 10	3.1771	0.7222	0.6250
Zhoukoudian 12	2.5597	0.8333	0.8297
Zhoukoudian 3	8.6560	0.9444	0.9641

The *H. sapiens* sample for the right lateral ridge curve had an N = 20, mean = 1.6149, variance = 0.9196, c = 0.2847, and d = 5.6722, K-S statistic = 0.0894 (acceptable with α<0.01).

Figure B.2 *H. sapiens* Right Lateral Ridge Curve Sample p-p Plot.

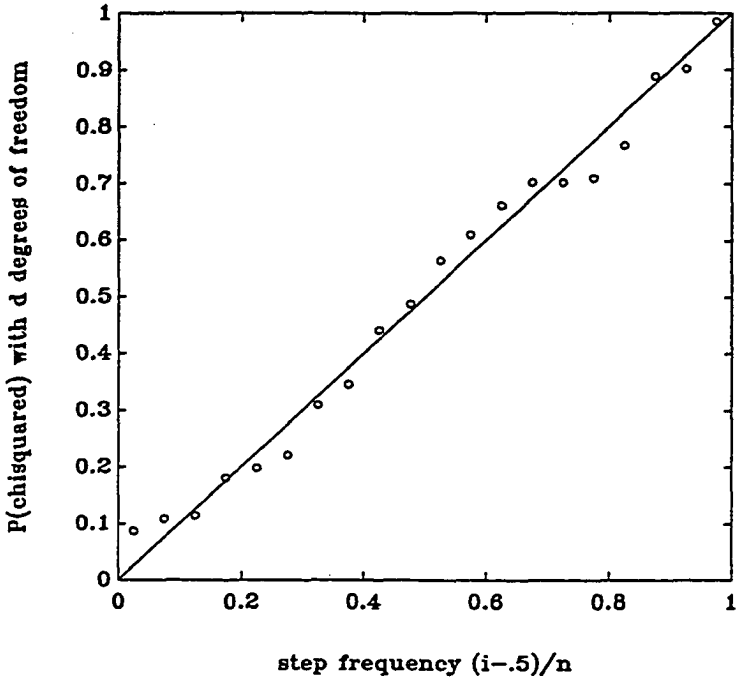

Table B.2 *H. sapiens* right lateral ridge curve intrasample data			
Specimen	T	Emp. Prob.	χ^2 Prob.
CMNH 1157	4.9276	0.0250	0.0869
CMNH 1253	5.9496	0.0750	0.1088
CMNH 1273	9.8786	0.1250	0.1143
CMNH 1759	15.3902	0.1750	0.1808
CMNH 2048	3.8821	0.2250	0.1979
CMNH 2401	2.6823	0.2750	0.2212
CMNH 2584	2.9861	0.3250	0.3097
CMNH 2860	6.4438	0.3750	0.3461
CMNH 514	2.8130	0.4250	0.4412
CMNH 560	4.5723	0.4750	0.4880
CMNH 630	2.0862	0.5250	0.5644
CMNH 667	1.8784	0.5750	0.6101
CMNH 681	2.1356	0.6250	0.6616
CMNH 856	3.6230	0.6750	0.7027
CMNH 881	6.8805	0.7250	0.7029
CMNH 883	10.2367	0.7750	0.7108
CMNH 919	6.9713	0.8250	0.7675
CMNH 920	7.6757	0.8750	0.8886
CMNH 939	6.8829	0.9250	0.9017
CMNH 962	5.5471	0.9750	0.9859

Left Lateral Ridge Curve

The *H. erectus* sample for the left lateral ridge curve had an N = 13. The mean = 3.0620, variance = 3.9690, c = 0.6481, and d = 4.7246. The K-S statistic = 0.1646. (acceptable with α<0.01).

Figure B.3 *H. erectus* Left Lateral Ridge Curve Sample p-p Plot.

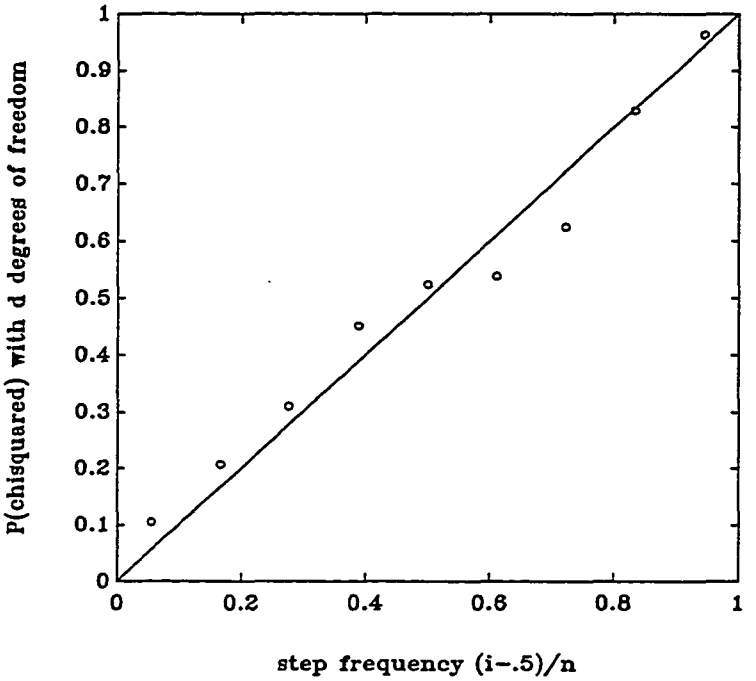

Table B.3 *H. erectus* left lateral ridge curve intrasample data			
Specimen	T	Emp. Prob.	χ^2 Prob.
KNM-ER 3733	0.6002	0.0385	0.0165
Lantian	6.1598	0.1154	0.0638
OH 9	3.4965	0.1923	0.1484
Sangiran 17	9.8055	0.2692	0.2273
Sangiran 2	4.8682	0.3462	0.3767
Solo 10	9.1055	0.4231	0.4140
Solo 12	3.2562	0.5000	0.4852
Solo 4	8.7189	0.5769	0.6042
Solo 5	1.8057	0.6538	0.7388
Solo 7	6.1569	0.7308	0.7390
Zhoukoudian 12	3.9735	0.8077	0.8953
Zhoukoudian 3	1.1522	0.8846	0.9095
Zhoukoudian 1966	2.3214	0.9615	0.9307

The *H. sapiens* sample for the left lateral ridge curve had an N = 20, mean = 1.2552, variance = 0.4433, c = 0.1766, and d = 7.1083, K-S statistic = 0.0872 (acceptable with α<0.01).

Figure B.4 *H. sapiens* Left Lateral Ridge Curve Sample p-p Plot.

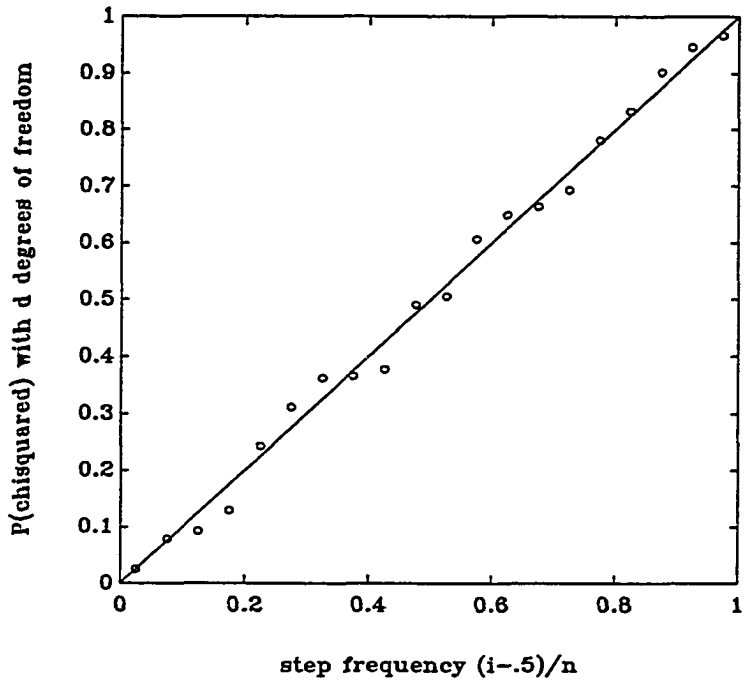

Table B.4 *H. sapiens* left lateral ridge curve intrasample data			
Specimen	T	Emp. Prob.	χ^2 Prob.
CMNH 1157	5.2792	0.0250	0.0253
CMNH 1253	5.4051	0.0750	0.0783
CMNH 1273	15.3979	0.1250	0.0927
CMNH 1759	9.6250	0.1750	0.1294
CMNH 2048	12.2544	0.2250	0.2434
CMNH 2401	8.4189	0.2750	0.3118
CMNH 2584	7.9175	0.3250	0.3622
CMNH 2860	5.3090	0.3750	0.3658
CMNH 514	3.2263	0.4250	0.3774
CMNH 560	4.8615	0.4750	0.4904
CMNH 630	8.0847	0.5250	0.5056
CMNH 667	2.6361	0.5750	0.6070
CMNH 681	1.7492	0.6250	0.6492
CMNH 856	2.8172	0.6750	0.6642
CMNH 881	4.2857	0.7250	0.6927
CMNH 883	14.0193	0.7750	0.7809
CMNH 919	6.5043	0.8250	0.8329
CMNH 920	7.4700	0.8750	0.9029
CMNH 939	10.5354	0.9250	0.9463
CMNH 962	6.3684	0.9750	0.9669

Right Temporal Ridge Curve

The *H. erectus* sample for the right temporal ridge curve had an N = 10. The mean = 89.8066, variance = 6274.2, c = 34.9315, and d = 2.5709. The K-S statistic = 0.2989. (acceptable with α<0.01).

Figure B.5 *H. erectus* Right Temporal Ridge Curve Sample p-p Plot.

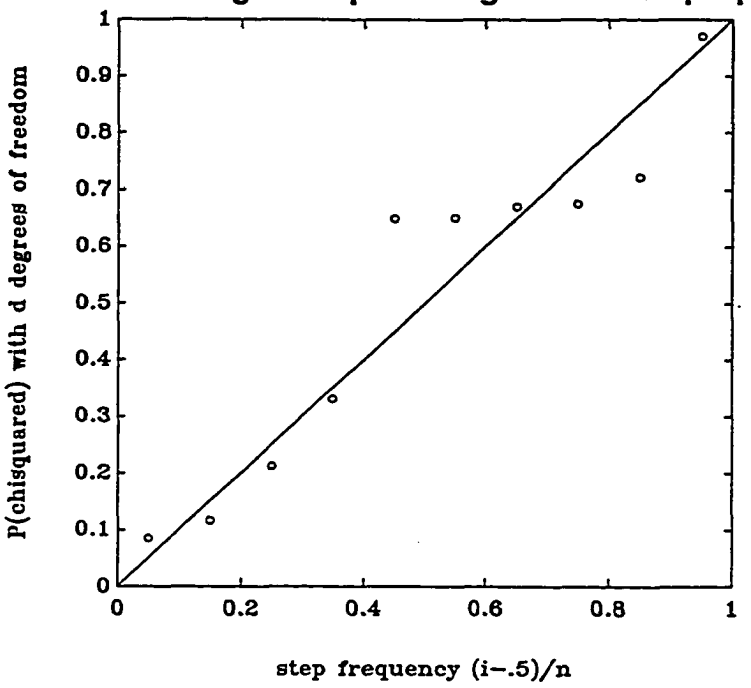

Table B.5 *H. erectus* right temporal ridge curve intrasample data			
Specimen	T	Emp. Prob.	χ^2 Prob.
KNM-ER 3733	1.2258	0.0500	0.0850
KNM-ER 3883	0.3554	0.1500	0.1160
Sangiran 2	8.1466	0.2500	0.2129
Solo 11	2.9174	0.3500	0.3311
Solo 12	3.2982	0.4500	0.6489
Solo 7	2.7821	0.5500	0.6504
Zhoukoudian 10	2.7724	0.6500	0.6704
Zhoukoudian 11	0.4631	0.7500	0.6753
Zhoukoudian 12	2.9517	0.8500	0.7212
Zhoukoudian 3	0.7966	0.9500	0.9700

The *H. sapiens* sample for the right temporal ridge curve had an N = 20, mean = 153.8496, variance = 18880.0, c = 61.3600, and d = 2.5073, K-S statistic = 0.1517 (acceptable with $\alpha<0.01$).

Figure B.6 *H. sapiens* Right Temporal Ridge Curve Sample p-p Plot

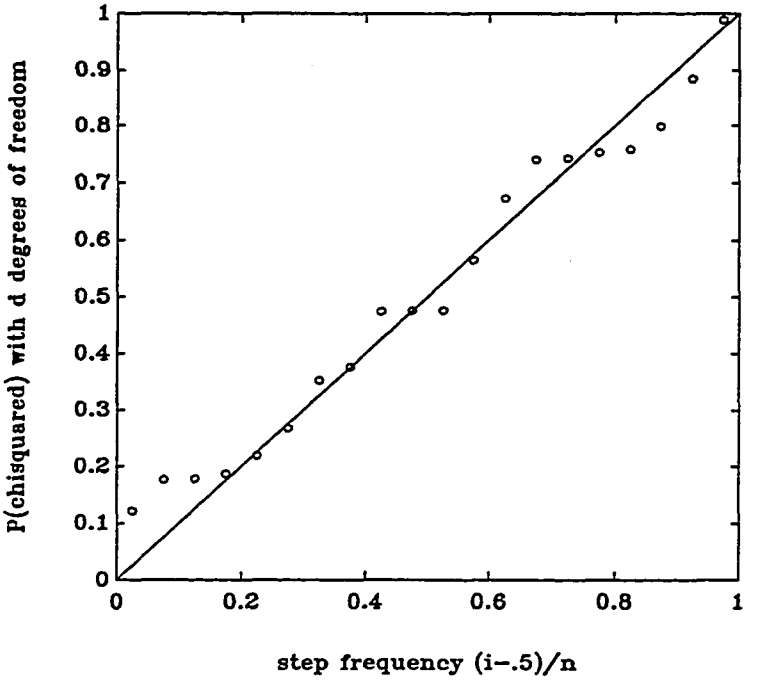

Table B.6 *H. sapiens* right temporal ridge curve intrasample data			
Specimen	T	Emp. Prob.	χ^2 Prob.
CMNH 1157	0.6720	0.0250	0.1219
CMNH 1253	1.7713	0.0750	0.1767
CMNH 1273	1.7697	0.1250	0.1780
CMNH 1759	1.7637	0.1750	0.1870
CMNH 2048	3.9432	0.2250	0.2193
CMNH 2401	5.1591	0.2750	0.2677
CMNH 2584	0.4563	0.3250	0.3524
CMNH 2860	3.4896	0.3750	0.3765
CMNH 514	3.5429	0.4250	0.4746
CMNH 560	3.3810	0.4750	0.4759
CMNH 630	0.7810	0.5250	0.4763
CMNH 667	0.6422	0.5750	0.5647
CMNH 681	0.6377	0.6250	0.6730
CMNH 856	1.3512	0.6750	0.7410
CMNH 881	1.2581	0.7250	0.7433
CMNH 883	0.9482	0.7750	0.7533
CMNH 919	3.4011	0.8250	0.7592
CMNH 920	0.1149	0.8750	0.7991
CMNH 939	2.2045	0.9250	0.8850
CMNH 962	2.8587	0.9750	0.9889

Left Temporal Ridge Curve

The *H. erectus* sample for the left temporal ridge curve had an N = 8. The mean = 77.0260, variance = 1577.9, c = 10.2429, and d = 7.5200. The K-S statistic = 0.2559 (acceptable with α<0.01).

Figure B.7 *H. erectus* Left Temporal Ridge Curve Sample p-p Plot.

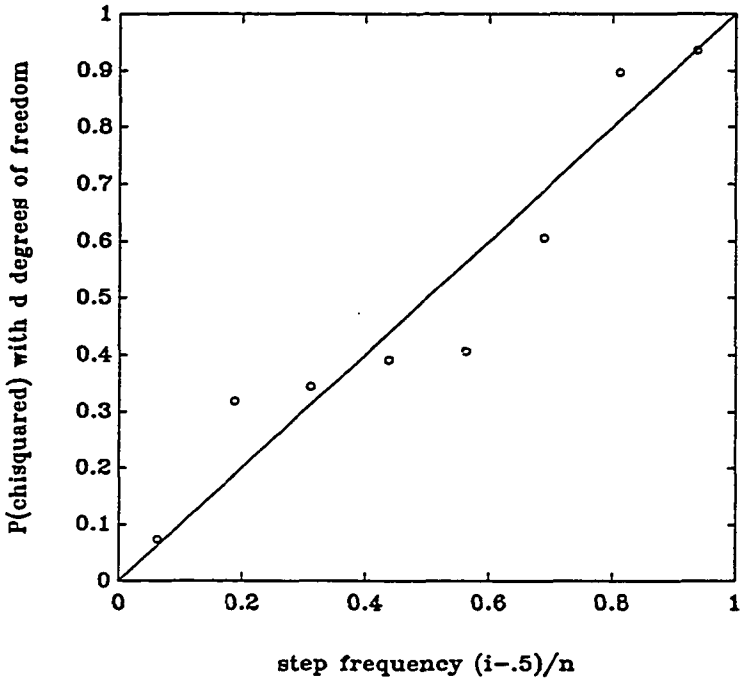

Table B.7 *H. erectus* left temporal ridge curve intrasample data			
Specimen	*T*	Emp. Prob.	χ^2 Prob.
KNM-ER 3733	5.4935	0.0625	0.0738
KNM-ER 3883	14.0802	0.1875	0.3184
OH 9	5.2735	0.3125	0.3440
Sangiran 17	12.6301	0.4375	0.3917
Solo 10	7.9119	0.5625	0.4073
Solo 12	2.8279	0.6875	0.6070
Solo 5	5.9039	0.8125	0.8971
Zhoukoudian 3	6.0387	0.9375	0.9359

The *H. sapiens* sample for the left temporal ridge curve had an N = 20, mean = 90.3641, variance = 6309.5, c = 34.9115, and d = 2.5884, K-S statistic = 0.1437 (acceptable with α<0.01).

Figure B.8 *H. sapiens* Left Temporal Ridge Curve Sample p-p Plot.

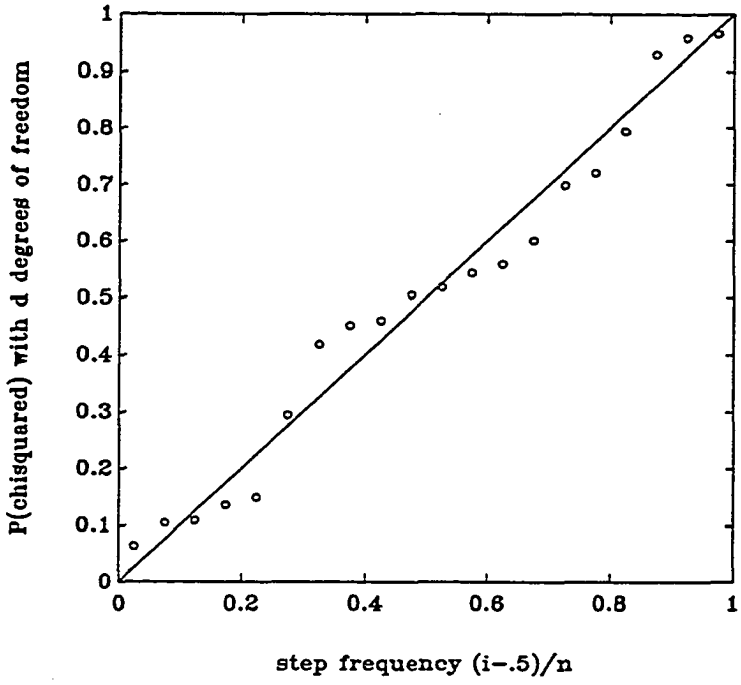

Table B.8 *H. sapiens* left temporal ridge curve intrasample data			
Specimen	T	Emp. Prob.	χ^2 Prob.
CMNH 1157	0.4320	0.0250	0.0642
CMNH 1253	6.3577	0.0750	0.1050
CMNH 1273	0.2865	0.1250	0.1093
CMNH 1759	1.9871	0.1750	0.1364
CMNH 2048	3.3165	0.2250	0.1494
CMNH 2401	1.5927	0.2750	0.2948
CMNH 2584	1.7348	0.3250	0.4187
CMNH 2860	0.4473	0.3750	0.4513
CMNH 514	1.7734	0.4250	0.4599
CMNH 560	7.9506	0.4750	0.5055
CMNH 630	7.5165	0.5250	0.5187
CMNH 667	3.1459	0.5750	0.5440
CMNH 681	1.1019	0.6250	0.5594
CMNH 856	0.5861	0.6750	0.6008
CMNH 881	2.2626	0.7250	0.6989
CMNH 883	0.5413	0.7750	0.7207
CMNH 919	2.1809	0.8250	0.7945
CMNH 920	2.0521	0.8750	0.9298
CMNH 939	2.4944	0.9250	0.9591
CMNH 962	4.0075	0.9750	0.9666

Coronal Ridge Curve

The *H. erectus* sample for the coronal ridge curve had an N = 13. The mean = 109.0743, variance = 14005.0, c = 64.2016, and d = 1.6989. The K-S statistic = 0.2680. (acceptable with α<0.01).

Figure 3.9 *H. erectus* Coronal Ridge Curve Sample p-p Plot.

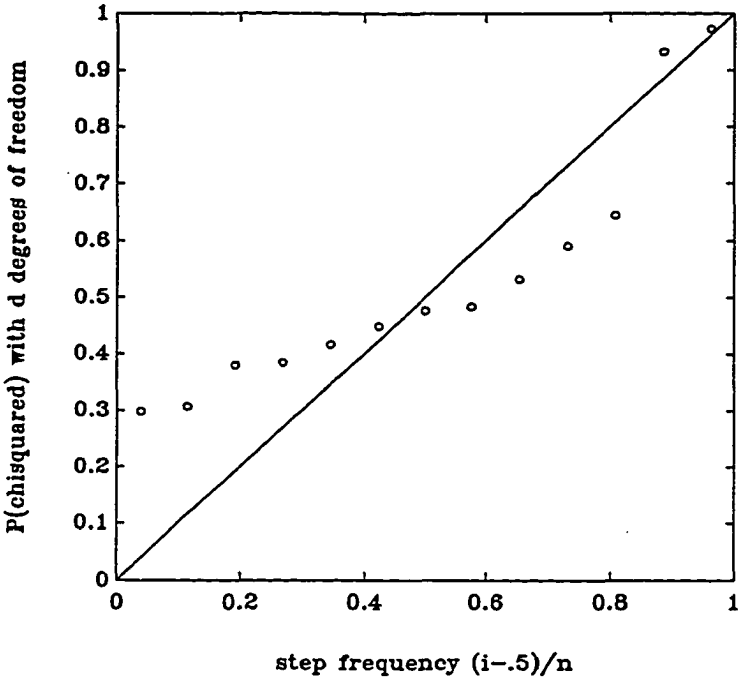

Table B.9 *H. erectus* coronal ridge curve intrasample data			
Specimen	T	Emp. Prob.	χ^2 Prob.
KNM-ER 3733	0.9277	0.0385	0.2978
KNM-ER 3883	1.0394	0.1154	0.3065
OH 9	1.0159	0.1923	0.3793
Sangiran 17	1.4505	0.2692	0.3847
Sangiran 2	6.5883	0.3462	0.4170
Solo 11	0.5154	0.4231	0.4492
Solo 12	0.5358	0.5000	0.4764
Solo 5	0.8293	0.5769	0.4834
Solo 7	1.2132	0.6538	0.5319
Solo 8	0.7369	0.7308	0.5902
Zhoukoudian 11	4.8110	0.8077	0.6432
Zhoukoudian 12	1.7006	0.8846	0.9322
Zhoukoudian 3	0.7221	0.9615	0.9731

The *H. sapiens* sample for the coronal ridge curve had an N = 20, mean = 79.3408, variance = 3707.6, c = 23.3648, and d = 3.3957, K-S statistic = 0.1435 (acceptable with α<0.01).

Figure B.10 *H. sapiens* Coronal Ridge Curve Sample p-p Plot.

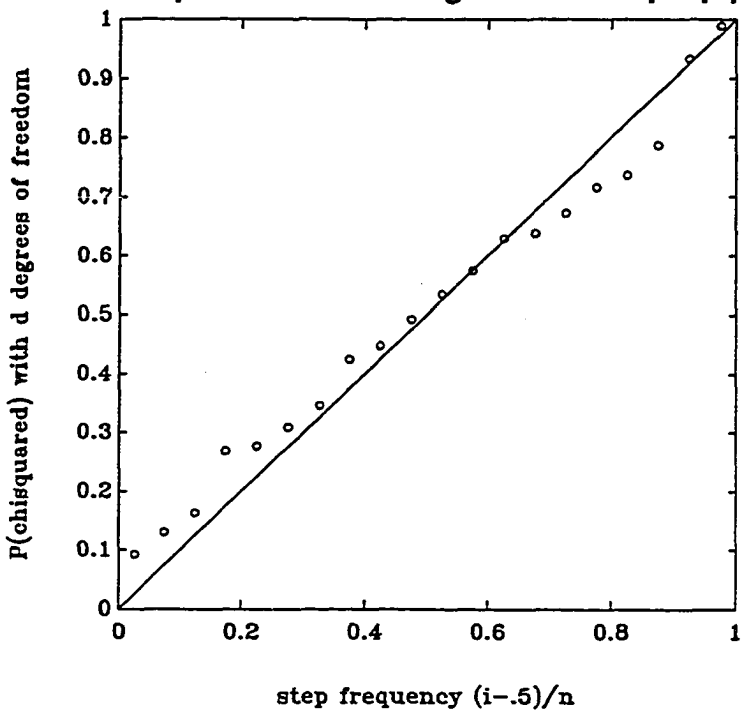

Table B.10 *H. sapiens* coronal ridge curve intrasample data			
Specimen	T	Emp. Prob.	χ^2 Prob.
CMNH 1157	2.7117	0.0250	0.0926
CMNH 1253	1.7650	0.0750	0.1302
CMNH 1273	5.0101	0.1250	0.1632
CMNH 1759	2.4655	0.1750	0.2685
CMNH 2048	4.2839	0.2250	0.2766
CMNH 2401	1.0775	0.2750	0.3087
CMNH 2584	0.9172	0.3250	0.3457
CMNH 2860	1.6125	0.3750	0.4246
CMNH 514	0.7250	0.4250	0.4476
CMNH 560	2.3434	0.4750	0.4920
CMNH 630	4.4794	0.5250	0.5338
CMNH 667	7.8167	0.5750	0.5738
CMNH 681	1.5744	0.6250	0.6285
CMNH 856	3.2081	0.6750	0.6374
CMNH 881	2.9569	0.7250	0.6717
CMNH 883	3.9126	0.7750	0.7152
CMNH 919	3.5830	0.8250	0.7360
CMNH 920	3.6482	0.8750	0.7858
CMNH 939	1.9444	0.9250	0.9332
CMNH 962	11.8796	0.9750	0.9888

Nuchal Ridge Curve

The complete *H. erectus* sample (sample one) for the nuchal ridge curve had an N = 15. The mean = 507.4488, variance = 863910.0, c = 851.2243, and d = 0.5961. The K-S statistic = 0.4278. (unacceptable with $\alpha<0.01$).

Figure B.11 *H. erectus* Nuchal Ridge Curve Sample One p-p Plot.

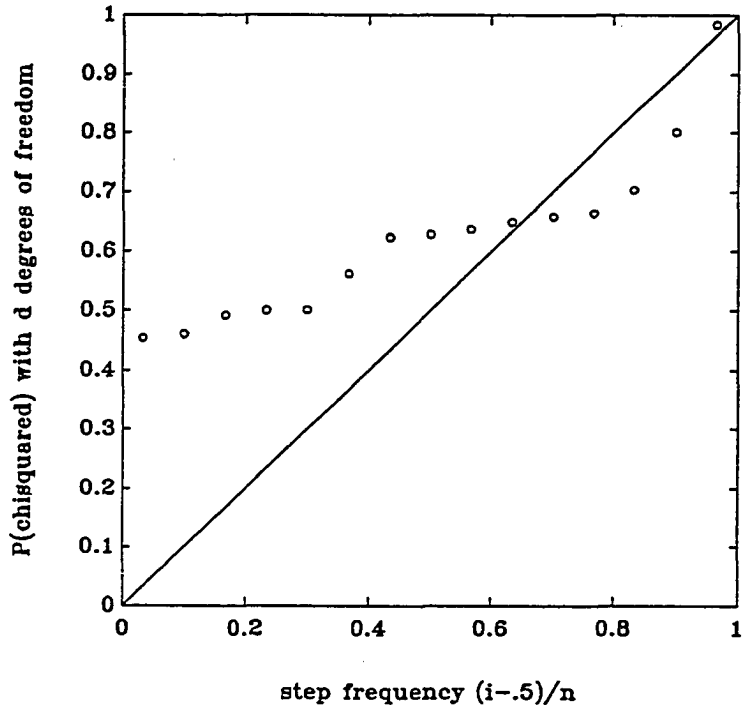

Table B.11 *H. erectus* right nuchal ridge curve intrasample one data			
Specimen	T	Emp. Prob.	χ^2 Prob.
KNM-ER 3733	0.1029	0.0333	0.4547
KNM-ER 3883	0.1082	0.1000	0.4612
OH 9	0.1362	0.1667	0.4924
Sangiran 17	0.1451	0.2333	0.5005
Sangiran 2	0.9173	0.3000	0.5013
Sangiran 4	4.4703	0.3667	0.5619
Solo 10	0.4102	0.4333	0.6230
Solo 11	0.3211	0.5000	0.6276
Solo 12	0.3963	0.5667	0.6366
Solo 5	0.5168	0.6333	0.6488
Solo 7	0.3488	0.7000	0.6579
Zhoukoudian 11	0.3753	0.7667	0.6637
Zhoukoudian 12	0.1443	0.8333	0.7030
Zhoukoudian 3	0.2188	0.9000	0.8008
Zhoukoudian 1966	0.3304	0.9667	0.9837

The *H. erectus*, minus Sangiran 4 (sample two), for the left nuchal ridge curve had an N = 14. The mean = 271.8947, variance = 34051.0, c = 62.6186, and d = 4.3421. The K-S statistic = 0.2004. (acceptable with α<0.01).

n = 14

Figure B.12 *H. erectus* Nuchal Ridge Curve (Sample 2) p-p Plot.

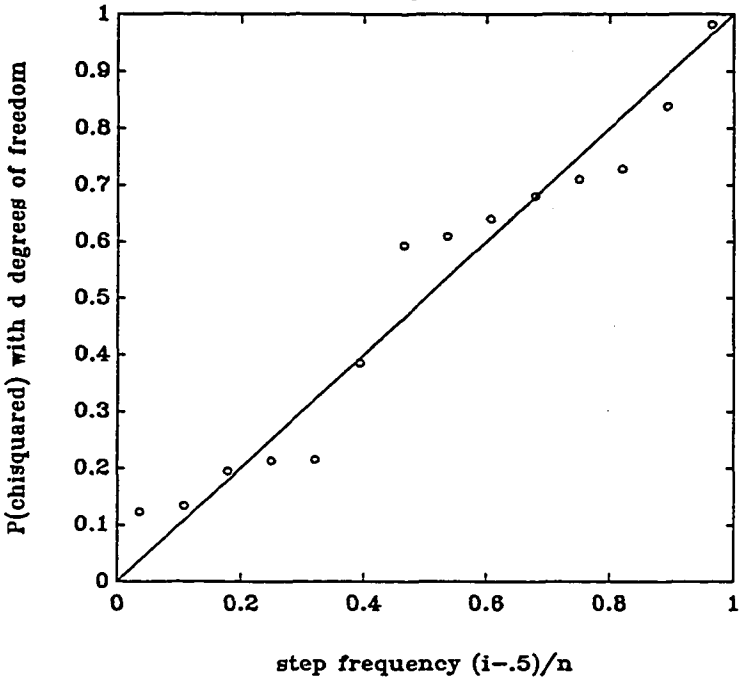

Table B.12 *H. erectus* nuchal ridge curve intrasample two data			
Specimen	*T*	Emp. Prob.	χ^2 Prob.
KNM-ER 3733	1.3992	0.0357	0.1227
KNM-ER 3883	1.4705	0.1071	0.1336
OH 9	1.8519	0.1786	0.1950
Sangiran 17	1.9727	0.2500	0.2135
Sangiran 2	12.4700	0.3214	0.2154
Solo 10	5.5760	0.3929	0.3859
Solo 11	4.3655	0.4643	0.5933
Solo 12	5.3867	0.5357	0.6093
Solo 5	7.0256	0.6071	0.6400
Solo 7	4.7421	0.6786	0.6806
Zhoukoudian 11	5.1016	0.7500	0.7101
Zhoukoudian 12	1.9620	0.8214	0.7284
Zhoukoudian 3	2.9743	0.8929	0.8388
Zhoukoudian 1966	4.4910	0.9643	0.9816

The *H. sapiens* sample for the nuchal ridge curve had an N = 20, mean = 460.5186, variance = 60985.0, c = 66.2133, and d = 6.9551, K-S statistic = 0.2186 (acceptable with $\alpha<0.01$).

Figure B.13 *H. sapiens* Nuchal Ridge Curve Sample p-p Plot.

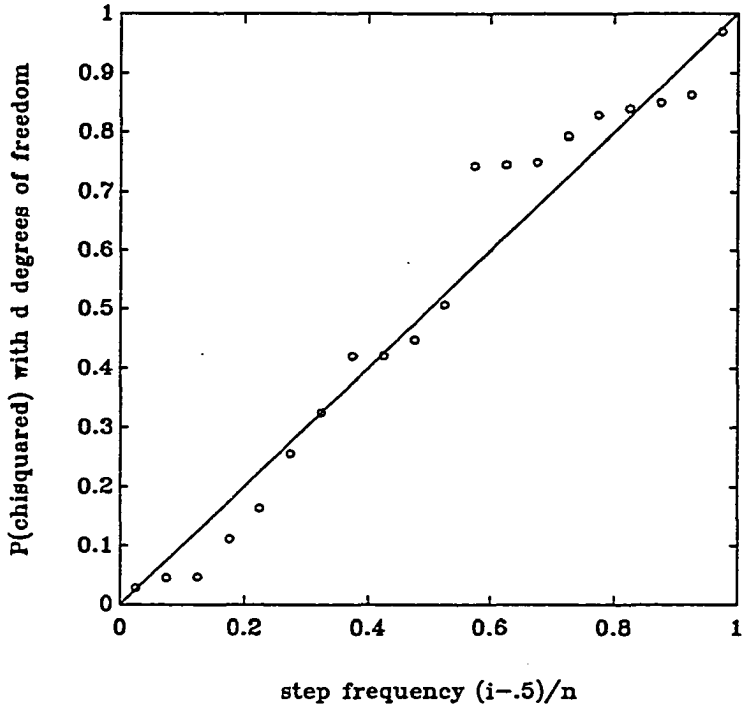

Table B.13 *H. sapiens* nuchal ridge curve intrasample data			
Specimen	T	Emp. Prob.	χ^2 Prob.
CMNH 1157	3.4584	0.0250	0.0278
CMNH 1253	10.6864	0.0750	0.0456
CMNH 1273	5.8498	0.1250	0.0467
CMNH 1759	8.8945	0.1750	0.1117
CMNH 2048	9.6345	0.2250	0.1638
CMNH 2401	2.0890	0.2750	0.2553
CMNH 2584	10.4591	0.3250	0.3253
CMNH 2860	2.0710	0.3750	0.4202
CMNH 514	6.3657	0.4250	0.4208
CMNH 560	8.9841	0.4750	0.4477
CMNH 630	5.6242	0.5250	0.5073
CMNH 667	8.9258	0.5750	0.7436
CMNH 681	4.8404	0.6250	0.7458
CMNH 856	1.7324	0.6750	0.7500
CMNH 881	10.2540	0.7250	0.7932
CMNH 883	15.4479	0.7750	0.8284
CMNH 919	4.2634	0.8250	0.8389
CMNH 920	5.6193	0.8750	0.8498
CMNH 939	10.9670	0.9250	0.8625
CMNH 962	2.9345	0.9750	0.9701

Literature Cited

Aitken MJ and Valladas H (1992) Luminescence dating relevant to human origins. Phil. Trans. R. Soc. Lond. B *337*:139-144.

Adam KD (1985) The chronological and systematic position of the Steinheim skull. In E Delson (ed.): Ancestors: The Hard Evidence. New York: Alan R. Liss, Inc., pp. 272-276.

Albrecht GH (1991) Thin plate splines and the primate scapula. Am. J. Phys. Anthropol. Suppl. *12*:42-43.

Albrecht GH (1992) Multivariate morphometrics with missing data: techniques for canonical variates and generalized distances. Am. J. Phys. Anthropol. Suppl. *14*:42.

An Z and Ho CK (1989) New magnetostratigraphic dates of Lantian *Homo erectus*. Quat. Res. *32*:213-221.

Andrews P (1984) An alternative interpretation of characters used to define *Homo erectus*. Cour. Forsch. Inst. Senckenberg *69*:167-175.

Andrews P and Franzen JL eds (1984) The Early Evolution of Man: With Special Emphasis On Southeast Asia and Africa. Cour. Forsch. Inst. Senckenberg *69*.

Ashton EH (1950) The endocranial capacities of the *Australopithecinae*. Proc. zool. Soc. Lond. *120*:715-721.

Aziz FJ, de Vos J, and Sondaar PV (1991) The *Homo* bearing deposits of Java and its ecological context. Abstract. 4th International Senckenberg Conference: 100 years of Pithecanthropus.

Bar-Yosef O (1989) Geochronology of the Levantine Middle Paleolithic. In P Mellars and CB Stringer (eds.): The Human Revolution: Behavioural and Biological Perspectives on the Origins of Modern Humans. Princeton: Princeton University Press, pp. 589-610.

Bar-Yosef O (1992a) Middle Palaeolithic chronology and the transition to the Upper Palaeolithic in southwest Asia. In G Bräuer and FH Smith (eds.): Continuity or

Replacement: Controversies in *Homo sapiens* Evolution. Rotterdam: Balkema, pp. 261-272.

Bar-Yosef O (1992b) The role of western Asia in modern human origins. Phil. Trans. R. Soc. Lond. *337*:193-200.

Bartstra GJ, Soegondho S, and van der Wijk A (1988) Ngandong Man: age and artifacts. J. Hum. Evol. *17*:325-337.

Begun DR (1992) Miocene fossil hominids and the chimp-human clade. Science *257*:1929-1933.

Biegert J (1963) The evaluation of characteristics of the skull, hands, and feet for primate taxonomy. In SL Washburn (ed.): Classification and Human Evolution, pp. 116-145.

Bilsborough A and Wood BA (1986) The origin and fate of *Homo erectus*. In B Wood, L Martin, and P Andrews (eds.): Major Topics in Primate and Human Evolution. Cambridge, UK: Cambridge University Press, pp. 295-316.

Birdsell JB (1967) Preliminary data on the trihybrid origin of the Australian aborigines. Arch. and Phys. Anthropol. in Oceania *2*:100-155.

Bonis L de (1986) *Homo erectus* et la transition vers *Homo sapiens* en Europe. In M Sakka (ed.): Définition et origines de l'Homme. Paris: CNRS, pp. 253-261.

Bookstein, FL (1991) Morphometric Tools for Landmark Data: Geometry and Biology. Cambridge: Cambridge University Press.

Bookstein FL, Chernoff B, Elder R, Humphries G, Smith G, and Strauss R (1985) Morphometrics in Evolutionary Biology: Geometry of Size and Shape Change, with Examples from Fishes. Philadelphia: Academy of Natural Sciences.

Bookstein FL and Cutting CB (1988) A proposal for the apprehension of curving craniofacial form in three dimensions. In K Vig and A Burdi (eds.): Craniofacial Morphogenesis and Dysmorphogenesis. Ann Arbor, MI: Center for Human Growth and Development, pp. 127-140

Bookstein FL and Cutting CB (1991) Proposal for an automated synthesis of morphometrics and image analysis for solid medical images. In SK Mun, R von Hanwehr, and P Gerity (eds.): Proc. Technology Requirements for Biomedical Imaging: SDI Technology Applications Symposium. Los Alamitos, CA: IEEE Press, pp. 118-122.

Boule M and Vallois HV (1957) Fossil Men: A Textbook of Human Paleontology. London: Thames and Hudson.

Bowen DQ, Hughes S, Sykes GA, and Miller GH (1989) Land-sea correlations in the Pleistocene based on isoleucine epimerization in non-marine molluscs. Nature *340*:49-51.

Brace CL (1964) The fate of the "classic" Neanderthals: A consideration of hominid catastrophism. Curr. Anthropol. *5*:3-43.

Brace CL (1988) The Stages of Human Evolution, 3rd ed. Englewood Cliffs, NJ: Prentice Hall.

Brace CL (1991) Monte Circeo, Neanderthals, and continuity in European cranial morphology, a rear end view. In M Piperno and G Scichilone (eds.): The Circeo 1 Neandertal Skull: Studies and Documentation. Rome: Libreria Dello Stato, pp. 175-195.

Bräuer G (1978) The morphological differentiation of anatomically modern man in Africa, with special regard to recent finds from East Africa. Zeitschrift für Morphologie und Anthropologie *69*:266-292.

Bräuer G (1981) New evidence on the transitional period between Neanderthal and modern Man. J. Hum. Evol. *10*:467-474.

Bräuer G (1982) Early anatomically modern man in Africa and the replacement of the Mediterranean and European Neandertals. In H de Lumley(ed.): L'*Homo erectus* et la Place de l'Homme de Tautavel parmi les Hominidés Fossiles. Nice: Louis-Jean Scientific and Literary Publications.

Bräuer G (1984a) The Afro-European *sapiens*-hypothesis, and hominid evolution in Asia during the Middle and Upper

Pleistocene. In J Franzen(ed.): Cour. Forsch. Inst. Senckenberg *69*:145-165.

Bräuer G (1984b) A craniological approach to the origin of anatomically modern *Homo sapiens* in Africa and implications for the appearance of modern Europeans. In FH Smith and F Spencer (eds.): The Origins of Modern Humans. New York: Alan R. Liss, Inc., pp. 327-410.

Bräuer G (1984c) Präsapiens-Hypothese oder Afro-europäische Sapiens-Hypothese. Zeitschrift für Morphologie und Anthropologie *75*:1-25.

Bräuer G (1989) The evolution of modern humans: A comparison of the African and non-African evidence. In The Human Revolution: Behavioural and Biological Perspectives on the Origins of Modern Humans. Princeton: Princeton University Press, pp. 123-154.

Bräuer G (1992) Africa's place in the evolution of *Homo sapiens*. In G Bräuer and FH Smith (eds.): Continuity or Replacement: Controversies in *Homo sapiens* Evolution. Rotterdam: Balkema, pp. 25-63.

Bräuer G, Deacon HJ, and Zipfel F (1992) Comment on the new maxillary finds from Klasies River, South Africa. J. Hum. Evol. *23*:419-422.

Bräuer G and Leakey, RE (1986) The ES-11693 cranium from Eliye Springs, West Turkana, Kenya. J. Hum. Evol. *15*:289-312.

Bräuer G and Mbua E (1992) *Homo erectus* traits used in cladistics and their variability in Asian and African hominids. J. Hum. Evol. *22*:79-108.

Bräuer G and Protsch, R (1980) New Upper Pleistocene hominids with neanderthaloid affinities from northern and eastern Germany. Am. J. Phys. Anthropol. *52*:207.

Bräuer G and Rimbach KW (1990) Late archaic and modern *Homo sapiens* from Europe, Africa, and southwest Asia: Craniometric comparisons and phylogenetic implications. J. Hum. Evol. *19*:789-807.

Bräuer G and Smith FH (1992) Continuity or Replacement: Controversies in *Homo sapiens* Evolution. Rotterdam: Balkema.

Bromage T (1992) The ontogeny of *Pan troglodytes* craniofacial architectural relationships and implications for early hominids. J. Hum. Evol. *23*:235-251.

Brown P (1989) Coobool Creek: A Morphological and Metrical Analysis of the Crania, Mandibles and Dentitions of a Prehistoric Australian Human Population. Terra Australis *13*:1-205.

Brown P (1992) Recent human evolution in East Asia and Australasia. Phil. Trans. R. Soc. Lond. B *337*:235-242.

Campbell BG (1965) The nomenclature of the Hominidae. Occas. Pap. Roy. Anthropol. Inst. *22*:1-34.

Campbell BG (1985) Human Evolution: An Introduction to Man's Adaptations, 3rd ed. New York: Aldine.

Cann RL, Stoneking M, and Wilson AC (1987) Mitochondrial DNA and human evolution. *325*:31-36.

Cave AJE (1961) The frontal sinus of the gorilla. Proc. Zool. Soc. Lond. *136*:359-373.

Cave AJE and Haines RW (1940) The paranasal sinuses of the anthropoid apes. J. Anat. *74*:493-523.

Chamberlain AT and Wood BA (1987) Early hominid phylogeny. J. Hum. Evol. *16*:119-133.

Chen T and Zhang Y (1991) Paleolithic chronology and possible coexistence of *Homo erectus* and *Homo sapiens* in China. World Archeology *23*:147-154.

Cheverud JM and Richtsmeier JT (1986) Finite-element scaling applied to sexual dimorphism in rhesus macaque (*Macaca mulatta*) facial growth. Syst. Zool. *35*:381-399.

Clarke R (1985) *Australopithecus* and early *Homo* in southern Africa. In E Delson (ed.): Ancestors: The Hard Evidence. New York: Alan R. Liss, Inc., pp. 171-177.

Clarke R (1990) The Ndutu cranium and the origin of *Homo sapiens*. J. Hum. Evol. *19*:699-736.

Cohen MM Jr (1986) Syndromes with craniosynostosis. In MM Cohen Jr (ed.): Craniosynostosis: Diagnosis, Evaluation, and Management. New York: Raven, pp. 413-590.

Conroy GC (1980) New evidence of Middle Pleistocene hominids from the Afar Desert-Ethiopia. Anthropos 7:96-107.

Coon CS (1962) The Origin of Races. New York: Knopf.

Countselinis A, Dritsas C, and Pitsios T (1991) Expertise médico-légale du crâne Pléistocène LA01/S2 (Apidima II), Apidima, Laconie, Grèce. L'Anthropologie *95*:401-408.

Cutting CB, Bookstein FL, Haddad B, and Dean D (in prep.) Averaging Three Dimensional Morphology.

Deacon JH (1992) Southern Africa and modern human origins. Phil. Trans. R. Soc. Lond. B *337*:1177-183.

Daegling D (1992) Shape variation in the hominoid mandibular symphysis as a taxonomic indicator. Am. J. Phys. Anthropol. Suppl. *14*:67.

Day MH (1986) Guide to Fossil Man, 4th Ed. Chicago: The University of Chicago Press.

Day M and Stringer C (1982) A reconsideration of the Omo Kibish remains and the *erectus-sapiens* transition. In H de Lumley (ed.): L'*Homo erectus* et la Place de l'Homme de Tautavel parmi les Hominidés Fossiles. Nice: Louis-Jean Scientific and Literary Publications, pp. 814-856.

De Villiers H and Fatti LP (1982) The antiquity of the Negro. S. Afr. J. Sci. *78*:321-333.

Dean D (1986) Covariation Between craniofacial form and chewing. M.A. thesis, Temple University.

Dean D and Delson E (1992) Second Gorilla or Third Chimpanzee? Nature *359*:676-677.

Dean D and Ziegler R (in prep.) Middle Pleistocene Hominid Cranial Remains From Reilingen (Southern Rhine Valley), Germany.

Dean MC and Wood BA (1982) Basicranial anatomy of Plio-Pleistocene hominids from East and South Africa. Am. J. Phys. Anthropol. 59:157-174.

Delfino VP, Eligio V, Potente F, Lettini T, and Ragone P (1991) Analytical morphometry of the Neanderthal cranium from Monte Circeo (Circeo 1). In M Piperno and G Scichilone (eds.): The Circeo 1 Neandertal Skull: Studies and Documentation. Rome: Libreria Dello Stato, pp. 197-251.

Delong RE and Getchell TV (1987) Nasal respiratory function -- vasomotor and secretory regulation. Chemical Senses *12*:3-36.

Delson E (1981) Paleoanthropology: Pliocene and Pleistocene human evolution. Paleobiol. 7:298-305.

Delson E (1992) Successor to Weidenreich. Nature *360*:544-545.

Delson E and Brooks AS (1988) Europe. In I Tattersall, E Delson, and J Van Couvering (eds.): Encyclopedia of Human Evolution and Prehistory, pp. 185-194.

Delson E, Eldredge N, and Tattersall IM (1977) Reconstruction of hominid phylogeny: A testable framework based on cladistic analysis. J. Hum. Evol. *6*:263-278.

Demes B (1987) Another look at an old face: Biomechanics of the Neandertal facial skeleton reconsidered. J. Hum. Evol. *16*:297-303.

Dhobzhansky T (1963) Genetic entities in hominid evolution. In SL Washburn (ed.): Classification and Human Evolution. New York: Aldine, pp. 347-362.

Dong X (1989) *Homo erectus* in China. In R Wu, X Wu, and S Zhang (eds.): Early Humankind in China. Beijing: Science Press, pp. 9-23.

Eldredge N and Tattersall IM (1982) The Myths of Human Evolution. New York: Columbia University Press.

Endo B (1966) Experimental studies on the mechanical significance of the form of the human facial skeleton. J. Fac. Sci. Univ. Tokyo, Sec. *VIII*:1-106

Endo B (1970) Analysis of stresses around the orbit due to masseter and temporalis muscles respectively. J. Anthropol. Soc. Nippon *78*:251-266.

Endo B and Adachi K (1988) Biomechanical simulation study on the forms of the frontal bone and facial bones of the recent human facial skeleton by using a two-dimensional frame model with stepwise variable cross-section members. Okajimas Folia Anat. Jpn. *64*:335-350.

Enlow DH (1990) Facial Growth, 3rd Ed. Philadelphia: WB Saunders.

Feibel CS, Brown FH, and McDougall I (1989) Stratigraphic context of fossil hominids from the Omo Group deposits: Northern Turkana Basin, Kenya and Ethiopia. Am. J. Phys. Anthropol. *78*:595-622.

Foley RA (1987) Another Unique Species: Patterns in Human Evolutionary Ecology. New York: John Wiley.

Foley RA (1989) The ecological conditions of speciation: A comparative approach to the origins of anatomically modern humans. In P Mellars and CB Stringer (eds.): The Human Revolution: Behavioural and Biological Perspectives on the Origins of Modern Humans. Princeton: Princeton University Press, pp. 298-318.

Foley RA and Lahr MM (1992) Beyond "out of Africa": Reassessing the origins of *Homo sapiens*. J. Hum. Evol. *22*:523-529.

Franciscus RG and Trinkaus E (1988) Nasal morphology and the emergence of *Homo erectus*. Am. J. Phys. Anthropol. 75:517-527.

Frayer D (1992a) The persistence of Neandertal features in post-Neandertal Europeans. In G Bräuer and FH Smith (eds.): Continuity or Replacement: Controversies in *Homo sapiens* Evolution. Rotterdam: Balkema, pp. 179-188.

Frayer D (1992b) Cranial base flattening in Europe: Neanderthals and more recent *Homo sapiens*. Am. J. Phys. Anthropol. Suppl. *14*:77.

Frayer DW, Jelínek J, Minugh-Purvis N, Oliva M, Seitl L, Smith FH, and Wolpoff MH (nd) Late Pleistocene Human Remains from Mladeč Cave, Moravia.

Gibbons A (1992) Jawing with our Georgian ancestors. Science *255*:401.

Graves P (1991) New models and metaphors for the Neandertal debate. Curr. Anthropol. *32*:513-541.

Greaves WS (1985) The mammalian postorbital bar as a torsion-resisting helical strut. J. Zool. Lond. *207*:125-136.

Greaves WS (1988) A functional consequence of an ossified mandibular symphysis. Amer. J. Phys. Anthropol. *77*:53-56.

Grimaud-Hervé D (1991) Evolution of the Javanese fossil hominid brain. Abstract. 4th International Senckenberg Conference: 100 years of Pithecanthropus.

Groves CP (1989a) A Theory of Human and Primate Evolution. Oxford: Oxford University Press.

Groves CP (1989b) A regional approach to the problem of the origin of modern humans in Australasia. In P Mellars and CB Stringer (eds.): The Human Revolution: Behavioural and Biological Perspectives on the Origins of Modern Humans. Princeton: Princeton University Press, pp. 274-297.

Groves CP and Mazák V (1975) An approach to the taxonomy of the Hominidae: gracile Villafranchian hominids of Africa. Casopis pro Mineralogii a Geologii *20*:225-246.

Habgood PJ (1989a) The evolution of modern humans: Evidence from Australasia seen in global context. In P Mellars and CB Stringer (eds.): The Human Revolution: Behavioural and Biological Perspectives on the Origins of Modern Humans. Princeton: Princeton University Press, pp. 245-273.

Habgood PJ (1989b) An examination of regional features on middle and early Late Pleistocene sub-Saharan African hominids. S. Afr. Arch. Bull. *44*:17-22.

Habgood PJ (1992) The origin of anatomically modern humans in east Asia. In G Bräuer and FH Smith (eds.): Continuity or Replacement: Controversies in *Homo sapiens* Evolution. Rotterdam: Balkema, pp. 273-288.

Hay RL (1990) Olduvai Gorge: A case history in the interpretation of hominid paleoenvironments in East Africa. In LF LaPorte (ed.): Establishment of a Geologic Framework for Paleoanthropology. Boulder, CO: Geological Society of America, Inc. pp. 23-37.

Hazout S, Loirat F, and Heim JL (1990) Modeles de phylogenie humaine assistés par ordinateur. Cahiers d'Anthropol. et Biom. Hum. *8*:85-100.

Heberer G (1963a) Die Ur- und Frühmenschen funde in Afrika. 2. Die Olduvai-Funde. Kosmos, Stuttgart *58*:84-88 (1962).

Heberer G (1963b) Über einen neuen archanthropinen typus aus der Oldoway-Schlucht. Zeit. Morph. Anthropol. *53*:171-177.

Hershkovits J, Pinhasov A, and Arbel G (1991) Skull surface contours by Moiré patterns: An experiment. Homo *42/43*:216-231.

Hilbert D and Cohn-Vossen S (1990) Geometry and the Imagination. New York: Chelsea.

Hoffecker JF, Powers WR, and Goebel T (1993) The colonization of Beringia and the peopling of the New World. Science *259*:46-53.

Holloway RL (1980) Indonesian "Solo" (Ngandong) endocranial reconstructions: Some preliminary observations and comparisons with Neandertal and *Homo erectus* groups. Am. J. Phys. Anthropol. *53*:285-295.

Hooton EA (1930) The Indians of Pecos Pueblo: A Study of Their Skeletal Remains. New Haven: Yale University Press.

Houghton P (1993) Neandertal supralaryngeal vocal tract. Am. J. Phys. Anthropol. *90*:139-146.

Howell FC (1960) European and Northwest African Middle Pleistocene Hominids. Curr. Anthropol. *1*:195-232.

Howell FC (1976) Some views of *Homo erectus* with special reference to its occurrence in Europe. In BA Sigmon and JS Cybulski (eds.): *Homo erectus* Papers in Honor of Davidson Black. Toronto: University of Toronto Press: 154-157.

Howell FC (1978) Hominidae. In VJ Maglio and HBS Cooke (eds.): Evolution of African Mammals. Cambridge: Harvard University Press, pp. 154-248.

Howell FC (1984) Introduction. In FH Smith and F Spencer (eds.): The Origins of Modern Humans. New York: Alan R. Liss, Inc., pp. xiii-xxii.

Howells WW (1944) Mankind So Far. New York: Doubleday.

Howells WW (1973) Cranial variation in man: A study by multivariate analysis of patterns of difference among recent human populations. Papers of the Peabody Museum of Archaeology and Ethnology *67*:1-259.

Howells WW (1974) Neanderthal Man: Facts and figures. Yrbk. Phys. Anthropol. *18*:7-18.

Howells WW (1976) *Homo erectus* in human descent: ideas and problems. In BA Sigmon and JS Cybulski (eds.): *Homo erectus* Papers in Honor of Davidson Black. Toronto: University of Toronto Press, pp. 63-85.

Howells WW (1980) *Homo erectus*: who, when and where. Yrbk. Phys. Anthropol. *23*:1-23.

Howells WW (1989) Skull Shapes and the Map: Craniometric Analysis in the Dispersion of Modern *Homo*. Papers of the Peabody Museum of Archaeology and Ethnology *67:1-189*.

Hrdlička A (1930) The skeletal remains of early man. Smithsonian Misc. Coll. *83*.

Hublin J-J (1982) Les anténéandertaliens: Presapiens ou prénéandertaliens. Geobios *6*:345-357.

Hublin J-J (1983) Les superstructures occipitales chez les prédécesseurs d'*Homo erectus* en Afrique: quelques remarques sur l'origine du torus occipital transverse. Bull. Mém. Soc. Anthrop. Paris *10*:303-312.

Hublin J-J (1985) Human fossils from the North African Middle Pleistocene and the Origin of *Homo sapiens*. In E Delson (ed.): Ancestors: The Hard Evidence. New York: Alan R. Liss, Inc., pp. 283-288.

Hublin J-J (1986) Some comments on the diagnostic features of *Homo erectus*. Anthropos. *23*:175-187.

Hublin J-J (1992) Recent human evolution in northwestern Africa. Phil. Trans. R. Soc. Lond. B *337*:185-191.

Hublin J-J and Braun M (1992) *Homo erectus*: Are the "autapomorphies" reversible? Am. J. Phys. Anthropol. Suppl. *14*:92.

Huxley T (1863) Evidence as to Man's Place in Nature. London: Macmillan.

Hylander WL, Picq PG, and Johnson KR (1991a) Masticatory-stress hypotheses and the supraorbital region of primates. Am. J. Phys. Anthropol. *86*:1-36.

Hylander WL, Picq PG, and Johnson KR (1991b) Function of the supraorbital region in primates. Arch. Oral Biol. 36:273-281.

Jacob T (1976) Solo Man and Peking Man. In BA Sigmon and JS Cybulski (eds.): Papers in Honor of Davidson Black. Toronto: University of Toronto Press, pp. 87-104.

Jelínek J (1980a) Variability and Geography. Anthropologie *18*:109-114.

Jelínek J (1980b) European *Homo erectus* and the origin of *Homo sapiens*. In L-K Konigsson (ed.): Current Arguments on Early Man. Oxford: Pergamon, pp. 137-144.

Jones R (1992) The human colonization of the Australian continent. In G Bräuer and FH Smith (eds.): Continuity or Replacement: Controversies in *Homo sapiens* Evolution. Rotterdam: Balkema, pp. 289-301.

Kalvin AD, Dean D, Hublin J-J, and Braun M (1992) Visualization in Anthropology: Reconstruction of Human Fossils from Multiple Pieces. In AE Kaufman and GM Nielson (eds.): Proceedings of IEEE Visualization '92. Los Alamitos, CA: IEEE Press, pp. 404-410.

Kamminga J and Wright RVS (1988) The Upper Cave at Zhoukoudian and the origins of the Mongoloids. J. Hum. Evol. *17*:739-767.

Kennedy GE (1991) On the autapomorphic traits of *Homo erectus*. J. Hum. Evol. *20*:375-412.

Kieth A (1915) The Antiquity of Man. London: Williams and Norgate.

Kieth A (1939) A Resurvey of the Anatomical Features of the Piltdown Skull, with Some Observations on the Recently Discovered Swanscombe Skull." J. Anat. (Lond) *73*:155-185.

Klein RG (1973) Geological antiquity of Rhodesian man. Nature *244*:311-312.

Klein RG (1983) The stone age prehistory of southern Africa. Ann. Rev. Anthropol. *12*:25-48.

Klein RG (1989) The Human Career. Human Biological and Cultural Origins. Chicago: University of Chicago Press.

Klein RG and Cruz-Uribe K (1991) The bovids from Elandsfontein, South Africa, and their implications for the age, paleoenvironment, and origins of the site. Afr. Arch. Rev. *9*:21-79.

Koenderink J (1990) Solid Shape. Cambridge: MIT Press.

Kraatz, R (1991) Type locality of *Homo erectus heidelbergensis*. Old sandpit "Grafenrain-Mauer). Abstract. 4th International Senckenberg Conference: 100 Years of Pithecanthropus.

Laitman JT (1985) Evolution of the hominid upper respiratory tract. In PV Tobias (ed.): Hominid Evolution: Past, Present and Future. New York: Alan R. Liss, Inc., pp. 281-286.

Laitman JT and Heimbuch RC (1982) The basicranium of Plio-Pleistocene hominids as an indicator of their upper respiratory systems. Am. J. Phys. Anthropol. *59*:323-344.

Laitman JT, Heimbuch RC, and Crelin ES (1978) Developmental changes in a basicranial line and its relationship to the upper respiratory system in living primates. Am. J. Anat. *152*:467-482.

Laitman JT, Heimbuch RC, and Crelin ES (1979) The basicranium of fossil hominids as an indicator of their upper respiratory system. Am. J. Phys. Anthropol. *51*:15-34.

Laitman JT, Reidenberg JS, and Gannon PJ (1992) Fossil skulls and hominid vocal tracts: New approaches to charting the evolution of human speech. In J Wind, B Chiarelli, B Birchmakjian, A Nocentini, and A Jonker (eds.): Language Origins: A Multidisciplinary Approach. Amsterdam: Kluwer, pp. 395-407.

Latham AG, and Schwarcz, HP (1992) The Petralona hominid site: Uranium-series re-analysis of 'Layer 10' calcite and associated palaeomagnetic analyses. Archaeometry *34*:135-140.

Leakey LSB (1963) East African fossil Hominoidea and the classification within this super-family. In SL Washburn (ed.): Classification and Human Evolution. New York: Aldine, pp. 32-49.

Leakey LSB (1966) *Homo habilis, Homo erectus,* and the australopithecines. Nature *209*:1279-1281.

Leakey LSB (1972) *Homo sapiens* in the Middle Pleistocene and the evidence of *Homo sapiens*' evolution. In F Bordes (ed.) The Origin of *Homo sapiens*. Paris: UNESCO, pp. 25-29.

Le Gros Clark WE (1955) The Fossil Evidence for Human Evolution, 3rd ed. Chicago: University of Chicago Press.

Le Gros Clark WE (1960) The Antecedents of Man. Chicago: Quadrangle.

Le Gros Clark WE (1967) Man Apes or Ape-Men. New York: Robert E. Krieger.

Li T and Etler DA (1992) New Middle Pleistocene hominid crania from Yunxian in China. Nature *357*:404-407.

Li T and Wang J (1991) The latest advance in Quaternary magneto-stratigraphy of China. In T Liu (ed.): Quaternary Geology and Environment of China. Beijing: Science Press, pp. 265-272.

Lieberman P, Laitman JT, Reidenberg JS, and Gannon PJ (1992) The anatomy, physiology, acoustics and perception of speech: Essential elements in analysis of the evolution of human speech. J. Hum. Evol. *23*:447-467.

Lipschutz MM (1969) Schaum's Outline of Theory and Problems of Differential Geometry. New York: McGraw-Hill.

Macintosh NWG and Larnach SL (1972) The persistence of *Homo erectus* traits in Australian Aboriginal crania. Oceania 7:1-7.

Maddison DR, Ruvolo M, and Swofford DL (1992) Geographic origins of human mitochondrial DNA: Phylogenetic evidence from control region sequences. Systematic Biology. 41:111-124.

Maier W and Nkini A (1984) Olduvai Hominid 9: New results of investigation. Cour. Forsch. Senckenberg *69*:123-130.

Marcus L, Dean D, and Bookstein FL (in prep.) Chi square model for discriminating biological space curve affinities. In: L Marcus (ed.): Proceedings of the Fifth Morphometrics Workshop. NATO Advanced Study Institute, Il Cioccio, Italy.

Mayr E (1951) Taxonomic categories in fossil hominids. Cold Spring Harbor Symp. Quant. Biol. *15*:109-117.

Mellars P and Stringer CB (1989) The Human Revolution: Behavioural and Biological Perspectives on the Origins of Modern Humans. Princeton: Princeton University Press.

Miller GH, Beaumont PB, Jull AJT, and Johnson B (1992) Pleistocene geochronology and palaeothermometry from

protein diagenesis in ostrich eggshells: implications for the evolution of modern humans. Phil. Trans. R. Soc. Lond. B *337*:149-157.

Moss ML and Young RW (1960) A functional approach to craniology. Am. J. Phys. Anthropol. *18*:281-292.

Olshan AF, Seigel AF, and Swindler, DR (1982) Robust and least squares orthogonal mapping: Methods for the study of craniofacial form and growth. Am. J. Phys. Anthropol. *59*:131-137.

Pesole G, Sbisá E, Preparata G, and Saccone C (1992) The evolution of the mitochondrial D-Loop region and the origin of modern Man. Mol. Biol. Evol. *9*:587-598.

Peterson R (1987) An Atlas of Mankind: Modern Europe. Washington: Cliveden.

Picq PG (1990) L'Articulation Temporo-mandibulaire des Hominidés. Cahiers de Paléoanthropologie. Paris: CNRS.

Picq PG (nd) Stasis vs. gradualism in *Homo erectus*: Evidence from the evolution of the TMJ.

Picq PG and Hylander WL (1989) Endo's stress analysis of the primate skull and the functional significance of the supraorbital region. Am. J. Phys. Anthropol. *79*:393-398.

Pope GG (1988) Recent advances in far eastern paleoanthropology. Ann. Rev. Anthropol. *17*:43-77.

Pope GG (1991) Evolution of the zygomaticomaxillary region in the genus *Homo* and its relevance to the origin of modern humans. J. Human. Evol. *21*:189-213.

Pope GG (1992) Craniofacial evidence for the origin of modern humans in China. Yrbk. of Phys. Anthropol. *35*:243-298.

Press WH, Flannery BP, Teukolsky SA, and Vetterling, WT (1988) Numerical Recipes in C. Cambridge: Cambridge University Press.

Preuschoft H, Demes B, Meyer M, and Bär HF (1986) The biomechanical principles realized in the upper jaw of long snouted primates. In JG Else and PC Lee (eds.):

Primate Evolution Vol. 1. Cambridge: Cambridge University Press, pp. 249-264.

Protsch R (1975) The absolute dating of Upper Paleolithic sub-Saharan fossil hominids and their place in human evolution. J. Hum. Evol. *4*:297-322.

Pycraft WP, Elliot GE, Yearsley M, Carter JT, Smith RA, Hopwood AT, Bate DMA, Swinton WE and Bather FA (1928) Rhodesian Man and Associated Remains. Oxford: Oxford University Press.

Rak Y (1983) The Australopithecine Face. London: Academic Press.

Rak Y (1986) The Neanderthal; a new look at an old face. J. Hum. Evol. *15*:151-164.

Ravosa, MJ (1988) Browridge development in Cercopithecidae: A test of two models. Am. J. Phys. Anthropol. *76*:535-555.

Ravosa MJ (1991a) Ontogenetic perspective on mechanical and non-mechanical models of circumorbital morphology. Am. J. Phys. Anthropol. *85*:95-112.

Ravosa MJ (1991b) Interspecific perspective on mechanical and nonmechanical models of primate circumorbital morphology. Am. J. Phys. Anthropol. *86*:369-396.

Richtsmeier JT (1989) Applications of finite-element scaling analysis in primatology. Folia Primatol. *53*:50-64.

Richtsmeier JT (1991) Similarities in *Aegyptopithecus* and *Afropithecus* facial morphology. Folia Primatol. *56*:65-85.

Richtsmeier JT, Cheverud JM, and Lele S (1992) Advances in anthropological morphometrics. Ann. Rev. Anthropol. 21:283-305.

Rightmire GP (1975) Problems in the study of later Pleistocene man in Africa. Am. Anthropol. 77:28-52.

Rightmire GP (1976) Relationships of Middle and Upper Pleistocene hominids from sub-Saharan Africa. Nature *260*:238-240.

Rightmire GP (1978) Florisbad and human population succession in southern Africa. Am. J. Phys. Anthropol. *48*:475-487.

Rightmire GP (1979) Implications of the Border Cave skeletal remains for later Pleistocene human evolution. Curr. Anthropol. *20*:23-35.

Rightmire GP (1980) *Homo erectus* and human evolution in the African Middle Pleistocene. In L-K Königsson (ed.) Current Argument on Early Man. Oxford: Pergamon, pp. 70-85.

Rightmire GP (1981a) Patterns in the evolution of *Homo erectus*. Paleobiol. *8*:307-308.

Rightmire GP (1981b) Later Pleistocene hominids of eastern and southern Africa. Anthropologie (Brno) *19*:15-26.

Rightmire GP (1984) *Homo sapiens* in sub-Saharan Africa. In FH Smith and F Spencer (eds.): The Origins of Modern Humans. New York: Alan R. Liss, Inc., pp. 295-325.

Rightmire GP (1985) The tempo of change in the evolution of mid-Pleistocene *Homo*. In E Delson (ed.): Ancestors: the hard evidence. New York: Alan R. Liss, pp. 255-264.

Rightmire GP (1986) Stasis in *Homo erectus* defended. Paleobiology *12*:324-325.

Rightmire GP (1988) *Homo erectus* and later Middle Pleistocene humans. Ann. Rev. Anthropol. *17*:239-59.

Rightmire GP (1989) Middle Stone Age Humans from Eastern and Southern Africa. In P Mellars and CB Stringer (eds.): The Human Revolution: Behavioural and Biological Perspectives on the Origins of Modern Humans. Princeton: Princeton University Press, pp. 109-122.

Rightmire GP (1990) The Evolution of *Homo erectus*. Cambridge: Cambridge University Press.

Rightmire GP (1991) The dispersal of *Homo erectus* from Africa and the emergence of more modern humans. J. Anthropol. Res. *47*:177-191.

Rightmire GP (1993) Variation among early Homo crania from Olduvai Gorge and the Koobi Fora region. Am. J. Phys. Anthropol. *90*:1-33.

Rightmire GP and Deacon HJ (1991) Comparative studies of Late Pleistocene human remains from Klasies River Mouth South Africa. J. Hum. Evol. *20*:131-156.

Rogers DF and Adams JA (1976) Mathematical Elements for Computer Graphics. New York: McGraw-Hill.

Rohlf FJ (1990) Rotational fit (Procrustes) methods. In FJ Rohlf and FL Bookstein (eds.) Proceedings of the Michigan Morphometrics Workshop. Ann Arbor, MI: University of Michigan Museum of Zoology, pp. 227-236.

Rohlf FJ and Bookstein FL eds (1990) Proceedings of the Michigan Morphometrics Workshop. Ann Arbor, MI: University of Michigan Museum of Zoology.

Rohlf FJ and Marcus LF (in press) A revolution in morphometrics. Trends in Ecol. and Evol.

Rohlf FJ and Slice D (1990) Extensions of the Procrustes method for optimal superimposition of landmarks. Syst. Zool. *39*:40-59.

Rohlf FJ and Sokal RR (1981) Statistical Tables. New York: WH Freeman.

Rosas A, Bermudez de Castro JM, and Aguirre E (1991) Mandibules et dents d'Ibeas (Espagne) dans le contexte de l'évolution humaine en Europe. L'Anthropologie *95*:89-102.

Rosas A (1987) Two new mandibular fragments from Atapuerca/Ibeas (SH site). A reassessment of the affinities of the Ibeas mandibles sample. J. Hum. Evol. 16:417-427.

Rosenberger AL (1986) Platyrrhines, catarrhines and the anthropoid transition. In B Wood, L Martin, and P Andrews (eds.): Major Topics in Primate and Human Evolution. Cambridge: Cambridge University Press, pp. 66-88.

Rouhani S (1989) Molecular genetics and the pattern of human evolution: Plausible and implausible models. In P Mellars and CB Stringer (eds.): The Human Revolution: Behavioural and Biological Perspectives on the Origins of Modern Humans. Princeton: Princeton University Press, pp. 47-61.

Russell MD (1983) The Functional and Adaptive Significance of the Supraorbital Torus. Ph.D. Thesis, The University of Michigan.

Russell MD (1985) The supraorbital torus: A most remarkable peculiarity. Curr. Anthropol. *26*:337-350.

Saban R (1991) Les vaisseaux méningés de l'homme d'Ehringsdorf d'après les moulages endocrâniens. L'Anthropologie *95*:113-122.

Saccone C, Pesole G, Sbisá E, and Preparata G (1992) Time and biosequences: a contribution to the origin of modern man. Human Evol. 7:37-46.

Santa Luca AP (1978) A re-examination of presumed Neandertal fossils. J. Hum. Evol. 7:619-636.

Santa Luca AP (1980) The Ngandong Fossil Hominids. Yale Univ. Publs. Anthropol. *78*:1-175.

Schwalbe G (1901) Der Neanderthalschädel. Bonner Jahrbuch *106*:1-72.

Schwarcz HP and Grün R (1992) Electron spin resonance (ESR) dating of the origin of modern man. Phil. Trans. R. Soc. Lond. B *337*:145-148.

Sémah F, Sémah A-M, and Djubiantono T (1990) They Discovered Java. Jakarta: PT Adiwarna Citra.

Shea BT (1985) On aspects of skull form in African apes and orangutans, with implications for hominoid evolution. Am. J. Phys. Anthropol. *68*:329-342.

Shea BT (1988) Phylogeny and skull form in the hominoid primates. In JH Schwartz (ed.) Orang-utan Biology. Oxford: Oxford University Press, pp. 233-245.

Shizumu M, Mubroto B, Siagian H, and Untung M (1985) A paleomagnetic study in the Sangiran area. In N Watanabe and D Kadar (eds.): Quaternary Geology of the Hominid Fossil Bearing Formations in Java. Bandung: Geol. Res. Dev. Centre, pp. 275-307.

Shreeve J (1992) The dating game. Discover *13*:76-83.

Simmons T, Falsetti AB, and Smith FH (1991) Evolutionary patterns in the frontal bones of Pleistocene hominids from western Asia. J. Hum. Evol. *20*:249-269.

Simmons T and Smith FH (1991) Human population relationships in the Late Pleistocene. Curr. Anth. *32*:623-627.

Simpson GG (1944) Tempo and Mode in Evolution. New York: Columbia Univ. Press.

Sokal RR and Rohlf FJ (1981) Biometry: The Principles and Practice of Statistics in Biological Research, 2nd ed. New York: WH Freeman.

Slice D, Dean D, Cutting CB, and Kim DH (1992) Techniques for Isolating Diagnostic Landmarks on Crouzon and Apert's Syndrome Crania. Am. J. Phys. Anthropol. *Supp. 14*:152.

Smith FH (1984) Fossil hominids from the Upper Pleistocene of central Europe and the origin of modern Europeans. In FH Smith and F Spencer (eds.): The Origins of Modern Humans. New York: Alan R. Liss, Inc., pp. 137-209.

Smith FH (1991) The Neandertals: Evolutionary dead ends or ancestors of modern people. J. Anth. Res. *47*:219-238.

Smith FH (1992a) The role of continuity in modern human origins. In G Bräuer and FH Smith (eds.): Continuity or Replacement: Controversies in *Homo sapiens* Evolution. Rotterdam: Balkema, pp. 145-156.

Smith FH (1992b) Models and realities in modern human origins: The African fossil evidence. Phil. Trans. R. Soc. Lond. B *337*:243-250.

Smith FH, Falsetti AB, and Donnelly SM (1989a) Modern Human Origins. Yrbk. Phys. Anthropol. *32*:35-68

Smith FH and Paquette SP (1989) The adaptive basis of Neandertal facial form, with some thoughts on the nature of modern human origins. In E Trinkaus (ed.): The Emergence of Modern Humans: Biocultural Adaptations in the Later Pleistocene. Cambridge: Cambridge University Press, pp. 181-210.

Smith FH and Ranyard GC (1980) Evolution of the supraorbital region in Upper Pleistocene fossil hominids from south-central Europe. Am. J. Phys. Anthropol. *53*:589-610.

Smith FH, Simek JF, and Harrill MS (1989b) Geographic variation in supraorbital torus reduction during the later Pleistocene. In P Mellars and CB Stringer (eds.): The Human Revolution: Behavioural and Biological Perspectives on the Origins of Modern Humans. Princeton: Princeton University Press, pp. 172-193.

Spitery E (1982) La face de l'homme de Tautavel. In H de Lumley (ed.): L'*Homo erectus* et la Place de l'Homme de Tautavel parmi les Hominidés Fossiles. Nice: Louis-Jean Scientific and Literary Publications, pp. 89-109.

Straney DO (1990) Median axis methods in morphometrics. In FJ Rohlf and FL Bookstein (eds.): Proceedings of the Michigan Morphometrics Workshop. Ann Arbor, MI: University of Michigan Museum of Zoology, pp. 179-200.

Stringer CB (1981) The dating of European Middle Pleistocene hominids and the existence of *Homo erectus* in Europe. Anthropologie *19*:3-14.

Stringer CB (1982) Towards a solution to the Neanderthal problem. J. Hum. Evol. *11*:431-438.

Stringer CB (1984) The definition of *Homo erectus* and the existence of the species in Africa and Europe. Cour. Forsch. Senckenberg *69*:131-143.

Stringer CB (1985) Pleistocene hominid variability and the origin of Late Pleistocene humans. In E Delson (ed.): Ancestors: the hard evidence. New York: Alan R. Liss, Inc., pp. 289-295.

Stringer CB (1988) "Archaic" *Homo sapiens*. In IM Tattersall, E Delson, and J Van Couvering (eds.): Encyclopedia of

Human Evolution and Prehistory. New York: Garland, pp. 49-54.

Stringer CB (1989a) The origins of early modern humans: A comparison of the European and non-European evidence. In P Mellars and CB Stringer (eds.): The Human Revolution: Behavioural and Biological Perspectives on the Origins of Modern Humans. Princeton: Princeton University Press, pp. 232-244.

Stringer CB (1989b) Documenting the origin of modern humans. In E Trinkaus (ed.): The Emergence of Modern Humans: Biocultural Adaptations in the Later Pleistocene. Cambridge: Cambridge University Press, pp. 67-96.

Stringer CB (1989c) *Homo sapiens*: Single or multiple origin? In J Durant (ed.): Human Origins. Oxford: Oxford University Press, pp. 63-80.

Stringer CB (1991) The concept of "archaic *Homo sapiens*." Abstract. 4th International Senckenberg Conference: 100 Years of Pithecanthropus.

Stringer CB (1992a) Replacement, continuity and the origin of *Homo sapiens*. In G Bräuer and FH Smith (eds.): Continuity or Replacement: Controversies in *Homo sapiens* Evolution. Rotterdam: Balkema, pp. 9-24.

Stringer CB (1992b) Reconstructing recent human evolution. Phil. Trans. R. Soc. Lond. B *337*:217-224.

Stringer CB and Andrews P (1988) Genetic and fossil evidence for the origin of modern humans. Science *239*:1263-1268.

Stringer CB and Burleigh R (1981) The Neanderthal problem and the prospects for direct dating of Neanderthal remains. Bull. Br. Mus. nat. Hist. (Geol.) *35*:225-241.

Stringer CB, Howell FC, and Melentis JK (1979) The significance of the fossil hominid skull from Petralona, Greece. J. Arch. Sci. *6*:235-253.

Stringer CB, Hublin, J-J, and Vandermeersch B (1984) The origin of anatomically modern humans in western Europe. In FH Smith and F Spencer (eds.): The Origins of Modern Humans. New York: Alan R. Liss, Inc., pp. 51-135.

Stoneking M, Sherry ST, and Vigilant L (1992a) Geographic origin of human mitochondrial DNA revisited. Syst. Biol. *41*:384-391.

Stoneking M, Sherry ST, Redd AJ, and Vigilant L (1992b) New approaches to dating suggest a recent age for the human mtDNA ancestor. Phil. Trans. R. Soc. Lond. B *337*:167-175.

Szalay FS and Delson E (1979) Evolutionary History of the Primates. London: Academic Press.

Tattersall IM (1986) Species recognition in human paleontology. J. hum. Evol. *15*:165-175.

Tattersall IM (1992a) Species concepts and species identification in human evolution. J. Hum. Evol. *22*:341-349.

Tattersall IM (1992b) Human origins and the origins of humanity. Human Evol. *7*:17-24.

Taylor M (1981) Physiology of the nose, paranasal sinuses, and nasopharynx. In GM English (ed.): Otolaryngology, Vol. II. Philadelphia: Harper and Row, pp. 1-63.

Tessier P (1986) Craniofacial surgery in syndromic craniosynostosis. In MM Cohen Jr. (ed.): Craniosynostosis: Diagnosis, Evaluation, and Management. New York: Raven, pp. 321-411.

Theunissen B (1989) Eugène Dubois and the Ape-man from Java. Dordrecht: Kluwer.

Thoma A (1973) New evidence for the polycentric evolution of *Homo sapiens*. J. Hum. Evol. *2*:529-536.

Thompson DW (1961) On Growth and Form. Cambridge: Cambridge University Press.

Thorne AG and Wolpoff MH (1981) Regional continuity in Australasian Pleistocene hominid evolution. Amer. J. Phys. Anthropol. *55*:337-349.

Thorne AG and Wolpoff MH (1991) 100 years of *Pithecanthropus* is enough. Abstr 4th International Senckenberg Conference: 100 Years of Pithecanthropus.

Tillier A-M (1975) Les Sinus Crâniens Chez les Hommes Actuels et Fossiles: Essai d'Interpretations. Paris: Thèse de 3e cycle.

Tillier A-M and Vandermeersch B (1982) Le problème de la radiation géographique de *Homo erectus*. Geobios *6*: 483-492.

Tobias PV (1980) A survey and synthesis of the African hominids of the late tertiary and early quaternary periods. In L-K Königsson (ed.) Current Argument on Early Man. Oxford: Pergamon, pp. 86-113.

Tobias PV (1991) Olduvai Gorge: The Skulls, Endocasts and Teeth of *Homo habilis*, Vol. 4. Cambridge: Cambridge University Press.

Trinkaus E (1982) A history of *Homo erectus* and *Homo sapiens* paleontology in America. In F Spencer (ed.): A History of Physical Anthropology: 1930-1980. London: Academic, pp. 261-280.

Trinkaus E (1987) The Neandertal face: Evolutionary and functional perspectives on a recent hominid face. J. Hum. Evol. *16*:429-443.

Trinkaus E (1989) The Emergence of Modern Humans: Biocultural Adaptations in the Later Pleistocene. Cambridge: Cambridge University Press.

Trinkaus E and Smith FH (1985) The fate of the Neandertals. In E Delson (ed.): Ancestors: The Hard Evidence. New York: Alan R. Liss, pp. 325-333.

Turner A (1992) Large carnivores and earliest European hominids: Changing determinants of resource availability during the Lower and Middle Pleistocene. J. Hum. Evol. *22*:109-126.

Turner A and Chamberlain A (1989) Speciation, morphological change and the status of African *Homo erectus*. J. Hum. Evol. *18*:115-130.

Vallois H (1949) The Fontéchevade fossil men. Am. J. Phys. Anthropol. 7:339-362.

Van der Meulen JC, Mazzola B, Stricker M, and Raphael B (1990) Classification of craniofacial malformations. In M Stricker, JC Van der Meulen, B Raphael, and R Mazzola (eds.): Craniofacial Malformations. Edinburgh: Churchill-Livingstone, pp. 149-309.

Vandermeersch, B (1989) The evolution of modern humans: Recent evidence from southwest Asia. In P Mellars and CB Stringer (eds.): The Human Revolution: Behavioural and Biological Perspectives on the Origins of Modern Humans. Princeton: Princeton University Press, pp. 155-164

Waddle D (1992) A quantitative approach to modern human origins. Am. J. Phys. Anthropol. Suppl. *14*:169.

Wang L (1989) New progress in chronology in Chinese paleoanthropology. In R Wu, X Wu, and S Zhang (eds.): Early Humankind in China. Beijing: Science Press, pp. 392-431.

Ward SC and Brown B (1986) The facial skeleton of *Sivapithecus indicus*. In D Swindler and J Erwin (eds.) Comparative Primate Biology, Vol. 1: Systematics, Evolution, and Anatomy. New York, Alan R. Liss, Inc., pp. 413-452.

Weidenreich F (1940) The torus occipitalis and related structures and their transformations in the course of human evolution. Bull. Geol. Soc. China. *19*:480-558.

Weidenreich F (1941) The brain and its role in the phylogenetic transformation of the human skull. Tr. Am. Phil. Soc. *31*:321-442.

Weidenreich F (1943) The skull of *Sinanthropus pekinensis*; a comparative study on a primitive hominid skull. Palaeontol. Sinica *Ser. D, 10*.

Weidenreich F (1945) Giant early man from Java and South China. Anthropol. Pap. Am. Mus. Nat. *40*:1-134.

Weidenreich F (1946) Apes, Giants and Man. Chicago: University of Chicago Press.

Weidenreich F (1951) Morphology of Solo Man. Anth. Pap. Am. Mus. Nat. Hist. 43:205-288.

White TD (1986) Cut marks on the Bodo cranium: A case of prehistoric defleshing. Am. J. Phys. Anthropol. *69*:503-509.

Wilk MB and Gnanadesikan R (1968) Probability plotting methods for the analysis of data. Biometrika *55*:1-17.

Wolpoff MH (1971) Vertesszöllös and the presapiens theory. Am. J. Phys. Anthropol. *35*:209-215.

Wolpoff MH (1980a) Cranial remains of Middle Pleistocene European hominids. J. Hum. Evol. *9*:339-358.

Wolpoff MH (1980b) Paleoanthropology. New York: Alfred A. Knopf.

Wolpoff MH (1983) Evolution in *Homo erectus*: the question of stasis. Paleobiol. *10*:389-406.

Wolpoff MH (1985) Human evolution at the peripheries: The pattern of the eastern edge. In Tobias PV (ed.): Hominid Evolution: Past, Present and Future. New York: Alan R. Liss, pp.

Wolpoff MH (1989a) Multiregional evolution: The fossil alternative to Eden. In P Mellars and CB Stringer (eds.): The Human Revolution: Behavioural and Biological Perspectives on the Origins of Modern Humans. Princeton: Princeton University Press, pp. 62-108.

Wolpoff MH (1989b) The place of the Neandertals in human evolution. In E Trinkaus (ed.) The Emergence of Modern Humans: Biocultural Adaptations in the Later Pleistocene. Cambridge: Cambridge University Press, pp. 97-141.

Wolpoff MH (1992a) Theories of modern human origins. In G Bräuer and FH Smith (eds.): Continuity or Replacement: Controversies in *Homo sapiens* Evolution. Rotterdam: Balkema, pp. 25-63.

Wolpoff MH (1992b) One hundred years of *Pithecanthropus* is enough. Am. J. Phys. Anthropol. Suppl. *14*:175-176.

Wolpoff MH and Caspari R (1990) Metric analysis of the skeletal material from Klasies River Mouth, Republic of South Africa. Am. J. Phys. Anthropol. *81*:319.

Wolpoff MH, Wu X, and Thorne AG (1984) Modern *Homo sapiens* origins: A general theory of hominid evolution involving the fossil evidence from East Asia. In FH Smith and F Spencer (eds.): The Origins of Modern Humans. New York: Alan R. Liss, Inc., pp. 411-483.

Wood BA (1984) The origin of *Homo erectus*. Cour. Forsch. Inst. Senckenberg *69*:99-111.

Wood BA (1985) Early *Homo* in Kenya and its systematic relationships. In E Delson (ed.): Ancestors: The Hard Evidence. New York: Alan R. Liss, pp. 206-214.

Wood BA (1991) Koobi Fora Research Project, Vol. 4.: Hominid Cranial Remains. Oxford: Oxford University Press.

Wood BA (1992) Early hominid species and speciation. J. Hum. Evol. *22*:351-365.

Wood BA and Chamberlain AT (1986) *Australopithecus*: Grade or clade? In B Wood, L Martin, and P Andrews (eds.): Major Topics in Primate and Human Evolution. Cambridge: Cambridge University Press, pp. 220-248.

Wright S (1969) Evolution and the Genetics of Populations, Vol. 2. The Theory of Gene Frequencies. Chicago: University of Chicago Press.

Wu R and Olsen JW (1985) Palaeoanthropology and Palaeolithic Archeology in the People's Republic of China. London: Academic.

Wu X (1990) The evolution of humankind in China. Acta Anthropol. Sin. *9*:312-321.

Wu X (1991) Early man in China, origin and dispersal of modern humans in East part of Asia. East Asian Tert/Quat. Newsletter *13*:82-83.

Wu X and Wu M (1985) Early *Homo sapiens* in China. In R Wu and JW Olsen (eds.): Palaeoanthropology and Palaeolithic

Archeology in the People's Republic of China. London: Academic Press, pp. 91-106.

Yokoyama Y, Nguyen HV, Falguères, Bibron R, and Léger C (1991) Datation directe par la spectrométrie gamma non destructive des restes humains: Comparaison avec d'autres méthodes. Cahiers du Quaternaire *16*:11-17.

Yuan S, Chen T, Gao S, and Hu Y (1991) Study on uranium series dating of fossil bones and teeth from Zhoukoudian site. Acta Anth. Sinica *10*:193.